ABSTRACT

Title of dissertation: STOCHASTIC VOLATILITY WITH LÉVY PROCESSES: CALIBRATION AND PRICING

Xianfang Wu, Doctor of Philosophy, 2005

Dissertation directed by: Professor Dilip B. Madan
Department of Finance, AMSC

In this thesis, stochastic volatility models with Lévy processes are treated in parameter calibration by the Carr-Madan fast Fourier transform (FFT) method and pricing through the partial integro-differential equation (PIDE) approach.

First, different models where the underlying log stock price or volatility driven by either a Brownian motion or a Lévy process are examined on Standard & Poor's (S&P) 500 data. The absolute percentage errors show that the calibration errors are different between the models. Furthermore, a new method to estimate the standard errors, which can be seen as a generalization of the traditional error estimation method, is proposed and the results show that in all the parameters of a stochastic volatility model, some parameters are well-identified while the others are not.

Next, the previous approach to parameter calibration is modified by making the volatility constrained under the volatilty process of the model and by making the other model parameters fixed. Parameters are calibrated over five consecutive days on S&P 500 or foreign exchange (FX) options data. The results show that the absolute percentage errors do not get much larger and are still in an acceptable

threshold. Moreover, the parameter calibrating procedure is stabilized due to the constraint made on the volatility process. In other words, it is more likely that the same calibrated parameters are obtained from different initial guesses.

Last, for the PIDEs with two or three space dimensions, which arise in stochastic volatility models or in stochastic skew models, it is in general inefficient or infeasible to apply the same numerical technique to different parts of the system. An operator splitting method is proposed to break down the complicated problem into a diffusion part and a jump part. The two parts are treated with a finite difference and a finite element method, respectively. For the PIDEs in 1-D, 2-D and 3-D cases, the numerical approach by the operator splitting is carried out in a reasonable time. The results show that the operator splitting method is numerically stable and has the monotonicity perserving property with fairly good accuracy, when the boundary conditions at volatility are estimated by Neumann conditions.

STOCHASTIC VOLATILITY WITH LÉVY PROCESSES: CALIBRATION AND PRICING

by

Xianfang Wu

Dissertation submitted to the Faculty of the Graduate School of the
University of Maryland, College Park in partial fulfillment
of the requirements for the degree of
Doctor of Philosophy
2005

Advisory Committee:

Professor Dilip B. Madan, Chair/Advisor
Professor Michael Fu
Professor C. David Levermore
Associate Professor Konstantina Trivisa
Professor Victor M. Yakovenko

DEDICATION

To my parents

and

in memory of

an infant child who died

five days after his birth

ACKNOWLEDGMENTS

Immanuel Kant says, *Sapere Aude* (dare to know)! This thesis is a manifestation of the sentence I have learned through my graduate experience that I will cherish forever. I owe my gratitude to all the people who have inspired me to establish such a determinant and passionate attitude toward the unknown world that challenges us in every corner of life.

I'd like to thank my advisor Professor Dilip B. Madan for giving me such an invaluable opportunity to work on computational finance. His insight and encouragement has always helped me get through the difficult problems that I dealt with. Thanks are also due to Dr. Peter Carr in Bloomberg L.P. for the inspiring and challenging project, which has pushed me to a new level I never knew I could achieve.

I would also like to convey my special thanks to Professor James A. Yorke who opened to me the United States, a world of love, of the brave, and of the free six years ago. Without him, my whole journey in the new world would have been a distant dream. His kindness, forbearance, and wisdom influence me profoundly on shaping my passionate and open philosophy toward freedom, which we cherish and defend unwieldly.

I owe my deepest thanks to my parents who have always stood by me with their endless love. They are the origin where my perseverance and curiosity come,

which are the key to my success to reach my every dream, never waivering even while I am in the toughest time of my life. Words cannot express the gratitude I owe them. I also thank my brother with his consistent support and encouragement that make me reach a stage far beyond my expectation from my humble beginning.

I thank Professor Michael Fu, Professor C. David Levermore, Associate Professor Konstantina Trivisa, Professor Victor M. Yakovenko for agreeing to serve on my thesis committee and for sparing their time reviewing the manuscript, and thank Professor Tobias von Petersdorff for discussions on the research topic.

I would also like to acknowledge help and support from Shuigen Xiao, Alverda McCoy. And I thank Forest Williams and Paul Higgins for providing free editing services for my dissertation. And I also thank Google Inc. for providing such a superb searching facility which has greatly enhanced my capability to obtain knowledge which I have long been thirsty for. Thanks also go to the illustrious who live or lived decades and centuries ago for the great works and thoughts which inspire me to establish my faith and vision on this step of a long journey exploring the challenging, yet beautiful world.

TABLE OF CONTENTS

LIST OF TABLES

LIST OF FIGURES

Chapter 1

Introduction

The main purpose of the thesis is to deal with stochastic volatility models using Lévy processes. Throughout the thesis, Lévy processes play a central role. For detailed treatments on Lévy processes see [Sat99, Ber96, JS03] and recently [App04]. Fundamental concepts on continuous martingales and stochastic calculus can be found in [KS97, RY99].

1.1 Stochastic Volatility Models

In the original Black-Scholes-Merton option pricing model ([BS73], [Mer73]), the price of an underlying asset S_t follows

$$dS_t = rS_t dt + \sigma S_t dB_t$$

under the risk neutral measure, where r is the interest rate, B_t is the standard Brownian motion and σ denotes the volatility which is constant across time t.

However, the constant volatility assumption contradicts the options data from the market. The daily set of the options data, which is composed by options with different strikes and maturities, results in a smile surface rather than flat, when converted to the volatility by the Black Scholes formula.

This contradiction indicates that the constant volatility asumption is not appropriate and there are different approches to circumvent this contradiction. One

is to model asset returns as processes with jumps, for example, [Mer76], [MCC98], [BN97], [Kou02]. Another approach is to assume that the volatility is not constant over time t. It includes the local volatility model and stochastic volatility models. The local volatility model proposed by [Dup94] assumes that the volatility is a deterministic function of the time t. Under this assumption, the market is still complete as in the Black Scholes case, and the derivative's risk can be perfectly hedged by the underlying asset without need to estimate the volatility risk premium.

Stochastic volatility models assume that the volatility is stochastic across time t and this is the assumption we take in the dissertation. The origin of the stochastic volatilty models goes back to as early as 1982 in Engle's ARCH model [Eng82] where the conditional variance is modeled in a discrete setting by

$$v_t|I_{t-1} \sim N(0, h_t),$$

$$h_t = \alpha_0 + \alpha_1 v_{t-1}^2,$$

where I_{t-1} denotes information set up to time $t-1$ and $N(0, h_t)$ denotes the normal distribution with mean 0 and variance h_t. In continuous time setting the volatility can be modeled as a mean reverting process, for example, Cox-Ingersoll-Ross (CIR) process [CIR85]

$$dv_t = \kappa(\theta - v_t)dt + \beta\sqrt{v_t}dB_t,$$

where κ denotes the rate of mean reversion, θ denotes the long term mean and β denotes the volatility of the process.

Stochastic volatility models have been widely accepted since it explains the empirical phenomena of volatility clustering and volatility persistence. The stochas-

tic volatility model also explains the volatility smile and its performance in option pricing is improved, compared with the Black Scholes model.

However, the daily return distribution is non-Gaussian. It has skewness, excess kurtosis and fat-tail. Thus stochastic volatility is naturally extended to Lévy processes since the study of a Lévy process can be carried out by study its characteristic function.

A Lévy process X_t is described by the Lévy-Khintchine formula in terms of its characteristic function

$$\phi_x(u) = E[e^{iuX_t}] = e^{-t\psi_x(u)}.$$

The characteristic exponent $\psi_x(u)$ is given by

$$\psi_x(u) = -iu\mu + \frac{1}{2}u^2\sigma^2 + \int (1 - e^{iux} + iux1_{|x|<1})\nu(dx),$$

where $\nu(dx)$ is the Lévy measure. An example of Lévy process is when $\nu(dx) = k(x)dx$, where

$$k(x) = \begin{cases} \lambda\frac{e^{-G|x|}}{|x|^{1+\alpha}}, & x < 0; \\ \lambda\frac{e^{-M|x|}}{|x|^{1+\alpha}}, & x > 0. \end{cases}$$

with $\alpha < 2$, which is known as CGMY process.

1.2 Models of Interest

In the current literature of stochastic volatility models, four classes of models are in the scope of interest where the underlying is modeled by a continuous Brownian motion or a Lévy process, and the volatility process is modeled by a mean reverting process driven by a continuous Brownian motion or a Lévy process.

There are two equivalent approaches in modeling these stochastic volatility models. One approach is to model asset returns as diffusions with stochastic volatility follows a Brownian driven mean reverting process (eg. Hull and White [HW87], Heston [Hes93]) or by an Ornstein-Uhlenbeck (OU) process driven by a one-sided pure jump Lévy process, termed Background Driving Lévy Process (BDLP) originated from a series of papers of Barndorff-Nielsen, Shephard and their co-workers ([BNS02], [BNNS02], see also [Sch03]). One example is the Heston model,

$$dS_t = rS_t dt + \sqrt{v_t} S_t dB_t^{(1)},$$

$$dv_t = \kappa(\theta - v_t)dt + \beta\sqrt{v_t} dB_t^{(2)},$$

where $B_t^{(1)}$ and $B_t^{(2)}$ are two Brownian motions with $dB_t^{(1)} dB_t^{(2)} = \rho dt$.

Another approach, proposed by Carr, Geman, Madan, and Yor [GMY01, CGMY03], constructs the stochastic volatility Lévy processes by evaluating Lévy processes subordinated to the integral of a mean reverting process, for example, Cox-Ingersoll-Ross (CIR) process or Ornstein-Uhlenbeck (OU) process. The approach is based on the Brownian scaling property which relates changes in scale to changes in time. Thus random changes in volatility can be represented by a random clock in time. Consider the instantaneous rate of time change process,

$$dv_t = \kappa(\theta - v_t)dt + \beta\sqrt{v_t} dB_t, \tag{1.1}$$

the new clock is given by its integral

$$Y(t) = \int_0^t v(s)ds.$$

Assuming $\{X(t); t \geq 0\}$ is a Lévy process independent of $\{Y(t); t \geq 0\}$, the stochastic volatility Lévy process is obtained by subordinating $X(t)$ to $Y(t)$

$$Z(t) = X(Y(t)),\ t \geq 0, \tag{1.2}$$

which can be written as

$$Z(t) = Z(0) + \int_0^t \int_{-\infty}^{\infty} xv(s)k(x)dsdx + \int_0^t \int_{-\infty}^{\infty} x(\mu(dx, ds) - v(s)k(x)dsdx), \tag{1.3}$$

where $k(x)$ denotes Lévy density and μ is the integer valued random measure. The characteristic function of $Z(t)$ is obtained by

$$E[e^{iuZ_t}] = e^{t\Psi(\log \phi(u))}, \tag{1.4}$$

where Ψ and ϕ are the characteristic functions of $X(t)$ and $Y(1)$, respectively.

It is known that Ψ is given by

$$E[e^{iuY(t)}] = \Psi(u, t, v(0); \kappa, \theta, \beta) = A(t, u) \exp(v(0)B(t, u)), \tag{1.5}$$

where

$$A(t, u) = \frac{\exp(\frac{\kappa^2 \theta t}{\beta^2})}{\left(\cosh(\frac{\gamma t}{2}) + \frac{\kappa}{\gamma} \sinh(\frac{\gamma t}{2})\right)^{\frac{2\kappa\theta}{\beta^2}}},$$

$$B(t, u) = \frac{2iu}{\kappa + \gamma \coth(\frac{\gamma t}{2})},$$

$$\gamma = \sqrt{\kappa^2 - 2\beta^2 iu}\ .$$

And ϕ is dependent on the density of the Lévy process.

Combining the two approaches the stochastic volatility models can be roughly classified into four categories with respect to the underlying stock price and volatility process:

i) Brownian underlying and Brownian volatility;

ii) Brownian underlying and Lévy volatility;

iii) Lévy underlying and Brownian volatility;

iv) Lévy underlying and Lévy volatility.

For each category the models we consider are

i) Heston model (and we also put Bates model here);

ii) Barndorff-Nielsen-Shephard (BNS) models;

iii) VGSA, NISGA, CGMYSA, VGSAM, NIGSAM, CGMYSAM (see [CGMY03]);

iv) VGIG, VGSG, VGSIG, NIGIG, NIGSG, NIGSIG (see [CGMY03]).

The detailed description of these models and their characteristic functions can be found in Appendix A.

Chapter 2

Standard Errors for Financial Market Data Analysis

2.1 Introduction

This chapter calibrates different models where the underlying log stock price or volatility driven by either a Brownian motion or a Lévy process on Standard & Poor's (S&P) 500 data. Furthermore, a new method to estimate the standard errors, which can be seen as a generalization of the traditional error estimation method, is proposed.

First, we re-state the reasoning on the proposed method for the standard error estimation which first appeared in [MW03].

Suppose we minimize a criterion $C(\boldsymbol{\theta})$ and estimate a vector $\boldsymbol{\theta}$. The first condition solved by our estimate $\boldsymbol{\theta}_0$ is

$$C_{\boldsymbol{\theta}}(\boldsymbol{\theta}_0) = \mathbf{0}.$$

Now consider the possibility that we in fact employed the wrong criterion and that the correct criterion was locally in the neighborhood of $\boldsymbol{\theta}_0$ actually of the form

$$\tilde{C} = C(\boldsymbol{\theta}) - \mathbf{a}^T(\boldsymbol{\theta} - \boldsymbol{\theta}_0).$$

The equation we should have been solving then is

$$C_{\boldsymbol{\theta}}(\boldsymbol{\theta}) = \mathbf{a}.$$

Suppose this solution is $\tilde{\boldsymbol{\theta}}$, so that

$$C_{\boldsymbol{\theta}}(\tilde{\boldsymbol{\theta}}) = \mathbf{a}.$$

We may now write

$$C_{\boldsymbol{\theta}}(\boldsymbol{\theta}_0) = C_{\boldsymbol{\theta}}(\tilde{\boldsymbol{\theta}}) + C_{\boldsymbol{\theta}\boldsymbol{\theta}'}(\bar{\boldsymbol{\theta}})(\boldsymbol{\theta}_0 - \tilde{\boldsymbol{\theta}})$$

for some $\bar{\boldsymbol{\theta}}$ on the line segment between $\boldsymbol{\theta}_0$ and $\tilde{\boldsymbol{\theta}}$. It follows that our error may be expressed as

$$\begin{aligned} \boldsymbol{\theta}_0 - \tilde{\boldsymbol{\theta}} &= -[C_{\boldsymbol{\theta}\boldsymbol{\theta}'}(\bar{\boldsymbol{\theta}})]^{-1} C_{\boldsymbol{\theta}}(\tilde{\boldsymbol{\theta}}) \\ &= -[C_{\boldsymbol{\theta}\boldsymbol{\theta}'}(\bar{\boldsymbol{\theta}})]^{-1}\mathbf{a}. \end{aligned}$$

If we contemplate a possible error in each direction of a magnitude proportional to the level of the criterion then our candidate for the potential vectors $\mathbf{a}$ are given by the columns of the matrix $C(\boldsymbol{\theta}_0)C_{\boldsymbol{\theta}}(\boldsymbol{\theta}_0)$ and our estimate of the impact on our parameter estimates is

$$\boldsymbol{\theta}_0 - \tilde{\boldsymbol{\theta}} = C(\boldsymbol{\theta}_0)[C_{\boldsymbol{\theta}\boldsymbol{\theta}'}(\boldsymbol{\theta}_0)]^{-1} C_{\boldsymbol{\theta}}(\boldsymbol{\theta}_0).$$

We therefore see the computation

$$\boldsymbol{\Sigma} = C(\boldsymbol{\theta}_0)[C_{\boldsymbol{\theta}\boldsymbol{\theta}'}(\boldsymbol{\theta}_0)]^{-1} \tag{2.1}$$

as a general error estimate addressing the impact on all parameters of a local misspecification of the criterion. Basically, if we got the criterion slopes wrong by the amount $C(\boldsymbol{\theta}_0)$ in the direction of the i^{th} parameter then the i^{th} column of $\boldsymbol{\Sigma}$ estimates the effect on the estimates.

We note further that $\mathbf{\Sigma}$ should be a positive definite matrix in general as it is the matrix of second order derivatives of a function computed at its minimum. We have here interpreted $\mathbf{\Sigma}$ in a very general setting in which we have not said what our criterion is or what the underlying model or data for the estimation are. We briefly relate this computation to standard error calculations in statistical estimation in the context of least squares, maximum likelihood and nonlinear least squares. We then consider its application in the context of estimating option pricing models where the standard assumptions of statistical estimation are problematic.

2.2 Relationship to Statistical Standard Error Calculations

Consider first the case of linear models estimated by least squares. The model formulation here is

$$\mathbf{y} = \mathbf{X}\boldsymbol{\beta} + \boldsymbol{\varepsilon},$$

where we suppose that $\boldsymbol{\varepsilon}$ is a zero mean finite variance random vector with identically distributed components that are independent of the explanatory variables $\mathbf{X}$. The least squares criterion is given by

$$C(\boldsymbol{\beta}) = \frac{(\mathbf{y} - \mathbf{X}\boldsymbol{\beta})^T(\mathbf{y} - \mathbf{X}\boldsymbol{\beta})}{N},$$

where N denotes the sample size. The least squares estimators have an asymptotic covariance matrix in this context given by

$$\mathbf{\Sigma}_{LS} = \hat{\sigma}^2(\mathbf{X}^T\mathbf{X})^{-1}.$$

We observe that asymptotically

$$\hat{\sigma}^2 = C(\boldsymbol{\beta}_{LS}),$$

where $\boldsymbol{\beta}_{LS}$ is the least squares estimate of $\boldsymbol{\beta}$. Furthermore we compute that

$$C_{\boldsymbol{\beta}\boldsymbol{\beta}'} = \frac{2}{N}(\mathbf{X}^T\mathbf{X}),$$

and hence that

$$\boldsymbol{\Sigma}_{LS} = \frac{2}{N}C(\boldsymbol{\beta}_{LS})[C_{\boldsymbol{\beta}\boldsymbol{\beta}'}]^{-1}. \tag{2.2}$$

The least squares standard errors are therefore proportional to our proposed error analysis matrix.

2.2.1 The Case of Maximum Likelihood

Suppose we have a set of independent observations of data $x_i, i = 1, ..., N$ and the probability model with parameter $\boldsymbol{\theta}$,

$$f(x_i; \boldsymbol{\theta}).$$

The likelihood of this data is defined by

$$l(\boldsymbol{\theta}) = \prod_{i=1}^{N} f(x_i; \boldsymbol{\theta}).$$

Our criterion for parameter estimation is to maximize this likelihood. This is equivalently done by minimizing the negative of the log likelihood. For the log likelihood we write

$$L(\boldsymbol{\theta}) = \ln(l(\boldsymbol{\theta})).$$

The matrix of standard errors is given by the inverse of the information matrix defined as

$$I(\boldsymbol{\theta}^*) = -E\left[\left.\frac{\partial^2 L}{\partial\boldsymbol{\theta}\partial\boldsymbol{\theta}'}\right|_{\boldsymbol{\theta}^*}\right].$$

We note that at the maximum likelihood estimate $\boldsymbol{\theta}_{ML}$

$$I(\boldsymbol{\theta}_{ML}) = -\frac{1}{l(\boldsymbol{\theta})}\frac{\partial^2 l}{\partial\boldsymbol{\theta}\partial\boldsymbol{\theta}'}.$$

This follows on noting that

$$\begin{aligned} L_{\boldsymbol{\theta}} &= \frac{1}{l(\boldsymbol{\theta})} l_{\boldsymbol{\theta}}, \\ L_{\boldsymbol{\theta}\boldsymbol{\theta}'} &= \frac{1}{l(\boldsymbol{\theta})} l_{\boldsymbol{\theta}\boldsymbol{\theta}'} - \frac{1}{l(\boldsymbol{\theta})^2} l_{\boldsymbol{\theta}} l_{\boldsymbol{\theta}'} \\ &= \frac{1}{l(\boldsymbol{\theta})} l_{\boldsymbol{\theta}\boldsymbol{\theta}'} - L_{\boldsymbol{\theta}} L_{\boldsymbol{\theta}'}. \end{aligned}$$

But at $\boldsymbol{\theta}_{ML}$ we have $L_{\boldsymbol{\theta}}(\boldsymbol{\theta}_{ML}) = \mathbf{0}$.

The inverse of the information matrix is

$$\boldsymbol{\Sigma}_{ML} = l(\boldsymbol{\theta}_{ML})\left[\left.-\frac{\partial^2 l}{\partial\boldsymbol{\theta}\partial\boldsymbol{\theta}'}\right|_{\boldsymbol{\theta}_{ML}}\right]^{-1}. \tag{2.3}$$

Once again we recognize the result as the level of the criterion function, the likelihood, times the inverse of matrix of second order derivatives of the criterion, here negated to get positive definiteness as the criterion is one of maximization as opposed to minimization.

2.2.2 Nonlinear Least Squares

The model for nonlinear least squares estimation is of the form

$$\mathbf{y} = \mathbf{f}(\mathbf{X}, \boldsymbol{\theta}) + \boldsymbol{\varepsilon},$$

where we make assumptions on $\boldsymbol{\varepsilon}$ that are similar to least squares estimation of linear models. The criterion here could be taken as

$$C(\boldsymbol{\theta}) = \frac{(\mathbf{y} - \mathbf{f}(\mathbf{X}, \boldsymbol{\theta}))^T(\mathbf{y} - \mathbf{f}(\mathbf{X}, \boldsymbol{\theta}))}{N}.$$

There are two estimates for the asymptotic covariance matrix of the parameter estimates, $\boldsymbol{\theta}_{NLS}$, that are asymptotically equivalent. The first is based on the approximating linear model and is given by

$$\boldsymbol{\Sigma}^{(1)}_{NLS} = \hat{\sigma}^2[\mathbf{f}_{\boldsymbol{\theta}}(\mathbf{X}, \boldsymbol{\theta}_{NLS})^T\mathbf{f}_{\boldsymbol{\theta}}(\mathbf{X}, \boldsymbol{\theta}_{NLS})]^{-1}, \tag{2.4}$$

while the second is developed in terms of an asymptotic analysis of the nonlinear estimator and is given by

$$\boldsymbol{\Sigma}^{(2)}_{NLS} = \hat{\sigma}^2[C_{\boldsymbol{\theta}\boldsymbol{\theta}'}(\boldsymbol{\theta}_{NLS})]^{-1}[\mathbf{f}_{\boldsymbol{\theta}}(\mathbf{X}, \boldsymbol{\theta}_{NLS})^T\mathbf{f}_{\boldsymbol{\theta}}(\mathbf{X}, \boldsymbol{\theta}_{NLS})][C_{\boldsymbol{\theta}\boldsymbol{\theta}'}(\boldsymbol{\theta}_{NLS})]^{-1}. \tag{2.5}$$

We recognize that

$$\hat{\sigma}^2 = C(\boldsymbol{\theta}_{NLS}).$$

We note further that

$$C_{\boldsymbol{\theta}\boldsymbol{\theta}'} = \frac{2}{N}\mathbf{f}_{\boldsymbol{\theta}}(\mathbf{X}, \boldsymbol{\theta}_{NLS})^T\mathbf{f}_{\boldsymbol{\theta}}(\mathbf{X}, \boldsymbol{\theta}_{NLS}) - \frac{2}{N}\sum_{i=1}^{N}(y_i - f_i(\mathbf{X}, \boldsymbol{\theta}))\frac{\partial^2 f_i}{\partial\boldsymbol{\theta}\partial\boldsymbol{\theta}'}. \tag{2.6}$$

Asymptotically one may show that the second term vanishes and recognizing this asymptotic equivalence we may write for the standard errors

$$\boldsymbol{\Sigma}_{NLS} = \frac{2}{N}C(\boldsymbol{\theta}_{NLS})[C_{\boldsymbol{\theta}\boldsymbol{\theta}'}(\boldsymbol{\theta}_{NLS})]^{-1}. \tag{2.7}$$

In all three contexts of statistical estimation we have seen that one may write the standard errors in terms of the criterion function directly as the inverse of its second

order derivative matrix times the level of the criterion function. In light of the discussion in our introductory section we propose using this formulation as a general recipe for the error analysis of parameter estimates in model estimation. We consider in the next section a situation that arises in estimating option pricing models or risk neutral models on financial market data where the classical assumptions of statistical theory are problematic and not easily reformulated.

2.3 Estimating Risk Neutral Models on Financial Market Data

The best context to focus on in considering these estimation problems is posed by the context of risk neutral estimation of parameters on swap market data. The swap market quote specifies a set of cash flows that may be traded against another set of cash flows for a zero initial cost at the time of the quote. Parameter estimation then specifies a model for the likelihood of paths of the underlying uncertainties such that the expected value of the cash flows is risk neutrally, or under this probability, zero. Our basic model is in the form

$$\mathbf{f}(\mathbf{X}, \boldsymbol{\theta}) = \mathbf{0},$$

where $\mathbf{f}(\mathbf{X}, \boldsymbol{\theta})$ amounts to the risk neutral model expectation, that may be made numerically or analytically. It is difficult to put this model in a classical statistical set up as the left hand side that is observed, is in fact zero. It is strange to contemplate that the value zero is now observed with error. The variance of the so-called left hand side is zero, along with the entire left hand side. The typical criterion for

estimation employed in practice is to choose $\boldsymbol{\theta}$ to minimize

$$C(\boldsymbol{\theta}) = \frac{1}{N}\mathbf{f}(\mathbf{X}, \boldsymbol{\theta})^T \mathbf{f}(X, \boldsymbol{\theta}).$$

This may be done and often we get some very good model calibrations with very little error. We may refer to these estimates as calibrated parameter estimates $\boldsymbol{\theta}_C$ that solve the condition

$$C_{\boldsymbol{\theta}}(\boldsymbol{\theta}_C) = \mathbf{0}.$$

We ask about the construction of $\boldsymbol{\Sigma}_C$ the matrix of standard errors associated with this estimation. We propose on the ground of the above presentation

$$\boldsymbol{\Sigma}_C = \frac{2}{N} C(\boldsymbol{\theta}_C)[C_{\boldsymbol{\theta}\boldsymbol{\theta}'}(\boldsymbol{\theta}_C)]^{-1}. \tag{2.8}$$

2.3.1 Data Set and Calibration Methodology

We use the monthly time series data of S&P call option prices for each second Monday of each month for year 2001 and 2002. The dates employed are *Jan 8, Feb12, Mar12, Apr 9, May 14, Jun 11, Juy 9, Aug 13, Sep 10, Oct 8, Nov 12, Dec 10* for 2001 and *Jan 14, Feb11, Mar 11, Apr 8, May 13, Jun 10, Jul 8, Aug 12, Sep 9, Oct 14, Nov11, Dec 9* for 2002. For each model described in Chapter 1 we use the uniform procedure of fast Fourier transform (FFT) for constructing the option prices developed by Carr and Madan [CM98]. More precisely, the price of a European call price with strike K and maturity T is:

$$P(K,T) = \frac{\mathrm{e}^{-\alpha \log(K)}}{2\pi} \int_{-\infty}^{+\infty} \mathrm{e}^{-iu\log(K)} \gamma(u,T) du, \tag{2.9}$$

where

$$\gamma(u,T) = \frac{\mathrm{e}^{-rT}\phi(u-(\alpha+1)i)}{\alpha^2+\alpha-u^2+i(2\alpha+1)u},$$

with $\phi(u)$ as the characteristic funtion for the log of the stock price. The model parameters are estimated by minimizing the root mean sqare error between market prices and model prices over all strikes and maturities. As a measure of fit, we compute the absolute percentage error (APE)

$$APE = \frac{\sum_{i=1}^{N} |P_i - \tilde{P}_i|}{\sum_{i=1}^{N} P_i} ,$$

where $P_i, \tilde{P}_i, i = 1, ..., N$ are the market prices and model prices of daily options panel.

2.3.2 Results of Parameter Estimations

The estimated parameters and the absolute percentage errors are presented in tables in Appendix C. As we can see, the estimated values of each parameter varies only in a certain range, while keeping stable in some sense when the panel of option data ranges over a period of two years. Comparisons of the APEs of the models are shown in Figure 1, Figure 2 and Figure 3. We can see that Heston (and Bates), SA and SG-class (except BNSSG) models have close absolute percentage errors and have a better performance than the other models: BNS, SAM, IG, and SIG-class models.

2.3.3 Standard Errors for Parameter Estimations

A major concern raised on the estimated parameters is how sure their values can be used in pricing other derivatives, since the estimated values are only the estimation of some local minimum based on certain criteria to stop the estimating procedure. Moreover, in order to study the stability property of parameters of the pricing models

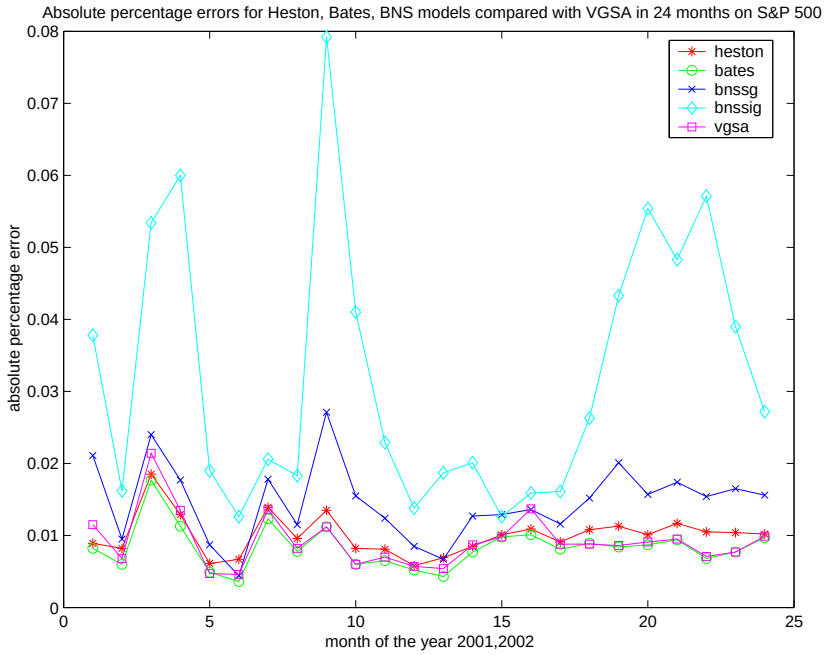

Figure 2.1: Absolute percentage errors for Heston, Bates, BNS-class models compared with VGSA on S&P 500 monthly second Monday data

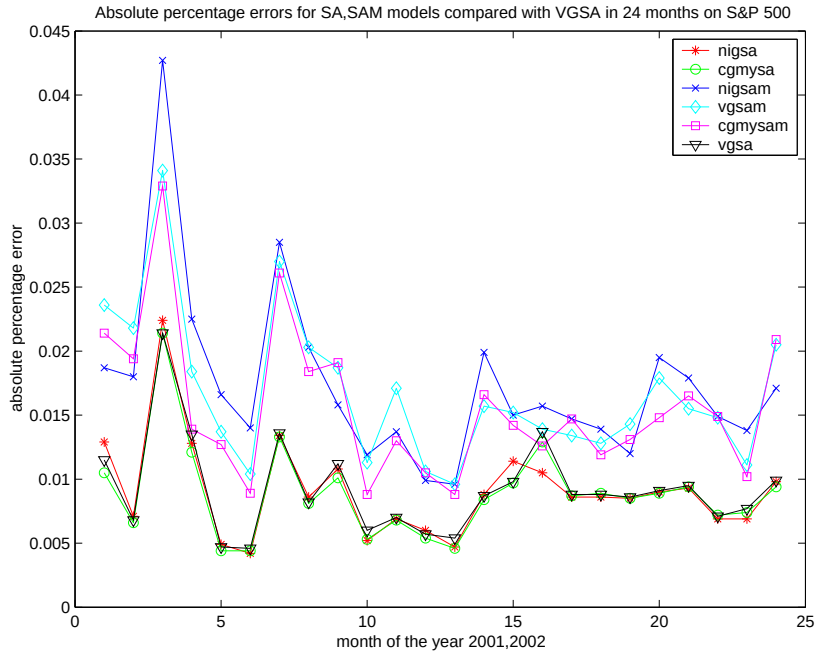

Figure 2.2: Absolute percentage errors for SA, SAM-class models compared with VGSA on S&P 500 monthly second Monday data

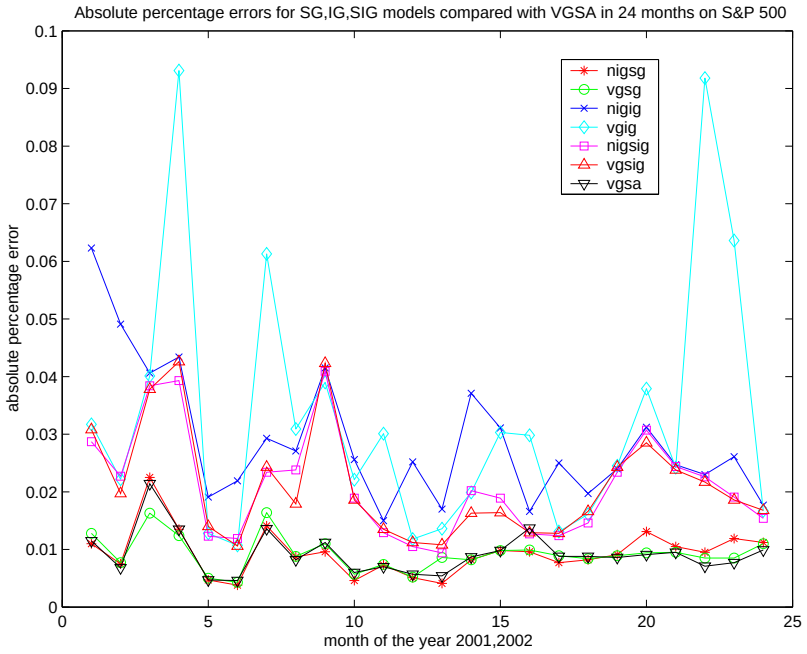

Figure 2.3: Absolute percentage errors for SG, IG, SIG-class models compared with VGSA on S&P 500 monthly second Monday data

over calendar time, one has to distinguish the drift of the estimated parameters over calendar time and the errors incurred by the model and the estimating procedure. In the rest of this chapter we are going to investigate the errors for parameter estimations and leave the dynamics of estimated parameters over calendar time to the next chapter.

As a traditional way, assuming the option pricing model $\mathbf{P}(\boldsymbol{\theta})$ and model price $\mathbf{P}(\boldsymbol{\theta}_0)$ with parameter estimation $\boldsymbol{\theta}_0$, we have

$$\mathbf{P}(\boldsymbol{\theta}) = \mathbf{P}(\boldsymbol{\theta}_0) + \left.\frac{\partial \mathbf{P}}{\partial \boldsymbol{\theta}}\right|_{\boldsymbol{\theta}_0} (\boldsymbol{\theta} - \boldsymbol{\theta}_0) + \boldsymbol{\varepsilon}.$$

Let $\left.\frac{\partial \mathbf{P}}{\partial \boldsymbol{\theta}}\right|_{\boldsymbol{\theta}_0} = \mathbf{A}$, $\boldsymbol{\theta} - \boldsymbol{\theta}_0 = \boldsymbol{\beta}$, $\mathbf{P}(\boldsymbol{\theta}) - \mathbf{P}(\boldsymbol{\theta}_0) = \mathbf{y}$, we have

$$\mathbf{y} = \mathbf{A}\boldsymbol{\beta} + \boldsymbol{\varepsilon},$$

and

$$\mathbf{A}^T\mathbf{A}\boldsymbol{\beta} = \mathbf{A}^T\mathbf{y}.$$

Since $\mathbf{A}$ may not be a full-rank matrix, we make the singular value decomposition (SVD) on $\mathbf{A}$:

$$\mathbf{A}_{m\times n} = \mathbf{U}\mathbf{D}\mathbf{V}^T = \mathbf{U}_{m\times n}\mathbf{D}_{n\times n}\mathbf{V}^T_{n\times n},\ m > n.$$

Thus we have

$$\mathbf{V}\mathbf{D}\mathbf{U}^T\mathbf{U}\mathbf{D}\mathbf{V}^T\boldsymbol{\beta} = \mathbf{V}\mathbf{D}\mathbf{U}^T\mathbf{y}.$$

Let $\mathbf{V} = (\mathbf{V}_1\ \ \mathbf{V}_2)$, and $\mathbf{D} = \mathrm{diag}(\mathbf{D}_1\ \ \mathbf{0})$ where $\mathbf{D}_1$ is a full-rank diagonal matrix, we have

$$\begin{pmatrix} \mathbf{V}_1 & \mathbf{V}_2 \end{pmatrix} \begin{pmatrix} \mathbf{D}_1^2 & \mathbf{0} \\ \mathbf{0} & \mathbf{0} \end{pmatrix} \begin{pmatrix} \mathbf{V}_1^T \\ \mathbf{V}_2^T \end{pmatrix} \boldsymbol{\beta} = \mathbf{V}\mathbf{D}\mathbf{U}^T\mathbf{y},$$

that is,

$$\mathbf{V}_1\mathbf{D}_1^2\mathbf{V}_1^T\boldsymbol{\beta} = \mathbf{V}\mathbf{D}\mathbf{U}^T\mathbf{y}.$$

So

$$\begin{aligned}
\mathbf{V}_1^T\boldsymbol{\beta} &= \mathbf{D}_1^{-2}\mathbf{V}_1^T\mathbf{V}\mathbf{D}\mathbf{U}^T\mathbf{y} \\
&= \mathbf{D}_1^{-2}\mathbf{V}_1^T \begin{pmatrix} \mathbf{V}_1 & \mathbf{V}_2 \end{pmatrix} \begin{pmatrix} \mathbf{D}_1 & \mathbf{0} \\ \mathbf{0} & \mathbf{0} \end{pmatrix} \mathbf{U}^T\mathbf{y} \\
&= \begin{pmatrix} \mathbf{D}_1^{-1} & \mathbf{0} \end{pmatrix} \begin{pmatrix} \mathbf{U}_1^T \\ \mathbf{U}_2^T \end{pmatrix} \mathbf{y} \\
&= \mathbf{D}_1^{-1}\mathbf{U}_1^T\mathbf{y},
\end{aligned}$$

where $\mathbf{U} = (\mathbf{U}_1\ \ \mathbf{U}_2)$. Assuming $\mathrm{var}(\boldsymbol{\varepsilon}) = \sigma^2\mathbf{I}$, we have

$$\mathrm{var}(\mathbf{V}_1^T\boldsymbol{\beta}) = \mathbf{D}_1^{-1}\mathbf{U}_1^T\sigma^2\mathbf{U}_1\mathbf{D}_1^{-1}$$

$$= \sigma^2 \mathbf{D}_1^{-2},$$

and

$$\begin{aligned} \mathrm{var}(\boldsymbol{\beta}) &= \sigma^2 \mathbf{V}_1 \mathbf{D}_1^{-2} \mathbf{V}_1^T \\ &= \sigma^2 \sum_{i=1}^{k} d_i^{-2} \mathbf{v}_i \mathbf{v}_i^T, \end{aligned}$$

with $\mathbf{V}_1 = (\mathbf{v}_1, ..., \mathbf{v}_k)$, and $\mathbf{D}_1 = \mathrm{diag}(d_1, ..., d_k)$. In this approach, the matrix $\mathbf{P}_{\boldsymbol{\theta}}^T(\boldsymbol{\theta}_0)\mathbf{P}_{\boldsymbol{\theta}}(\boldsymbol{\theta}_0)$ is always positive definite (or semi-definite). Thus the standard errors for the estimated parameters can be obtained by the singular value decomposition or the Moore-Penrose pseudoinverse of the matrix.

As stated in the previous section, the proposed method of the standard error estimation

$$\boldsymbol{\Sigma} = \frac{2}{N} C(\boldsymbol{\theta}_0)[C_{\boldsymbol{\theta}\boldsymbol{\theta}'}(\boldsymbol{\theta}_0)]^{-1} \tag{2.10}$$

is asymptotically equivalent to the traditional method and the difference is that the positive definite (semi-definite) matrix $\mathbf{P}_{\boldsymbol{\theta}}^T(\boldsymbol{\theta}_0)\mathbf{P}_{\boldsymbol{\theta}}(\boldsymbol{\theta}_0)$ is replaced by

$$C_{\boldsymbol{\theta}\boldsymbol{\theta}'} = \frac{2}{N}\mathbf{P}_{\boldsymbol{\theta}}^T(\boldsymbol{\theta}_0)\mathbf{P}_{\boldsymbol{\theta}}(\boldsymbol{\theta}_0) - \frac{2}{N}\sum_{i=1}^{N}(\tilde{P}_i - P_i(\boldsymbol{\theta}_0))\frac{\partial^2 P_i}{\partial\boldsymbol{\theta}\partial\boldsymbol{\theta}'}. \tag{2.11}$$

The $C_{\boldsymbol{\theta}\boldsymbol{\theta}'}$ is not necessarily a positive definite (semi-definite) matrix and care must be taken when we make the inverse of it.

2.3.4 Numerical Implementations

To compute $\frac{\partial \mathbf{P}}{\partial \boldsymbol{\theta}}(\boldsymbol{\theta}_0)$ and $\frac{\partial^2 \mathbf{P}}{\partial \boldsymbol{\theta}\partial\boldsymbol{\theta}'}(\boldsymbol{\theta}_0)$, we use the option prices computed at specific parameters by fast Fourier transform [CM98] as stated in the previous section and approximate the derivatives by the center difference scheme. Of the sixteen models

described in Chapter 1, we computed the standard error matrices of fourteen models and disregard the CGMYSA and CGMYSAM model. The last two models are extensions of the VGSA and VGSAM model with similar absolute percentage errors but have a set of nine paramters which is much larger than the other ones. Therefore this costs much more computing time since the approximate computing time is proportional to the square of the number of parameters.

Of the fourteen models, all the standard error matrices have large condition numbers but are different on the eigenvalues of the matrices of $\frac{\partial^2 \mathbf{P}}{\partial \boldsymbol{\theta} \partial \boldsymbol{\theta}'}(\boldsymbol{\theta}_0)$. Four models, Heston, BNSSG, NIGSA, VGSA have all positive eigenvalues, which mean they keep the property of positive definiteness. The other five models, Bates, NIGSG, VGSG, NIGSIG, VGSIG have some occasions that the matrices have small negative eigenvalues. Thus the property of positive definiteness no longer hold in these cases. The rest five models BNSSIG, NIGIG, VGIG, NIGSAM, VGSAM often have very large negative eigenvalues in their matrices and thus make the results meanless.

To compute the standard error matrices of the nine models, we set some reasonable tolerance value to make sure that the computed Moore-Penrose pseudoinverses still keep the property of positive definiteness. This is achieved by zeroing the absolute values of the small eigenvalues which are less than the tolerance value. Denote $\|M\|$ the norm of a standard error matrix, we set the tolerance value to $10^{-14} * \|M\|$ for Heston, BNSSG, NIGSA, VGSA and the other five models to $10^{-4} * \|M\|$ to $10^{-7} * \|M\|$ based on the negative eigenvalues of the matrices. Compared with the default tolerance value $10^{-16} * \|M\|$, the computed standard errors of these five models still have plenty of information lost and thus we only put the results of four

Jan	33.62	2366.07	48556.00	3710252.65	45545913.55
Feb	13.21	1617.52	45033.59	5947043.19	50153362.67
Mar	39.93	1473.10	30127.74	2591448.43	26687521.66
Apr	7.69	535.09	29699.21	948801.54	37255706.86
May	9.68	1096.96	29370.95	3619145.78	42359170.78
Jun	2.62	936.68	20377.04	2383137.51	43218510.46
Jul*	-1.78	37.67	39832.32	4303122.22	56410024.75
Aug	7.21	466.49	26759.77	3936912.51	47628980.69
Sep	14.86	651.52	20989.70	1373814.77	28168819.67
Oct	10.67	682.19	24569.83	945541.42	34655200.53
Nov	13.30	692.01	24430.69	1945525.57	32444198.28
Dec	4.15	625.08	17924.50	1947885.43	34205704.20

Table 2.1: Eigenvalues of infomation matrix for Heston model on S&P 500 monthly second Monday data in 2001 with proposed method

models, Heston, BNSSG, NIGSA, VGSA in Appendix D.

We show that our proposed method has the similar results of standard errors compared with the traditional method. Furthermore, the results show that in all the parameters of each model, some parameters are better identified, in other words, they have smaller standard errors than the other ones. For example, in the VGSA model, the first three parameters C, G, M are better identified than the last three ones κ, η, λ.

Chapter 3

Stability on Calibration of Stochastic Volatility Models

3.1 Introduction

The estimation of parameters under risk neutral measure is the first step to price various options. The previous chapter has shown a way to estimate the parameters of the stochastic volatility models with explicit characteristic functions from the panel of the daily options data and it yields directly the parameters of the required risk neutral measure. However, this approach does not produce a stable set of parameters that can be used consistently and with confidence over time, although the numerical evidence shows that some of the calibrated parameters have small variances which indicate that they are well-identified and fairly stable over time.

In practice, obtaining stability over time of calibrated parameters is crucial for pricing path-dependent volatility-dependent options and for hedging. The issue of stability has led to the interest of term structure of implied volatility surfaces.

Recall that a local volatility model assumes the volatility is a function of the static local volatility surface and the dynamics of the underlying $\sigma_t = \sigma(S_t, t)$, where S_t follows

$$dS_t = rS_t dt + \sigma(S_t, t)S_t dB_t.$$

The function $\sigma(S_t, t)$ can be determined from the panel of daily European call op-

tions $C(K,T)$ by

$$\frac{\partial C}{\partial T}(K,T) + rK\frac{\partial C}{\partial K}(K,T) - \frac{1}{2}\sigma^2(K,T)K^2\frac{\partial^2 C}{\partial K^2}(K,T) = 0. \tag{3.1}$$

A generalization of the local volatility can be viewed as the risk neutral expectation of the future squared stochastic valitility of a continous martingale M_t with quadratic variation $\langle M\rangle_t = \sigma_t^2 t$,

$$\sigma^2(K,T) = E^Q(\sigma_T^2 | M_t = K), \tag{3.2}$$

where Q is the risk neutral measure [Kle02].

Stability of parameters over time has drawn attention on multifactor volatility models where volatility are driven by two processes, one fluctuating on a fast time-scale, and the other fluctuating on a slowly varying process. These models have been extensively used in the bond pricing literature. Bates ([Bat96], [Bat00]) proposes a two-factor geometric jump-diffusion model and develops a nonlinear generalized least squares/Kalman filtration method for estimating parameters from a series of options data with restrictions on the dynamics of the volatility process. The results indicate that two-factor models performs well over one-factor models in capturing the term structures of implied volatilities over time.

Fouque, Papanicolaou, and Sircar [FPS00] propose an approach which approximately fits the volatility surface to a straight line in a composite variable based on a multiscale volatility model under risk neutral measure,

$$dS_t = rS_t dt + f(v_t^{(1)}, v_t^{(2)})S_t dB_t^{(0)},$$

$$dv_t^{(1)} = \frac{1}{\varepsilon}(\theta(t) - v_t^{(1)})dt + \frac{\beta(t)}{\sqrt{\varepsilon}}dB_t^{(1)},$$

$$dv_t^{(2)} = \delta c(v_t^{(2)})dt + \sqrt{\delta} g(v_t^{(2)})dB_t^{(2)},$$

where $dB_t^{(0)}dB_t^{(1)} = \rho_1(t)dt$ and $dB_t^{(0)}dB_t^{(2)} = \rho_2(t)dt$, and gets fairly good stability properties. Those issues are discussed in detail in [FPSS03], and a simple extension is introduced which improves the performance with parameters over time t. More importantly the variation of the estimated parameters over time is relatively small, indicating that the procedure have good stability properties.

In general, close formulas or characteristic functions of the multiscale stochastic volatility models do not exist and the estimation on the historical options data would need heavy duty of simulations. The [FPS00, FPSS03] approach of approximation is quite straight forward but does not satisfy the non-arbitrage criteria.

This chapter proposes a stabilizing strategy that takes advantage of the viable Carr-Madan FFT approach on calibrating stochastic volatility models with one driving volatility process by increasing the sample of options data to the five days in a row. The results show quite encouraging that the parameters are widely stabilized while the calibration errors remain in a fairly low range.

3.2 Methodology

Since the volatility is another random variable besides the stock price in stochastic volatility models, we modify the previous approach by fixing the model parameters over a short time period, say, five days when calibrating S&P 500 options data, and by making the volatility constrained under the volatility process of the model.

Specifically, assuming the market price is $C(K, T, t)$, and the model price is

$f(\boldsymbol{\theta}, S_t, v_t, K, T, t)$, $t = 1, 2, ..., N$ with paramter vector $\boldsymbol{\theta}$, which we should distinguish from the scalar θ in the CIR process, we wish to choose $\boldsymbol{\theta}^*$ and $v_t^*, t = 1, ..., N$ satisfying

$$(\boldsymbol{\theta}^*, \{v_t^*\}_{t=1,...,N}) = \arg\min_{\boldsymbol{\theta}, v_t} \sum_{K,T,t} D^2(\boldsymbol{\theta}, S_t, v_t, K, T, t) - \sum_{t=1}^{N-1} P(\boldsymbol{\theta}, v_{t+1}|v_t), \qquad (3.3)$$

where

$$D(\boldsymbol{\theta}, S_t, v_t, K, T, t) = C(K, T, t) - f(\boldsymbol{\theta}, S_t, v_t, K, T, t),$$

and $P(\boldsymbol{\theta}, v_{t+1}|v_t)$ is the conditional probability of the volatility $\{v_t, t = 1, ..., N\}$ following the stochastic volatility model.

Of the above two approaches on constructing the stochastic volatility Lévy processes, we consider the Heston and Bates model for the first approach, while for the second approach we consider the VGSA and NIGSA model.

The transition probability $P(\boldsymbol{\theta}, v_{t+1}|v_t)$ of the first approach is quite straight forward and it is the transition probability of the CIR model (1.1) given by (see [CIR85], and also [Fel51]),

$$P(v(s), s; v(t), t) = c\ e^{-u-v} \left(\frac{v}{u}\right)^{q/2} I_q(2(uv)^{1/2}), \qquad (3.4)$$

where $u = cv(t)e^{-\kappa(s-t)}$, $v = cv(s)$, $q = \frac{2\kappa\theta}{\beta^2} - 1$, with

$$c = \frac{2\kappa}{\beta^2(1 - e^{-\kappa(s-t)})},$$

and $I_q(\cdot)$ is the modified Bessel function of the first kind of order q.

The transition probability $P(\boldsymbol{\theta}, v_{t+1}|v_t)$ of the second approach is a little tricky. From the observation of the factorization of the compensator in Equation (1.3), it

is clear that the constant in the Lévy density, that is σ for the NIG model (A.11) and C for the VG model (A.14), can be absorbed into a scaling of the process $v(t)$. Thus the scaling constant in the Lévy density can be identified with the initial value for the volatility process, which is the CIR process in both cases. The option prices are constructed by the Carr-Madan FFT method (2.9).

3.3 S&P 500 Data and Results

We use the daily time series data of S&P call option prices of five consecutive days including each second Monday of each month for year 2001 and 2002. The results compared with the previous approach are mainly in the following aspects:

1. The APEs do not get much larger and are still in an acceptable threshold.

2. The standard errors of some calibrated parameters are reduced due to the increased sample of options data.

3. More importantly, the calibrating procedure for the parameters are stabilized under the constraint of the volatility process. It is more likely that the same calibrated parameters are obtained from different initial guesses.

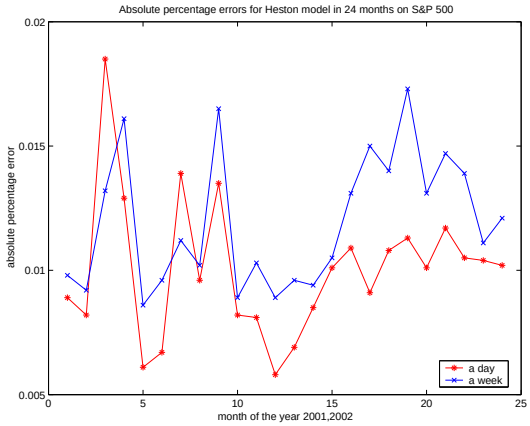

(a) Heston model

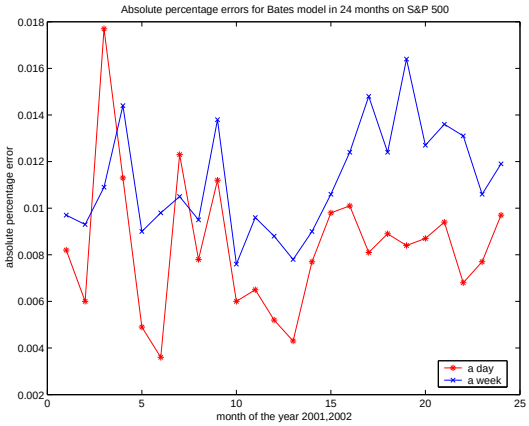

(b) Bates model

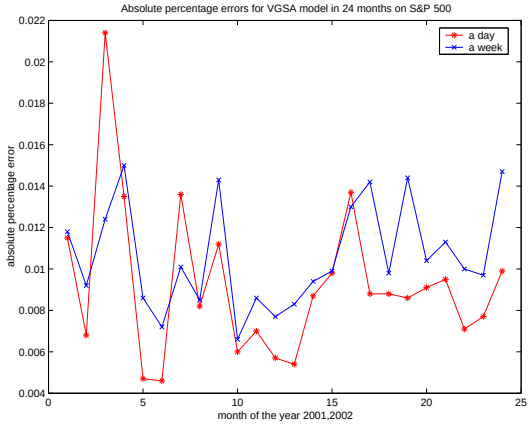

(c) VGSA model

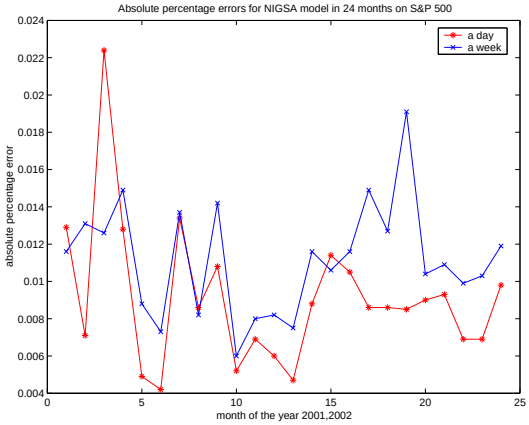

(d) NIGSA model

Figure 3.1: Comparisons of absolute percentage errors on S&P 500 monthly data: second Mondays vs. second weeks

	κ	θ	β	σ_0^2	ρ	ape
x_{init}	1.4175	0.0638	0.4506	0.0681	-0.7268	N/A
x_{opt}	3.8202	0.0497	0.6547	0.0432	-0.6862	0.0067
x_{init}	10.1306	0.0360	0.5781	0.0554	-0.8297	N/A
x_{opt}	6.7113	0.0484	0.9967	0.0453	-0.6731	0.0069
x_{init}	4.7427	0.0462	0.6360	0.0327	-0.7083	N/A
x_{opt}	4.2801	0.0494	0.7084	0.0435	-0.6837	0.0067

Table 3.1: Parameter estimates with different initial guesses for Heston model on S&P 500 on second Monday of June, 2001

	κ	θ	β	ρ	v_1	v_2	v_3	v_4	v_5	ape
x_{init}	1.4175	0.0638	0.4506	-0.7268	0.0681	0.0564	0.0575	0.0493	0.0527	N/A
x_{opt}	2.3789	0.0486	0.4107	-0.7181	0.0358	0.0389	0.0361	0.0385	0.0416	0.0096
x_{init}	10.1306	0.0360	0.5781	-0.8297	0.0681	0.0564	0.0575	0.0493	0.0527	N/A
x_{opt}	2.3790	0.0486	0.4108	-0.7181	0.0358	0.0389	0.0361	0.0385	0.0416	0.0096
x_{init}	4.7427	0.0462	0.6360	-0.7083	0.0327	0.0445	0.0315	0.0389	0.0458	N/A
x_{opt}	2.3790	0.0486	0.4108	-0.7181	0.0358	0.0389	0.0361	0.0385	0.0416	0.0096

Table 3.2: Parameter estimates with different initial guesses for Heston model on S&P 500 on second week of Jun, 2001

2001	κ	θ	β	ρ	v_1	v_2	v_3	v_4	v_5	ape
Jan	1.4175	0.0638	0.4506	-0.7268	0.0681	0.0564	0.0575	0.0493	0.0527	0.0098
Feb	0.8343	0.0637	0.3131	-0.7478	0.0356	0.0399	0.0374	0.0418	0.0388	0.0092
Mar	2.8567	0.0555	0.4799	-0.9040	0.0560	0.0528	0.0490	0.0497	0.0738	0.0132
Apr	2.9768	0.0474	0.3502	-0.9710	0.0934	0.0650	0.0679	0.0632	0.0482	0.0161
May	1.9600	0.0511	0.4092	-0.7154	0.0464	0.0470	0.0506	0.0499	0.0474	0.0086
Jun	2.3789	0.0486	0.4107	-0.7181	0.0358	0.0389	0.0361	0.0385	0.0416	0.0096
Jul	2.0586	0.0420	0.2436	-0.8693	0.0313	0.0396	0.0399	0.0393	0.0402	0.0112
Aug	1.8521	0.0457	0.2916	-0.8201	0.0345	0.0352	0.0361	0.0347	0.0344	0.0102
Sep	4.4529	0.0473	0.4270	-1.0000	0.0490	0.0615	0.0630	0.0740	0.0953	0.0165
Oct	4.9609	0.0539	0.9918	-0.7035	0.1093	0.1098	0.0884	0.0869	0.1187	0.0089
Nov	5.3782	0.0595	1.1175	-0.7082	0.0830	0.0919	0.0919	0.0813	0.0734	0.0103
Dec	2.8475	0.0508	0.4547	-0.7592	0.0493	0.0494	0.0486	0.0451	0.0499	0.0089
2002	κ	θ	β	ρ	v_1	v_2	v_3	v_4	v_5	ape
Jan	5.5026	0.0514	0.8785	-0.7485	0.0475	0.0390	0.0498	0.0587	0.0606	0.0096
Feb	2.4165	0.0475	0.3855	-0.8032	0.0450	0.0460	0.0427	0.0412	0.0358	0.0094
Mar	1.3032	0.0447	0.2378	-0.7993	0.0351	0.0336	0.0337	0.0261	0.0256	0.0105
Apr	5.2608	0.0292	0.1961	-1.0000	0.0280	0.0282	0.0283	0.0287	0.0283	0.0131
May	2.3762	0.0312	0.1261	-1.0000	0.0322	0.0319	0.0369	0.0370	0.0369	0.0150
Jun	7.8406	0.0388	0.3974	-1.0000	0.0482	0.0491	0.0494	0.0667	0.0677	0.0140
Jul	6.1273	0.0386	0.3657	-1.0000	0.0704	0.0919	0.0930	0.0922	0.0890	0.0173
Aug	5.1970	0.0435	0.6498	-0.6449	0.1753	0.1425	0.1255	0.1206	0.1322	0.0131
Sep	3.6347	0.0581	0.7503	-0.7087	0.1126	0.1202	0.1050	0.1349	0.1305	0.0147
Oct	3.4894	0.0673	0.7142	-0.7193	0.1814	0.1901	0.1606	0.1533	0.1427	0.0139
Nov	4.9416	0.0580	0.6199	-0.8078	0.0851	0.0895	0.0889	0.0805	0.1081	0.0111
Dec	2.2775	0.0575	0.2341	-1.0000	0.0724	0.0711	0.0706	0.0709	0.0703	0.0121

Table 3.3: Parameter estimates for Heston model for five consecutive days on S&P 500 monthly second week data

2001	κ	θ	β	ρ
Jan	0.04141	0.00039	0.00849	0.00837
Feb	0.06138	0.00132	0.00927	0.01101
Mar	0.08475	0.00031	0.01502	0.02208
Apr*	0.06109	0.00012	0.00000	0.00000
May	0.09134	0.00026	0.01165	0.01200
Jun	0.17555	0.00042	0.01841	0.01445
Jul	0.10736	0.00022	0.01295	0.03868
Aug	0.09785	0.00033	0.00993	0.01834
Sep	0.10658	0.00025	0.03283	0.06837
Oct	0.07232	0.00021	0.01646	0.00768
Nov	0.13810	0.00027	0.02423	0.00936
Dec	0.17693	0.00027	0.01867	0.01848
2002	κ	θ	β	ρ
Jan	0.34486	0.00021	0.04117	0.01246
Feb	0.10579	0.00025	0.01130	0.01589
Mar	0.08175	0.00059	0.01226	0.02913
Apr	4.12621	0.00031	0.07608	0.16343
May	0.22021	0.00021	0.01126	0.07602
Jun	0.30313	0.00013	0.02511	0.06115
Jul	0.09587	0.00013	0.02799	0.07168
Aug	0.05562	0.00020	0.02120	0.01698
Sep	0.06321	0.00034	0.01838	0.01263
Oct	0.03999	0.00034	0.01446	0.01038
Nov	0.12697	0.00025	0.02375	0.02541
Dec	0.12856	0.00038	0.01530	0.06195

Table 3.4: Standard errors of Heston model for five consecutive days on S&P 500 monthly second week data

2001	κ	θ	β	ρ	λ	μ	δ	v_1	v_2	v_3	v_4	v_5	ape
Jan	1.4400	0.0629	0.4425	-0.7552	0.0232	0.1005	0.1294	0.0678	0.0559	0.0571	0.0488	0.0522	0.0097
Feb	0.8355	0.0613	0.3112	-0.7486	0.0415	-0.1915	0.0528	0.0346	0.0388	0.0364	0.0406	0.0378	0.0093
Mar	1.7948	0.0473	0.4299	-0.7105	0.0509	-0.4240	0.2072	0.0493	0.0470	0.0444	0.0448	0.0630	0.0109
Apr	2.8918	0.0457	0.4141	-0.9246	0.3496	0.0275	0.0992	0.0876	0.0599	0.0612	0.0581	0.0423	0.0144
May	0.4653	0.0310	0.2552	-0.5757	0.4317	-0.1600	0.1182	0.0335	0.0339	0.0354	0.0350	0.0339	0.0090
Jun	0.3358	0.0302	0.1159	-0.8004	0.1186	-0.3481	0.0436	0.0303	0.0307	0.0304	0.0307	0.0311	0.0098
Jul	1.5498	0.0331	0.1892	-1.0000	0.4333	-0.0514	0.1292	0.0261	0.0333	0.0334	0.0331	0.0336	0.0105
Aug	1.4976	0.0357	0.1719	-0.9997	0.0791	-0.2004	0.2734	0.0315	0.0318	0.0322	0.0317	0.0315	0.0095
Sep	3.1947	0.0462	0.5058	-0.8599	0.3583	0.0889	0.0251	0.0468	0.0564	0.0584	0.0670	0.0857	0.0138
Oct	4.5583	0.0378	0.9240	-0.6125	0.1763	-0.2692	0.1107	0.0961	0.0966	0.0773	0.0755	0.1047	0.0076
Nov	4.8821	0.0040	0.1047	-0.9702	0.9023	-0.1656	0.1790	0.0483	0.0478	0.0473	0.0465	0.0458	0.0096
Dec	4.4096	0.0496	0.6421	-0.7544	0	-0.2883	0.7082	0.0557	0.0557	0.0542	0.0444	0.0573	0.0088
2002	κ	θ	β	ρ	λ	μ	δ	v_1	v_2	v_3	v_4	v_5	ape
Jan	1.6370	0.0236	0.1545	-0.7679	0.1415	-0.4172	0.0370	0.0321	0.0318	0.0321	0.0384	0.0383	0.0078
Feb	2.5738	0.0453	0.3318	-1.0000	0.0477	0.1743	0.0427	0.0438	0.0444	0.0421	0.0413	0.0325	0.0090
Mar	0.6018	0.0363	0.1850	-0.6783	0.1671	-0.2220	0.0911	0.0294	0.0283	0.0282	0.0220	0.0216	0.0106
Apr	2.8294	0.0253	0.1210	-1.0000	0.1066	-0.1751	0.0000	0.0275	0.0276	0.0275	0.0277	0.0277	0.0124
May	3.6681	0.0293	0.1537	-1.0000	0.0736	-0.1622	0.0000	0.0294	0.0291	0.0381	0.0381	0.0380	0.0148
Jun	3.0490	0.0369	0.2216	-1.0000	0.0114	0.0425	0.3197	0.0440	0.0446	0.0448	0.0553	0.0557	0.0124
Jul	5.9794	0.0380	0.3791	-1.0000	0.0044	0.3779	0.0002	0.0701	0.0912	0.0925	0.0917	0.0884	0.0164
Aug	5.1949	0.0405	0.5382	-0.8411	0.0335	0.2730	0.0242	0.1736	0.1394	0.1235	0.1194	0.1292	0.0127
Sep	3.7445	0.0197	0.4561	-0.7127	0.5095	-0.1779	0.2033	0.0902	0.0925	0.0835	0.1085	0.1056	0.0136
Oct	3.8050	0.0418	0.4563	-0.9280	0.1824	-0.2189	0.3213	0.1703	0.1760	0.1457	0.1399	0.1319	0.0131
Nov	4.7046	0.0565	0.5462	-0.9096	0.0101	0.2083	0.2989	0.0827	0.0871	0.0868	0.0792	0.1043	0.0106
Dec	1.4061	0.0390	0.1436	-1.0000	0.2472	-0.2357	0.0513	0.0583	0.0577	0.0576	0.0575	0.0573	0.0119

Table 3.5: Parameter estimates for Bates model for five consecutive days on S&P 500 monthly second week data

2001	κ	θ	β	ρ	λ	μ	δ
Jan	0.00172	0.00043	0.00779	0.01109	0.00602	0.00188	0.00323
Feb*	0.00025	0.00061	0.00635	0.01129	0.00000	0.00000	0.00000
Mar	0.00039	0.00076	0.00749	0.00961	0.00242	0.00253	0.00351
Apr	0.00061	0.00052	0.00593	0.00267	0.00122	0.01043	0.00715
May	0.00077	0.00168	0.01117	0.01179	0.01399	0.00296	0.01003
Jun*	0.00000	0.00167	0.00344	0.00000	0.00000	0.00000	0.00000
Jul	0.00022	0.00056	0.00406	0.00042	0.00090	0.00522	0.00269
Aug	0.00009	0.00045	0.00180	0.00040	0.00253	0.00036	0.00107
Sep	0.00047	0.00022	0.00523	0.00307	0.00016	0.00259	0.00172
Oct	0.00055	0.00075	0.00248	0.00708	0.00556	0.00382	0.00337
Nov	0.00001	0.00025	0.00045	0.00005	0.00012	0.00148	0.00201
Dec	0.00030	0.00033	0.00306	0.00354	0.00087	0.00002	0.00001
2002	κ	θ	β	ρ	λ	μ	δ
Jan	0.00010	0.00059	0.00546	0.00168	0.00341	0.00484	0.00212
Feb	0.00024	0.00019	0.00346	0.00096	0.00298	0.00212	0.00083
Mar	0.00055	0.00102	0.00469	0.00323	0.00282	0.00249	0.01023
Apr*	0.00011	0.00066	0.00504	0.00038	0.00587	0.00831	0.00000
May*	0.00022	0.00062	0.00521	0.00063	0.00910	0.01000	0.00000
Jun	0.00013	0.00021	0.00306	0.00068	0.00165	0.00010	0.00016
Jul*	0.00012	0.00016	0.00536	0.00199	0.00100	0.00036	0.00000
Aug	0.00028	0.00026	0.00635	0.00376	0.00280	0.00157	0.00049
Sep	0.00143	0.00080	0.00693	0.00273	0.00927	0.00267	0.00502
Oct	0.00102	0.00087	0.00655	0.00339	0.00876	0.00900	0.00635
Nov	0.00034	0.00022	0.00490	0.00313	0.00128	0.00024	0.00044
Dec*	0.00016	0.00127	0.00411	0.00035	0.01022	0.00581	0.00000

Table 3.6: Standard errors of Bates model for five consecutive days on S&P 500 monthly second week data

2001	G	M	κ	θ	β	v_1	v_2	v_3	v_4	v_5	ape
Jan	27.5433	39.7557	3.7777	16.3734	15.8624	39.6389	31.9389	33.3981	27.1095	30.2924	0.0118
Feb	22.4619	39.1710	1.9712	8.5342	6.6719	15.1548	17.4934	15.5623	18.2277	16.3137	0.0092
Mar	27.5061	41.8339	5.1406	15.6597	19.6009	32.6856	30.6012	27.8919	28.7891	41.5230	0.0124
Apr	26.1995	41.5157	6.2173	14.9024	17.2927	52.6841	35.5401	38.0701	34.2621	25.3640	0.0150
May	16.7377	31.3790	2.2619	5.8369	5.1964	11.6544	11.7284	12.6523	12.4345	11.7505	0.0086
Jun	18.6906	36.1930	2.8737	7.5077	6.0333	11.5735	13.3044	11.4335	12.5456	13.5754	0.0072
Jul	30.2061	51.0747	3.7921	16.0018	9.8707	23.6903	29.4413	30.8028	28.1531	31.1505	0.0101
Aug	16.4313	34.2169	1.6353	5.0960	3.5271	9.1136	9.3130	9.8202	9.1761	9.1774	0.0085
Sep	25.6489	42.7651	6.6691	13.9818	17.4420	26.6476	32.5258	33.3645	39.3850	48.9936	0.0143
Oct	12.4698	25.5884	7.4083	4.6029	11.6673	15.9058	16.0780	12.9627	12.8043	17.2174	0.0066
Nov	9.9118	22.4011	6.7587	3.4641	8.6181	8.3409	9.1983	9.2094	8.3121	7.5710	0.0086
Dec	15.7316	31.6457	3.4586	6.2288	6.1264	11.5619	11.6996	11.6300	10.1753	11.9771	0.0077
2002	G	M	κ	θ	β	v_1	v_2	v_3	v_4	v_5	ape
Jan	8.0901	21.5771	1.0024	1.6771	1.3609	3.4155	3.3677	3.4020	3.7758	3.7631	0.0083
Feb	23.8162	43.8980	5.0712	11.4343	11.6644	22.2880	24.7877	21.1673	21.2052	17.1038	0.0094
Mar	15.5851	32.7791	1.0000	4.1599	2.3795	8.3690	7.7200	7.9392	6.8222	6.6211	0.0099
Apr	28.9526	84.7482	8.6044	17.1824	7.3371	24.0102	26.4502	20.9632	29.6137	27.7921	0.0130
May	27.3283	63.6496	2.6370	13.4527	3.3386	24.3570	20.4983	25.5337	26.2586	25.8325	0.0142
Jun	22.9094	47.0200	4.9504	11.3291	7.0793	21.1325	23.4181	23.6137	27.0085	29.0071	0.0098
Jul	24.9683	45.5987	10.7385	13.7990	17.4931	41.0500	52.2309	57.0122	56.8662	50.2467	0.0144
Aug	14.0772	29.7482	7.3954	5.7442	7.7600	33.9464	27.7954	24.2438	23.0509	25.9609	0.0104
Sep	11.5934	26.0073	6.2981	4.4798	8.6714	15.5932	17.0692	14.4218	18.8886	18.1228	0.0113
Oct	10.7124	23.8542	5.9075	4.5887	7.9560	21.3466	22.6618	18.9888	18.1587	16.7383	0.0100
Nov	17.7678	35.5789	7.8784	9.8071	13.3611	24.2968	26.5924	26.7370	22.5349	31.1577	0.0097
Dec	12.6554	37.0922	1.1000	4.3224	1.0000	11.7668	11.7108	11.6818	11.6708	11.6342	0.0147

Table 3.7: Parameter estimates for VGSA model for five consecutive days on S&P 500 monthly second week data

2001	G	M	κ	θ	β
Jan	0.12837	0.26498	0.11822	0.18815	0.34321
Feb	0.08569	0.40149	0.06463	0.20322	0.17717
Mar	0.11983	0.32954	0.13264	0.16414	0.38720
Apr	0.18667	0.55655	0.18199	0.21452	0.43608
May	0.06586	0.37799	0.10776	0.14239	0.19394
Jun	0.07644	0.43944	0.09761	0.10964	0.17903
Jul	0.16337	0.74343	0.15010	0.25190	0.34158
Aug	0.06085	0.37981	0.07530	0.13100	0.12103
Sep	0.12752	0.44575	0.14296	0.13314	0.32402
Oct	0.04538	0.21325	0.10521	0.02435	0.16176
Nov	0.05653	0.27975	0.18890	0.02669	0.21385
Dec	0.08501	0.49038	0.18613	0.09504	0.27510
2002	G	M	κ	θ	β
Jan	0.04446	0.37662	0.26138	0.25620	0.15169
Feb	0.13356	0.59979	0.18598	0.12399	0.34536
Mar	0.08546	0.54481	0.05640	0.15179	0.08404
Apr*	0.00000	0.00000	0.43805	0.40082	0.85126
May	0.32888	3.40938	0.21773	0.40572	0.30760
Jun	0.13402	0.95353	0.16663	0.10692	0.28448
Jul*	0.09867	0.39664	0.00000	0.10860	0.00000
Aug	0.07017	0.40663	0.10275	0.03586	0.20731
Sep	0.05816	0.34954	0.10856	0.03199	0.17371
Oct	0.03866	0.22845	0.06784	0.02318	0.11658
Nov	0.12112	0.66827	0.23123	0.10056	0.38779
Dec*	0.05076	1.09355	0.04156	0.00000	0.11646

Table 3.8: Standard errors of VGSA model for five consecutive days on S&P 500 monthly second week data

2001	ν	θ_{NIG}	κ	θ_{CIR}	β	v_1	v_2	v_3	v_4	v_5	ape
Jan	22.6354	-6.1288	3.7366	0.6735	3.1827	1.6333	1.3252	1.3719	1.1315	1.2460	0.0116
Feb	36.1501	-5.1398	1.8961	1.0000	2.7306	1.3841	1.5404	1.4264	1.6134	1.4670	0.0131
Mar	19.3551	-6.9303	4.3926	0.5270	3.1175	1.0670	1.0068	0.9286	0.9542	1.3375	0.0126
Apr	22.7929	-7.6846	6.2493	0.6251	3.5324	2.2113	1.4974	1.5843	1.4340	1.0673	0.0149
May	16.9603	-8.1831	1.6003	0.2804	1.0000	0.7360	0.7407	0.7739	0.7641	0.7409	0.0088
Jun	18.2758	-11.0731	2.4459	0.3442	1.0000	0.5802	0.6420	0.5985	0.6340	0.6691	0.0073
Jul	47.2666	-27.3071	6.4232	0.5987	2.1976	1.1188	1.4242	1.4597	1.4947	1.4215	0.0137
Aug	31.9068	-13.0825	3.5043	0.5487	1.8522	1.0024	1.0315	1.0936	1.0084	1.0048	0.0082
Sep	21.0765	-8.3662	6.3448	0.5406	3.2479	1.0303	1.2385	1.2770	1.4953	1.8529	0.0142
Oct	10.9108	-7.0345	6.8566	0.3028	2.4054	1.0258	1.0288	0.8450	0.8306	1.1053	0.0060
Nov	7.6758	-6.6332	6.0399	0.2384	1.0000	0.5455	0.5743	0.5709	0.5364	0.5021	0.0080
Dec	14.7279	-8.6539	2.2234	0.3029	1.0007	0.6337	0.6421	0.6305	0.6149	0.6706	0.0082
2002	ν	θ_{NIG}	κ	θ_{CIR}	β	v_1	v_2	v_3	v_4	v_5	ape
Jan	12.8720	-8.7931	2.4358	0.2689	1.0000	0.5183	0.5009	0.5068	0.5920	0.5784	0.0075
Feb	14.3397	-7.7806	2.1642	0.3229	1.0000	0.5807	0.5881	0.5543	0.5406	0.5017	0.0116
Mar	42.0405	-11.4410	4.3114	0.7865	2.6585	1.6441	1.3386	1.4758	1.1166	1.0520	0.0106
Apr	50.0000	-23.8747	28.2069	0.7938	6.4590	1.5884	1.7188	1.3010	1.9963	1.8022	0.0116
May	49.9298	-16.9930	20.1622	1.0000	6.0267	1.7926	1.2895	2.3778	2.4619	2.3275	0.0149
Jun	27.6282	-13.4352	2.7243	0.4469	1.0000	1.1021	1.1154	1.1265	1.3043	1.3184	0.0127
Jul	39.5842	-10.4118	9.1286	1.0000	4.0081	2.9747	3.5851	3.7462	3.7963	3.5397	0.0191
Aug	14.2960	-8.8464	7.2769	0.3764	1.6910	2.2156	1.7946	1.5933	1.5367	1.6731	0.0104
Sep	11.1876	-7.8725	5.9683	0.3185	1.8906	1.1059	1.1764	1.0257	1.3194	1.2748	0.0109
Oct	10.6435	-7.2994	5.8064	0.3643	1.9248	1.7087	1.7870	1.5104	1.4435	1.3443	0.0099
Nov	13.8864	-9.0852	5.5196	0.4135	1.6784	0.9728	1.0109	1.0046	0.9246	1.1812	0.0103
Dec	21.5496	-11.7889	2.4954	0.4865	1.0000	1.3055	1.2905	1.2746	1.2916	1.2781	0.0119

Table 3.9: Parameter estimates for NIGSA model for five consecutive days on S&P 500 monthly second week data

2001	ν	θ_{NIG}	κ	θ_{CIR}	β
Jan	0.18124	0.15588	0.11385	0.00796	0.06745
Feb	0.21058	0.10743	0.09347	0.01994	0.08593
Mar	0.16778	0.17781	0.11086	0.00568	0.06054
Apr	0.30023	0.34594	0.18097	0.00943	0.08821
May	0.15700	0.25498	0.08153	0.01545	0.03619
Jun	0.21317	0.35112	0.10040	0.00656	0.02806
Jul	0.79747	0.83504	0.13378	0.00701	0.00897
Aug	0.26556	0.32381	0.12899	0.00739	0.04935
Sep	0.20942	0.26727	0.13315	0.00527	0.06115
Oct	0.09622	0.13908	0.08899	0.00142	0.03179
Nov	0.21141	0.17955	0.74134	0.00190	0.11474
Dec*	0.15914	0.28500	0.00000	0.00000	0.00000
2002	ν	θ_{NIG}	κ	θ_{CIR}	β
Jan*	0.00000	0.00000	0.00000	0.00000	0.00000
Feb	0.13913	0.21812	0.11900	0.00550	0.03604
Mar	0.51816	0.49267	0.30397	0.01416	0.13638
Apr*	0.00000	0.00000	0.00000	0.00255	0.01058
May	1.00408	0.14467	0.41257	0.02106	0.01839
Jun	0.37342	0.61347	0.11006	0.01190	0.03988
Jul	0.55640	0.13695	0.15361	0.02018	0.05508
Aug	0.21111	0.34272	0.09319	0.00226	0.05334
Sep	0.16303	0.26448	0.09752	0.00226	0.04034
Oct	0.10997	0.18099	0.06255	0.00187	0.03033
Nov	0.27101	0.43533	0.16977	0.00401	0.05299
Dec*	0.23823	0.33705	0.00000	0.00000	0.00000

Table 3.10: Standard errors of NIGSA model for five consecutive days on S&P 500 monthly second week data

3.4 Stability on Calibration of Stochastic Skew Model on FX Data

The stochastic skew model is proposed by Carr and Wu [CW04] to capture the average symmetric behavior of currency option implied volatilities across moneyness and maturity, and the dynamic properties of the asymmetric return distribution which varies greatly over time.

3.4.1 Stochastic Skew Model

The stochastic skew model (SSM) assumes that under the risk neutral measure the log currency return follows the time changed Lévy process

$$x_t = \ln S_t/S_0 = (r_d - r_f)t + (L^R_{T^R_t} - \xi^R T^R_t) + (L^L_{T^L_t} - \xi^L T^L_t), \tag{3.5}$$

where r_d and r_f denote the continuously compounded domestic and foreign risk free rates, L^R and L^L denote two Lévy processes that exhibit right and left skewness, ξ^R and ξ^L denote convexity adjustments of the two Lévy processes. Furthermore, $L^j = \sigma B^j_t + J^j_t, j = R, L$ where $J^j_t, j = R, L$ denote pure Lévy jump components. T^R_t and T^L_t are separate stochastic time changes applied to the two Lévy processes L^R and L^L respectively. Let $v^i_t = \partial T^i_t/\partial t, i = R, L$, and assume

$$dv^i_t = \kappa(1 - v^i_t)dt + \sigma_v\sqrt{v^i_t}dZ^i_t,\ \ i = R, L, \tag{3.6}$$

where Z^i_t are Brownian motions with $dB^i_t dZ^i_t = \rho^i dt, i = R, L$.

By the generalized Fourier transform [CW02], the characteristic function of x_t is given by,

$$\phi_x(u) = \exp(iu(r_d - r_f)t - b^R(t)v^R_0 - c^R(t) - b^L(t)v^L_0 - c^L(t)), \tag{3.7}$$

where

$$b^j(t) = \frac{2\psi^j(1-\mathrm{e}^{-\eta^j t})}{2\eta^j - (\eta^j - \kappa^j)(1-\mathrm{e}^{-\eta^j t})},$$
$$c^j(t) = \frac{\kappa}{\sigma_v^2}\left[2\ln\left(1 - \frac{\eta^j - \kappa^j}{2\eta^j}(1-\mathrm{e}^{-\eta^j t})\right) + (\eta^j - \kappa^j)t\right],$$

with $\eta^j = \sqrt{(\kappa^j)^2 + 2\sigma_v^2\psi^j}$, $\kappa^j = \kappa - iu\rho^j\sigma\sigma_v$, $j = R, L$. The characteristic exponents $\psi^j, j = R, L$ are dependent on the choice of the Lévy components. For the CGMY model with the Lévy density ($\alpha \leq 2$)

$$k(x) = \lambda e^{-\frac{|x|}{\nu_j}}|x|^{-\alpha-1},\ x \neq 0,$$

and the characteristic exponent for the convexity adjusted Lévy component is

$$\begin{aligned}\psi(u) &= \lambda\Gamma(-\alpha)\left[\left(\frac{1}{\nu_j}\right)^\alpha - \left(\frac{1}{\nu_j} - iu\right)^\alpha\right] - iu\lambda\Gamma(-\alpha)\left[\left(\frac{1}{\nu_j}\right)^\alpha - \left(\frac{1}{\nu_j} - 1\right)^\alpha\right] \\ &+ \lambda\Gamma(-\alpha)\left[\left(\frac{1}{\nu_j}\right)^\alpha - \left(\frac{1}{\nu_j} + iu\right)^\alpha\right] - iu\lambda\Gamma(-\alpha)\left[\left(\frac{1}{\nu_j}\right)^\alpha - \left(\frac{1}{\nu_j} + 1\right)^\alpha\right] \\ &+ \psi^D, \end{aligned} \tag{3.8}$$

where

$$\psi^D = \frac{1}{2}\sigma^2(iu + u^2).$$

3.4.2 Methodology

As in the previous section on S&P data, we fix the model parameters over five consecutive days in the calibration of foreign exchange (FX) over-the-counter currency options data, while making the volatilities constrained under the two time change volatility processes of the model.

Specifically, assuming the market price is $C(K, T, t)$, and the model price is $f(\boldsymbol{\theta}, S_t, v_t^R, v_t^L, K, T, t)$ with t=1,2,...,N, we wish to choose $\boldsymbol{\theta}^*$, v_t^{R*} and v_t^{L*}, $t =$

$1, ..., N$ satisfying

$$(\boldsymbol{\theta}^*, \{v_t^{R*}\}_{t=1,...,N}, \{v_t^{L*}\}_{t=1,...,N})$$
$$= \arg \min_{\boldsymbol{\theta}, v_t^R, v_t^L} \sum_{K,T,t} D^2(\boldsymbol{\theta}, S_t, v_t^R, v_t^L, K, T, t) - \sum_{t=1}^{N-1} P(\boldsymbol{\theta}, v_{t+1}^R | v_t^R) - \sum_{t=1}^{N-1} P(\boldsymbol{\theta}, v_{t+1}^L | v_t^L), \tag{3.9}$$

where

$$D(\boldsymbol{\theta}, S_t, v_t^R, v_t^L, K, T, t) = C(K, T, t) - f(\boldsymbol{\theta}, S_t, v_t^R, v_t^L, K, T, t),$$

and $P(\boldsymbol{\theta}, v_{t+1}^j | v_t^j)$ is the conditional probability of the volatility $\{v_t^j, t = 1, ..., N\}$, $j = R, L$ following the stochastic skew model.

The transition probability $P(\boldsymbol{\theta}, v_{t+1} | v_t)$ is the transition probability of the CIR model as given in the previous section. And the model call option prices $f(\boldsymbol{\theta}, S_t, v_t^R, v_t^L, K, T, t)$, t=1,2,...,N are constructed by the Carr-Madan FFT method (2.9).

3.4.3 FX Data and Results

The FX data set is from the over-the-counter currency options market. It includes daily quotes of currency option implied volatilities. Moneyness is conventionally quoted in terms of Black-Scholes delta rather than strike price. Options on each currency pair have 12 maturities: 7 days, 1 month, 2 months, 3 months, 6 months, 9 months, 1 year, 18 months, 2 years, 3 years, 4 years, and 5 years. At each maturity, the implied volatility quotes are available at five strikes in the form of deltas: ten-delta call, 25-delta call, at-the-money, ten-delta put, and 25-delta put. Given the implied volatility quote $\sigma(\delta, T)$ at a certain delta and maturity, the strike prices are

computed by

$$K_{call} = S_0 \exp\left[(r_d - r_f)T + \frac{T}{2}\sigma(\delta_{call}, T)^2 - \sqrt{T}\sigma(\delta_{call}, T)N^{-1}(e^{r_f T}\delta_{call})\right],$$

$$K_{put} = S_0 \exp\left[(r_d - r_f)T + \frac{T}{2}\sigma(\delta_{put}, T)^2 + \sqrt{T}\sigma(\delta_{put}, T)N^{-1}(-e^{r_f T}\delta_{put})\right],$$

$$K_{ATM} = S_0 e^{(r_d - r_f)T + \frac{T}{2}\sigma(ATM,T)^2},$$

where $N(x)$ denotes the standard normal distribution.

We use the daily time series data of USD-GBP FX call option prices of five consecutive days including each second Monday of each month for year 2002 and 2003. And we use the VG model which is a special case of the CGMY model with $\alpha = 0$.

As in the case of S&P 500, the results show that the calibrating procedure for the parameters are stabilized due to the constraint of the volatility processes, while the APEs do not get much larger and are still in an acceptable threshold. And since the two driving time change volatility processes are normalized, the volatility parameters from the calibrations are in a range that are close to the value of unit.

2002	σ	λ	ν_j	κ	σ_v	ρ^R	ρ^L	ape
Jan	0.0399	14.5653	0.0164	1.5643	3.3467	-0.1462	-0.2932	0.0100
Feb	0.0408	10.5885	0.0183	2.1095	3.8299	-0.5009	0.0399	0.0080
Mar	0.0350	9.2143	0.0188	1.3216	2.9499	-0.3852	-0.0149	0.0075
Apr	0.0265	7.3702	0.0213	2.2069	4.0526	-0.1499	-0.4647	0.0100
May	0.0467	7.8233	0.0154	1.7451	3.5315	0.0093	-0.2820	0.0097
Jun	0.0246	16.1583	0.0145	1.2612	3.0178	-0.1438	-0.4671	0.0101
Jul	0.0388	10.3796	0.0180	1.8827	3.7592	0.1306	-0.1760	0.0094
Aug	0.0420	11.7442	0.0158	1.2262	3.2298	0.0288	0.0205	0.0081
Sep	0.0312	16.0111	0.0149	1.6522	3.4823	-0.0572	0.0609	0.0060
Oct	0.0362	14.7986	0.0151	1.6818	3.4447	-0.2459	0.4225	0.0070
Nov	0.0349	13.7633	0.0152	1.9384	4.0937	0.2266	-0.1203	0.0082
Dec	0.0350	14.0767	0.0149	1.6996	3.5879	0.0010	0.1235	0.0079
2003	σ	λ	ν_j	κ	σ_v	ρ^R	ρ^L	ape
Jan	0.0394	15.4791	0.0147	1.0850	2.6249	0.3057	-0.2265	0.0057
Feb	0.0346	15.1394	0.0156	1.4853	3.2076	-0.0647	0.1468	0.0093
Mar	0.0357	14.3725	0.0152	1.0834	2.5201	0.1601	0.0357	0.0081
Apr	0.0438	14.9556	0.0144	0.9230	2.4208	-0.0167	0.0146	0.0057
May	0.0337	14.4143	0.0153	1.1437	2.8160	0.2992	-0.3549	0.0076
Jun	0.0328	15.5731	0.0152	1.3204	3.2581	0.3140	-0.4127	0.0099
Jul	0.0334	14.8984	0.0155	1.0511	2.9423	0.2246	-0.3143	0.0112
Aug	0.0341	14.8688	0.0151	1.2330	3.1017	0.1503	-0.1926	0.0104
Sep	0.0431	9.1531	0.0179	1.1904	2.7436	-0.4430	0.4735	0.0125
Oct	0.0398	11.0993	0.0178	2.9126	4.9416	0.2121	-0.1638	0.0104
Nov	0.0290	17.1979	0.0150	1.5616	3.4481	0.2491	-0.1655	0.0093
Dec	0.0301	10.4178	0.0204	1.9112	3.5859	0.2776	-0.2016	0.0088

Table 3.11: Parameter estimates for SSM model for five consecutive days on USD-GBP monthly second week data in year 2002-2003

2002	v_1^R	v_2^R	v_3^R	v_4^R	v_5^R	v_1^L	v_2^L	v_3^L	v_4^L	v_5^L
Jan	0.6869	0.9117	0.9993	0.5619	0.8250	0.5543	0.7598	0.5981	0.7538	0.5910
Feb	0.7403	0.5917	0.6589	0.6803	0.6091	0.7466	0.6178	0.7569	0.6236	0.7146
Mar	0.5346	0.6456	0.4947	0.6101	0.4693	0.6093	0.4610	0.6228	0.5523	0.5680
Apr	0.6372	0.3540	0.7896	0.3698	0.6050	0.4483	0.6773	0.3760	0.5046	0.4595
May	0.7440	0.2821	0.9212	0.2736	0.8992	0.3162	0.8349	0.2133	0.8079	0.2252
Jun	0.6490	0.3689	0.6925	0.3511	0.6758	0.3756	0.6393	0.4058	0.7291	0.4451
Jul	1.1072	0.7550	1.1310	0.6811	1.1400	0.6594	1.0191	0.7067	1.0871	0.6915
Aug	1.1326	0.5184	0.9380	0.8147	0.9543	0.8548	0.8881	0.8144	1.1397	0.5394
Sep	0.8620	0.8091	1.0882	0.6385	0.8970	0.8623	1.0162	0.8029	0.8383	0.9830
Oct	0.8075	0.5965	0.9026	0.5566	0.7381	0.6361	0.8427	0.6140	0.7027	0.5756
Nov	0.8249	0.5117	0.8525	0.5460	0.7296	0.6794	0.8163	0.5889	0.8066	0.5255
Dec	0.8284	0.3794	0.6797	0.5899	0.8118	0.4921	0.6481	0.6148	0.7648	0.4942
2003	v_1^R	v_2^R	v_3^R	v_4^R	v_5^R	v_1^L	v_2^L	v_3^L	v_4^L	v_5^L
Jan	1.0550	0.3596	0.9076	0.4793	0.9175	0.4886	0.8223	0.5487	1.0075	0.3749
Feb	1.0295	0.4316	0.9566	0.5596	0.8837	0.6049	0.7501	0.6935	0.7446	0.6123
Mar	0.8587	0.6730	0.7849	0.5797	0.8387	0.5980	0.8078	0.6401	0.6221	0.7780
Apr	0.4943	0.8807	0.8309	0.5054	0.7853	0.5417	0.7062	0.6347	0.9562	0.3945
May	1.1117	0.4284	0.8929	0.7198	0.8577	0.7068	1.0155	0.5054	1.0847	0.4947
Jun	1.0992	0.4450	1.1981	0.3537	1.1210	0.3584	1.0260	0.5244	1.1934	0.2872
Jul	1.1067	0.3319	1.2081	0.3131	1.1522	0.3131	0.8826	0.6818	1.0850	0.3452
Aug	1.1640	0.3840	1.0053	0.5950	0.9758	0.4944	0.7561	0.7783	0.8165	0.7534
Sep	0.5713	0.9832	0.5821	0.9244	0.9575	0.5244	0.5862	0.9326	0.5081	0.8904
Oct	1.2750	0.7549	1.1852	0.8314	1.3214	0.5907	1.3898	0.6276	1.1636	0.8087
Nov	0.9205	0.7501	1.1611	0.4684	1.1648	0.5343	0.9175	0.6961	1.2875	0.3418
Dec	0.9427	0.7045	1.1803	0.5333	1.1566	0.5602	1.1381	0.5861	1.1779	0.5654

Table 3.12: Parameter estimates for SSM model for five consecutive days on USD-GBP monthly second week data in year 2002-2003

Chapter 4

Operator Splitting Method for PIDEs

4.1 Introduction

In Black-Scholes theory, the price of a risky asset in risk neutral measure follows the stochastic differential equation

$$dS_t = rS_t dt + \sigma S_t dB_t. \tag{4.1}$$

Let $x_t = \log S_t$, and denote $u(x,t)$ as the value of an European or barrier option written on the underlying S_t, the Black-Scholes PDE can be derived from Ito's formula as

$$\frac{\partial u}{\partial t} + \mathcal{L}_t u = 0, \tag{4.2}$$

where

$$\mathcal{L}_t u = \frac{1}{2}\sigma^2 \frac{\partial^2 u}{\partial x^2} + (r - \frac{1}{2}\sigma^2)\frac{\partial u}{\partial x} - ru. \tag{4.3}$$

Generally if x_t is a Lévy process with convexity adjustments

$$x_t = rt + (\sigma B_t - \frac{1}{2}\sigma^2 t) + (J_t - \xi t), \tag{4.4}$$

where J_t and ξ denote a pure Lévy jump component and its convexity adjustment, by Ito's lemma (B.9), $u(x,t)$ follows the parabolic integro-differential equation (PIDE)

$$\frac{\partial u}{\partial t} + \mathcal{L}_t^D u + \mathcal{L}_t^J u = 0, \tag{4.5}$$

where

$$\mathcal{L}_t^D u = \frac{1}{2}\sigma^2 \frac{\partial^2 u}{\partial x^2} + (r - \frac{1}{2}\sigma^2)\frac{\partial u}{\partial x} - ru, \tag{4.6}$$

and

$$\mathcal{L}_t^J u = \int_{-\infty}^{\infty} \left[u(x+y,t) - u(x,t) - (e^y - 1)\frac{\partial u}{\partial x}(x,t) \right] k(y)dy, \tag{4.7}$$

where $k(y)$ is the jump kernel. In this case, the infinitesimal generator of the Lévy process x_t is an integro-differential operator which is composed of a differential operator $\mathcal{L}_t^D$ accounting for the diffusion part of x_t, and a nonlocal operator $\mathcal{L}_t^J$ corresponding to the pure jump part.

A common approach of numerical solutions to the PIDEs in option pricing literature is the finite difference method [CT03, CV03, HM02]. The finite difference method is intuitive, easy to implement and has the monotonicity perserving property. And more importantly, its superiority in handling convection-diffusion type evolution partial differential equations make it popular since many partial differential equations from option pricing are of this type.

On the other hand, the introduction of jumps of stochastic processes has become an impetus for the study of numerical methods for the corresponding parabolic integro-differential equations [CT03]. Although it is feasible to use a finite difference method in handling the integral operator of the PIDE with one space dimension, different approaches are proposed to improve the efficiency in discretization and the viability on the PIDEs with more than one space dimensions. Matache, von Petersdorff, and Schwab [MvPS03] propose a finite element method under weighted Sobolev spaces for PIDEs with one space dimension on European options and the

method results in a sparse representation of the integral operator. The extension of the method to American options can be found in [MNS03].

On the parabolic differential equations with more than one space dimensions, Jaillet, Lamberton, and Lapeyre [JLL90] give a theoretical framework of variational analysis on the pricing of American options. Hilber, Matache, and Schwab [HMS04] propose a wavelet based finite element method on solving PDEs with stochastic volatility using weighted Sobolev spaces. Von Petersdorff and Schwab [vPS03] extend the work of [MvPS03] to high dimensional PIDEs by using the wavelet based sparse grid.

However, for the PIDEs in two or three space dimensions, it is in general inefficient or infeasible to apply the same numerical technique to different parts of the system. From the view of the diffusion part, it is a typical convection dominated convection diffusion equation and is desirable to apply a finite difference discretization. On the other hand, the jump part is composed of nonlocal operator(s), a Galerkin scheme is preferred to avoid dense matrices from the finite difference discretization.

The general idea behind the operator splitting method is to break down the complicated problem into smaller parts and to treat each of them with corresponding numerical techniques. It was developed during 1950's and 60's by Russian academician Yanenko and Marchuk (with the name 'fractional steps') [Yan71] and by Douglas, Peaceman, and Rachford in U.S. (with the name 'alternating direction implicit') dealing with high dimensional problems in fluid dynamics [HV03]. See also [Smo03] and the references therein.

4.2 Operator Splitting for 1-D PIDEs

Assuming $r = 0$ and we are to compute a European call option, and we have made a change of variable $T - t \to t$, the 1-D PIDE (4.5) becomes

$$\frac{\partial u}{\partial t} = \frac{\sigma^2}{2}\frac{\partial^2 u}{\partial x^2} - \frac{\sigma^2}{2}\frac{\partial u}{\partial x} + \int_{-\infty}^{\infty}\left[u(x+y,t) - u(x,t) - (e^y - 1)\frac{\partial u}{\partial x}(x,t)\right]k(y)dy, \quad (4.8)$$

with boundary conditions

$$u(x,0) = (e^x - K)^+,$$

$$u(-\infty, t) = 0,$$

$$\frac{\partial u}{\partial x}(x,t) = e^x, \text{ when } x \text{ is large.}$$

The last boundary condition is based on the fact that when x goes to infinity, the call price converges to the terminal payoff:

$$u(x,t) \to (e^x - K)^+, \ t > 0.$$

For computational purpose, we approximate jumps smaller than $\varepsilon > 0$ by a Brownian motion in infinite activity cases.

4.2.1 Approximation of Small Jumps by Brownian Motion

Let $\{X_t; t \geq 0\}$ be an infinite activity Lévy process with the characteristic triplet $(0, \nu, \gamma)$. By the Lévy Itô decomposition (see [Sat99]) X_t can be written as a sum of a compound Poisson process and an almost sure limit of compensated compound Poisson processes

$$X_t = \gamma t + \int_0^t \int_{|x|\geq 1} x\mu(dx, ds) + \lim_{\varepsilon \downarrow 0} M_t^{\varepsilon}, \quad (4.9)$$

where

$$M_t^\varepsilon = \int_0^t \int_{\varepsilon \le |x| < 1} x\mu(dx, ds) - t \int_{\varepsilon \le |x| < 1} x\nu(dx), \tag{4.10}$$

and μ is the random Poisson measure with intensity ν. It implies that X_t can be approximated by truncating the jumps smaller than ε,

$$X_1^\varepsilon(t) = \gamma_\varepsilon t + M_t^\varepsilon, \tag{4.11}$$

where

$$\gamma_\varepsilon = \gamma - \int_{\varepsilon \le |x| \le 1} x\nu(dx), \tag{4.12}$$

and

$$M_t^\varepsilon = \int_0^t \int_{|x| \ge \varepsilon} x\mu(dx, ds) \tag{4.13}$$

is a compound Poisson process with jumps larger than ε.

Moreover, the approximation can be improved by incorporating the contribution from the variation of small jumps which is approximated by a Brownian motion,

$$X_2^\varepsilon(t) = \gamma_\varepsilon t + \sigma(\varepsilon) B_t + M_t^\varepsilon, \tag{4.14}$$

where

$$\sigma^2(\varepsilon) = \int_{|x| < \varepsilon} x^2 \nu(dx). \tag{4.15}$$

This fact is verified by the following theorem,

Theorem 4.2.1 ([AR01]) *Denote $X_t^\varepsilon = X_t - X_1^\varepsilon(t)$. For every function f that is continuous with respect to the uniform metric, bounded, and measurable with respect to the projection σ-field, it holds $Ef(\sigma(\varepsilon)^{-1} X_t^\varepsilon) \to Ef(B_t)$ as $\varepsilon \to 0$ if and only if*

for each $\kappa > 0$,

$$\sigma(\kappa\sigma(\varepsilon) \wedge \varepsilon) \sim \sigma(\varepsilon), \ \ as\ \varepsilon \to 0.$$

The last condition is implied by

$$\lim_{\varepsilon \to 0} \frac{\sigma(\varepsilon)}{\varepsilon} = \infty.$$

4.2.2 Operator Splitting

After the approximation of small jumps by a Brownian motion, the PIDE (4.8) becomes

$$\begin{aligned} \frac{\partial u}{\partial t} &= \frac{\sigma^2 + \sigma^2(\varepsilon)}{2}\frac{\partial^2 u}{\partial x^2} - \frac{\sigma^2 + \sigma^2(\varepsilon)}{2}\frac{\partial u}{\partial x} \\ &\quad + \int_{|y| \geq \varepsilon} \left[u(x+y,t) - u(x,t) - \frac{\partial u}{\partial x}(x,t)(e^y - 1) \right] k(y) dy, \end{aligned} \tag{4.16}$$

where $\sigma^2(\varepsilon)$ is defined in (4.15).

We discretize the above equation with time steps $t_n, n = 1, ..., N$ and use the θ-scheme for each step. For each time step $[t_n, t_{n+1}]$, we split the right hand side of the PIDE into two parts and discretize the space dimension of the diffusion part with the finite difference method and that of the jump part with the finite element method independently.

1. Diffusion step

$$\frac{\partial u}{\partial t} = \frac{\sigma^2 + \sigma^2(\varepsilon)}{2}\frac{\partial^2 u}{\partial x^2} - \frac{\sigma^2 + \sigma^2(\varepsilon)}{2}\frac{\partial u}{\partial x}, \ t \in (t_n, t_{n+1}), \tag{4.17}$$

$$u(-\infty, t) = 0, \ \frac{\partial u}{\partial x}(x,t) = e^x, \text{ when } x \text{ is large,}$$

$$u\big|_{t=t_n} = u_n,$$

$$\Longrightarrow u_n^*.$$

2. Jump step

$$\frac{\partial u}{\partial t} = \int_{|y|\geq\varepsilon} \left[u(x+y,t) - u(x,t) - \frac{\partial u}{\partial x}(x,t)(e^y - 1) \right] k(y)dy, \ t \in (t_n, t_{n+1}) \quad (4.18)$$

$$\text{(no spatial boundary conditions)} \ , u|_{t=t_n} = u_n^*,$$

$$\Longrightarrow u_{n+1}.$$

We further truncate the x space $(-\infty, \infty)$ to $[R_{xa}, R_{xb}]$, and denote $x_i, u_i, i = 0, ..., N_x$ be uniform grid points and values on $[R_{xa}, R_{xb}]$. Let $h_x = x_i - x_{i-1}$ and

$$\frac{\partial u}{\partial x} \approx \frac{u_i - u_{i-1}}{h_x},$$

$$\frac{\partial^2 u}{\partial x^2} \approx \frac{u_{i+1} - 2u_i + u_{i-1}}{h_x^2}.$$

Then the diffusion operator becomes

$$\begin{aligned} \mathcal{L}^D u &\approx \frac{\sigma^2 + \sigma^2(\varepsilon)}{2} \frac{u_{i+1} - 2u_i + u_{i-1}}{h_x^2} - \frac{\sigma^2 + \sigma^2(\varepsilon)}{2} \frac{u_i - u_{i-1}}{h_x} \\ &= (\sigma^2 + \sigma^2(\varepsilon)) \left(\frac{1}{2h_x^2} + \frac{1}{2h_x} \right) u_{i-1} \\ &\quad -(\sigma^2 + \sigma^2(\varepsilon)) \left(\frac{1}{h_x^2} + \frac{1}{2h_x} \right) u_i + \frac{\sigma^2 + \sigma^2(\varepsilon)}{2h_x^2} u_{i+1}. \end{aligned} \quad (4.19)$$

The boundary values are

$$u_0 = 0,$$

$$\frac{u_{N_x} - u_{N_x - 1}}{h_x} = e^{R_{xb}}.$$

For the jump step

$$\frac{\partial u}{\partial t} = \int_{|y|\geq\varepsilon} \left[u(x+y,t) - u(x,t) - \frac{\partial u}{\partial x}(x,t)(e^y - 1) \right] k(y)dy, \ t \in (t_n, t_{n+1}), \quad (4.20)$$

$$u|_{t=t_n} = u_n^*,$$

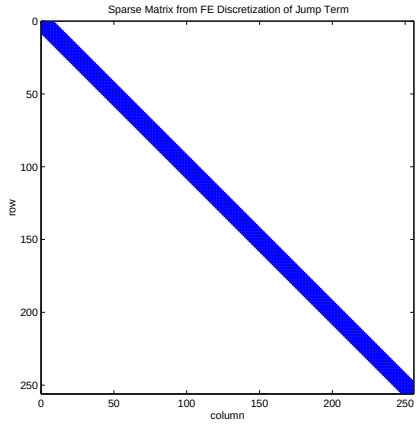

Figure 4.1: Illustration of sparse matrix from finite element discretization of integral operator

we further make a variable change $u - h(x,t) \to u$ where $h(x,t)$ denotes the terminal payoff

$$h(x,t) = (e^x - K)^+.$$

We get

$$\frac{\partial u}{\partial t}(x,t) = \int_{|y|\geq\varepsilon} \left[u(x+y,t) - u(x,t) - \frac{\partial u}{\partial x}(x,t)(e^y - 1) \right] k(y)dy + F(x,t), \quad (4.21)$$

where

$$F(x,t) = -\frac{\partial h}{\partial t}(x,t) + \int_{|y|\geq\varepsilon} \left[h(x+y,t) - h(x,t) - \frac{\partial h}{\partial x}(x,t)(e^y - 1) \right] k(y)dy. \quad (4.22)$$

The above equation is semi-discretized by a finite element method using piecewise linear hat functions on uniform grids. This discretization on the space dimension by the Galerkin scheme results in a sparse matrix if we truncate the small elements of the matrix.

4.2.3 Variational Formulation of Integral Operator

For the jump step in the operator splitting method, a variational formulation is needed to establish the existence of the solution for the finite element discretization. This formulation is carried out by [MvPS03] through weighted Sobolev spaces and is briefly described in this subsection. For a review on Sobolev spaces, see [AF03].

In the case of the European options, the payoff $h(x,t)$ does not belong to $L^2(\mathbb{R})$, and the solutions have exponential growth at infinity. Hence standard Solobev spaces fail to serve as function spaces. Weighted Sobolev spaces are introduced.

Definition 4.2.2 *Let $\nu \in \mathbb{R}$ and denote $L^2_\nu(\mathbb{R}) = \{v \in L^1_{loc}(\mathbb{R}) | ve^{\nu|x|} \in L^2(\mathbb{R})\}$, The weighted Sobolev space H^1_ν is defined by*

$$H^1_\nu(\mathbb{R}) := \{v \in L^1_{loc}(\mathbb{R}) | ve^{\nu|x|}, v'e^{\nu|x|} \in L^2(\mathbb{R})\}.$$

Denote

$$\begin{aligned} a^\eta(u,v) &= -(\mathcal{L}^J u, v)_{L^2_\eta(\mathbb{R})} \\ &= -\int\int_{\mathbb{R}^2} \left[u(x+y,t) - u(x,t) - \frac{\partial u}{\partial x}(x,t)(e^y - 1)\right] k(y)v(x)e^{2\eta(x)}dydx, \end{aligned} \tag{4.23}$$

and

$$\begin{aligned} &(F(\cdot,t), v)_{(H^1_\eta(\mathbb{R}))^* \times H^1_\eta(\mathbb{R})} \\ &= \int\int_{\mathbb{R}^2} \left[h(x+y,t) - h(x,t) - \frac{\partial h}{\partial x}(x,t)(e^y - 1)\right] k(y)v(x)e^{2\eta(x)}dydx. \end{aligned} \tag{4.24}$$

Theorem 4.2.3 ([MvPS03]) *Let $\eta \in L^1_{loc}(\mathbb{R})$ with $\frac{\partial \eta}{\partial x} \in L^\infty(\mathbb{R})$.*

1. Assume that

$$\eta(x+\theta y) - \eta(x) \leq \eta(y),\ \forall x, y \in \mathbb{R},\ \forall \theta \in [0,1],$$

and that

$$C(\eta) := \int_{\mathbb{R}} e^{\eta(y)} |y| \mathbf{1}_{\{|y| \geq 1\}}(y) k(y) dy < +\infty.$$

Then there exist $\alpha(\eta) > 0$, $\beta(\eta) > 0$ and $C(\eta) > 0$ such that

$$|a^{-\eta}(u,v)| \leq C(\eta) \|u\|_{H^1_{-\eta}(\mathbb{R})} \|v\|_{H^1_{-\eta}(\mathbb{R})},\ \forall u, v \in H^1_{-\eta}(\mathbb{R}),$$

$$a^{-\eta}(u,u) \geq \alpha(\eta) \|u\|_{H^1_{-\eta}(\mathbb{R})} - \beta(\eta) \|u\|_{L^1_{-\eta}(\mathbb{R})},\ \forall u \in H^1_{-\eta}(\mathbb{R}).$$

2. Assume that

$$-\eta(x+\theta y) + \eta(x) \leq \eta(-y),\ \forall x, y \in \mathbb{R},\ \forall \theta \in [0,1],$$

and that

$$C_2(-\eta) := \int_{\mathbb{R}} e^{\eta(-y)} |y| \mathbf{1}_{\{|y| \geq 1\}}(y) k(y) dy < +\infty.$$

Then there exist $\alpha_2(\eta) > 0$, $\beta_2(\eta) > 0$ and $C_2(\eta) > 0$ such that

$$|a^{-\eta}(u,v)| \leq C_2(-\eta) \|u\|_{H^1_{-\eta}(\mathbb{R})} \|v\|_{H^1_{-\eta}(\mathbb{R})},\ \forall u, v \in H^1_{-\eta}(\mathbb{R}),$$

$$a^{-\eta}(u,u) \geq \alpha_2(\eta) \|u\|_{H^1_{-\eta}(\mathbb{R})} - \beta_2(\eta) \|u\|_{L^1_{-\eta}(\mathbb{R})},\ \forall u \in H^1_{-\eta}(\mathbb{R}).$$

The finite element method for the jump part of the operator splitting can be cast into the following weak form: find $u \in L^2(H^1_{-\mu}(\mathbb{R}); (0,T)) \cap H^1((H^1_{-\mu}(\mathbb{R}))^*; (0,T))$ such that

$$\frac{d}{dt}(u(\cdot,t), v)_{L^2_{-\mu}(\mathbb{R})} + a^{-\mu}(u(\cdot,t), v) = (F(\cdot,t), v)_{(H^1_{-\mu}(\mathbb{R}))^* \times H^1_{-\mu}(\mathbb{R})},\ \forall v \in H^1_{-\mu}(\mathbb{R}), \tag{4.25}$$

$$u(\cdot, 0) = 0.$$

By Theorem 4.2.3, there exists a unique weak solution $u \in L^2(H^1_{-\mu}(\mathbb{R}); (0,T)) \cap H^1((H^1_{-\mu}(\mathbb{R}))^*; (0,T))$.

4.2.4 Space Discretization of Integral Operator

Assuming $u \in C^2(\mathbb{R})$ in the integral operator (4.7), then for every x and small y,

$$u(x+y) - u(x) - (e^y - 1)\frac{\partial u}{\partial x} \approx C(u)y^2 \tag{4.26}$$

for a certain function $C(u)$. Thus in the infinite variation case

$$\int_{-\infty}^{\infty} y^2 k(y) dy = \infty,$$

the function $J[u](x)$ is unbounded on $\mathbb{R}$ if u is the European call option. Therefore special care must be taken in the discretization under the finite element bases. In practice on computing the double integral of the jump part (4.23),

$$\mathbf{J}^{(x+)}_{(i,j)} = \int_{-R_x}^{R_x} \int_{\varepsilon}^{R_J} \left[\psi_i(x+y) - \psi_i(x) - (e^y - 1)\frac{\partial \psi_i}{\partial x}(x) \right] k(y) dy \psi_j(x) dx, \tag{4.27}$$

$$\mathbf{J}^{(x-)}_{(i,j)} = \int_{-R_x}^{R_x} \int_{-R_J}^{-\varepsilon} \left[\psi_i(x+y) - \psi_i(x) - (e^y - 1)\frac{\partial \psi_i}{\partial x}(x) \right] k(y) dy \psi_j(x) dx, \tag{4.28}$$

where $\psi_i(x), i = 0, ..., N$ denote hat functions as finite element bases, we switch the order of integration and first compute

$$Q^{(\psi)}_{(i,j)}(y) = \int_{-R_x}^{R_x} \left[\psi_i(x+y) - \psi_i(x) - (e^y - 1)\frac{\partial \psi_i}{\partial x}(x) \right] \psi_j(x) dx, \tag{4.29}$$

by the piecewise quadrature rule. And then

$$\mathbf{J}^{(x+)}_{(i,j)} = \int_{\varepsilon}^{R_J} Q^{(\psi)}_{(i,j)}(y) k(y) dy, \tag{4.30}$$

$$\mathbf{J}_{(i,j)}^{(x-)} = \int_{-R_J}^{-\varepsilon} Q_{(i,j)}^{(\psi)}(y)k(y)dy. \tag{4.31}$$

Similarly, for the right hand side double integrals (4.24),

$$H_i^{(x+)} = \int_{-R_x}^{R_x}\int_{\varepsilon}^{R_J}\left[h(x+y) - h(x) - (e^y - 1)\frac{\partial h}{\partial x}(x)\right]k(y)dy\psi_i(x)dx, \tag{4.32}$$

$$H_i^{(x-)} = \int_{-R_x}^{R_x}\int_{-R_J}^{-\varepsilon}\left[h(x+y) - h(x) - (e^y - 1)\frac{\partial h}{\partial x}(x)\right]k(y)dy\psi_i(x)dx, \tag{4.33}$$

we first compute

$$Q_i^{(h)}(y) = \int_{-R_x}^{R_x}\left[h(x+y) - h(x) - (e^y - 1)\frac{\partial h}{\partial x}(x)\right]\psi_i(x)dx. \tag{4.34}$$

And then

$$H_i^{(x+)} = \int_{\varepsilon}^{R_J} Q_i^{(h)}(y)k(y)dy, \tag{4.35}$$

$$H_i^{(x-)} = \int_{-R_J}^{-\varepsilon} Q_i^{(h)}(y)k(y)dy. \tag{4.36}$$

4.2.5 Results

A pure CGMY model is computed with paramters $C = 0.05, G = M = 10, Y = 1.6$, and $K = 10, \varepsilon = 10^{-5}, \Delta t = 0.1$, $T = 1$. The computing space domain is $[-6, 6]$, with 256 uniform grids. Compared with the values from the Carr-Madan FFT method, the result shows that for the pure CGMY model, the operator splitting method is fast and accurate. Moreover, it shows that the operator splitting method is numerically stable and has the monotonicity perserving property as the finite difference method does. The relative prices (prices subtracted by final payoff) and price difference by the operator splitting (OS) and FFT method are shown in Figure 4.2.

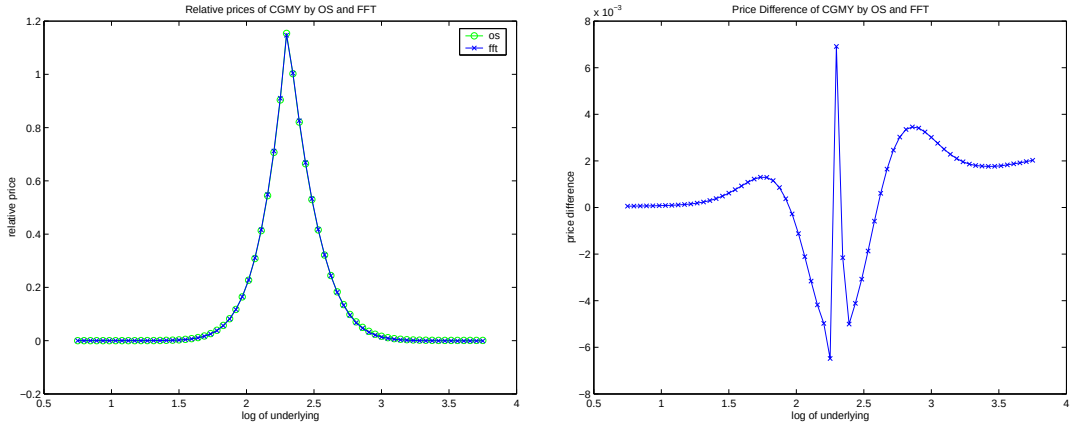

(a) Relative prices

(b) Price difference

Figure 4.2: European call prices under CGMY model by OS and FFT

4.3 Operator Splitting for 2-D PIDEs

4.3.1 Time Changed Lévy Process Model

In stochastic volatility models, a Lévy process is further subordinated by the time integral of a mean reverting CIR process to generate the desired volatility properties — stochastic volatility and volatility persistence:

$$X_t = rt + (\sigma B_{T_t} - \frac{1}{2}\sigma^2 T_t) + (J_{T_t} - \xi T_t), \tag{4.37}$$

where T_t denotes the stochastic clock with activity rate given by $v_t = \partial T_t / \partial t$, which follows

$$dv_t = \kappa(1 - v_t)dt + \sigma_v \sqrt{v_t} dZ_t, \tag{4.38}$$

with $dB_t dZ_t = \rho dt$. Here the long-run mean of the mean reverting process is normalized to the unit.

Accordingly the parabolic integro-differential equation has two variables in

space dimension:

$$\begin{aligned}
&\frac{\partial u}{\partial t}(x,v,t) + \left(r - \frac{\sigma^2 v}{2}\right)\frac{\partial u}{\partial x}(x,v,t) + \kappa(1-v)\frac{\partial u}{\partial v}(x,v,t) \\
&+\frac{\sigma^2 v}{2}\frac{\partial^2 u}{\partial x^2}(x,v,t) + \sigma\rho\sigma_v v\frac{\partial u^2}{\partial x \partial v}(x,v,t) + \frac{\sigma_v^2 v}{2}\frac{\partial^2 u}{\partial v^2}(x,v,t) \\
&+v\int_{-\infty}^{\infty}\left[u(x+y,v,t) - u(x,v,t) - \frac{\partial u}{\partial x}(x,v,t)(e^y - 1)\right]k(y)dy \\
&-ru(x,v,t) = 0. \qquad (4.39)
\end{aligned}$$

Assuming $r = 0$ and after a change of variable $T - t \to t$, the 2-D PIDE (4.39) becomes:

$$\begin{aligned}
\frac{\partial u}{\partial t}(x,v,t) \;=\; & -\frac{\sigma^2 v}{2}\frac{\partial u}{\partial x}(x,v,t) + \kappa(1-v)\frac{\partial u}{\partial v}(x,v,t) \\
&+\frac{\sigma^2 v}{2}\frac{\partial^2 u}{\partial x^2}(x,v,t) + \sigma\rho\sigma_v v\frac{\partial^2 u}{\partial x \partial v}(x,v,t) + \frac{\sigma_v^2 v}{2}\frac{\partial^2 u}{\partial v^2}(x,v,t) \\
&+v\int_{-\infty}^{\infty}\left[u(x+y,v,t) - u(x,v,t) - \frac{\partial u}{\partial x}(x,v,t)(e^y - 1)\right]k(y)dy, \qquad (4.40)
\end{aligned}$$

with boundary conditions for European call options,

$$u(x,v,0) = (e^x - K)^+,$$

$$u(-\infty,v,t) = 0,\ \frac{\partial u}{\partial x}(x,v,t) = e^x,\ \text{when } x \text{ is large},$$

$$g_1(u,u_t,u_x,u_v,\cdot)|_{v=0} = 0,$$

$$g_2(u,u_t,u_x,u_v,\cdot)|_{v=\infty} = 0.$$

where g_1, g_2 denote the boundary conditions at $v = 0$ and $v = \infty$, respectively.

4.3.2 Operator Splitting in Diffusion Step

Similar to the case in 1-D, we have the diffusion step

$$\begin{aligned}\frac{\partial u}{\partial t}(x,v,t) &= -v\frac{\sigma^2+\sigma^2(\varepsilon)}{2}\frac{\partial u}{\partial x}(x,v,t)+\kappa(1-v)\frac{\partial u}{\partial v}(x,v,t)\\ &\quad +v\frac{\sigma^2+\sigma^2(\varepsilon)}{2}\frac{\partial^2 u}{\partial x^2}(x,v,t)+\sigma\rho\sigma_v v\frac{\partial^2 u}{\partial x\partial v}(x,v,t)+\frac{\sigma_v^2 v}{2}\frac{\partial^2 u}{\partial v^2}(x,v,t),\end{aligned} \tag{4.41}$$

$$u(-\infty,v,t)=0,\ \frac{\partial u}{\partial x}(x,v,t)=e^x,\ \text{when } x \text{ is large},$$

$$g_1^D(u,u_t,u_x,u_v,\cdot)|_{v=0}=0,$$

$$g_2^D(u,u_t,u_x,u_v,\cdot)|_{v=\infty}=0,$$

$$u(x,v,t)|_{t=t_n}=u_n,$$

$$\Longrightarrow u_n^*.$$

The g_1^D, g_2^D denote the boundary conditions for the diffusion step at $v=0$ and $v=\infty$, respectively. Note that g_1^D, g_2^D are different from g_1, g_2.

Similar to 1-D, denote $u_{i,j}, i=0,...,N_x, j=0,...,N_v$ be grid point values, let

$$\frac{\partial u}{\partial x}\approx\frac{u_{i,j}-u_{i-1,j}}{h_x}, \tag{4.42}$$

$$\frac{\partial u}{\partial v}\approx\begin{cases}\frac{u_{i,j}-u_{i,j-1}}{h_v} & \text{if } v\geq\theta;\\ \frac{u_{i,j+1}-u_{i,j}}{h_v} & \text{if } v<\theta,\end{cases} \tag{4.43}$$

$$\frac{\partial^2 u}{\partial x^2}\approx\frac{u_{i+1,j}-2u_{i,j}+u_{i-1,j}}{h_x^2}, \tag{4.44}$$

$$\frac{\partial^2 u}{\partial v^2}\approx\frac{u_{i,j+1}-2u_{i,j}+u_{i,j-1}}{h_v^2}, \tag{4.45}$$

$$\frac{\partial^2 u}{\partial x \partial v} \approx \frac{u_{i+1,j+1} - 2u_{i,j} + u_{i-1,j-1}}{2h_x h_v} - \frac{h_x}{2h_v}\frac{\partial^2 u}{\partial x^2} - \frac{h_v}{2h_x}\frac{\partial^2 u}{\partial v^2}. \tag{4.46}$$

The diffusion operator is discretized with a 7-point stencil[IT04],

$$\begin{aligned}
\mathcal{L}u &\approx \frac{\rho\sigma_v v_j}{2h_x h_v} u_{i-1,j-1} \\
&+ \left[\frac{1}{h_v^2}\left(\frac{\sigma_v^2}{2}v_j - \frac{h_v}{2h_x}\rho\sigma_v v_j\right) - \frac{\kappa(\theta - v_j)1_{\{v_j \geq \theta\}}}{h_v}\right] u_{i,j-1} \\
&+ \left[\frac{1}{h_x^2}\left(\frac{1}{2}v_j - \frac{h_x}{2h_v}\rho\sigma_v v_j\right) + \frac{v_j}{2h_x}\right] u_{i-1,j} \\
&+ \left[-\frac{1}{h_x^2}\left(v_j - \frac{h_x}{h_v}\rho\sigma_v v_j\right) - \frac{1}{h_v^2}\left(\sigma_v^2 v_j - \frac{h_v}{h_x}\rho\sigma_v v_j\right)\right. \\
&\quad \left. -\frac{\rho\sigma_v v_j}{h_x h_v} - \frac{1}{2h_x}v_j + \frac{\kappa(\theta - v_j)\mathrm{sign}(v_j - \theta)}{h_v}\right] u_{i,j} \\
&+ \frac{1}{h_x^2}\left(\frac{1}{2}v_j - \frac{h_x}{2h_v}\rho\sigma_v v_j\right) u_{i+1,j} \\
&+ \left[\frac{1}{h_v^2}\left(\frac{\sigma_v^2}{2}v_j - \frac{h_v}{2h_x}\rho\sigma_v v_j\right) + \frac{\kappa(\theta - v_j)1_{\{v_j < \theta\}}}{h_v}\right] u_{i,j+1} \\
&+ \frac{\rho\sigma_v v_j}{2h_x h_v} u_{i+1,j+1}.
\end{aligned} \tag{4.47}$$

4.3.3 Operator Splitting in Jump Step

For the jump step

$$\frac{\partial u}{\partial t}(x,v,t) = v\int_{|y|\geq\varepsilon}\left[u(x+y,v,t) - u(x,v,t) - \frac{\partial u}{\partial x}(x,v,t)(e^y - 1)\right]k(y)dy, \tag{4.48}$$

$$u(x,v,t)|_{t=t_n} = u_n^*,$$

$$\Longrightarrow u_{n+1},$$

let $u(x,v,t) - h(x,t) \to u(x,v,t)$, we have

$$\begin{aligned}
\frac{\partial u}{\partial t}(x,v,t) &= v\int_{|y|\geq\varepsilon}\left[u(x+y,v,t) - u(x,v,t) - \frac{\partial u}{\partial x}(x,v,t)(e^y - 1)\right]k(y)dy \\
&+ F(x,v,t),
\end{aligned} \tag{4.49}$$

where

$$F(x,v,t) = -\frac{\partial h}{\partial t}(x,t) + v\int_{|y|\geq\varepsilon}\left[h(x+y,t) - h(x,t) - \frac{\partial h}{\partial x}(x,t)(e^y-1)\right]k(y)dy, \tag{4.50}$$

with

$$u(x,v,t)|_{t=t_n} = u_n^* \text{ (or: } u_n^* - h(x,t) \text{),}$$

$$\Longrightarrow u_{n+1}.$$

Let $V = H^1_{-\mu}(\mathbb{R}\times\mathbb{R}_+)$ as defined similarly in the 1-D case. The variational formulation reads: find $u \in L^2(V;(0,T)) \cap H^1(V^*;(0,T))$, such that

$$\frac{d}{dt}(u(\cdot,t),w)_{L^2_{-\mu}(\mathbb{R}\times\mathbb{R}_+)} = (\mathcal{L}u(\cdot,t),w)_{V^*\times V} + (F(\cdot,t),w)_{V^*\times V},\ \forall w\in V, \tag{4.51}$$

$$u(\cdot,0) = 0.$$

where

$$(\mathcal{L}u,w)$$
$$= \int_{\mathbb{R}\times\mathbb{R}_+} v\int_{\varepsilon\leq|y|\leq R_j}\left[u(x+y,v,t) - u(x,v,t) - \frac{\partial u}{\partial x}(x,v,t)(e^y-1)\right]k(y)dywdxdv, \tag{4.52}$$

which can be written as

$$\mathbf{A} = \mathbf{J}^{(x)}\otimes\mathbf{M}_v^{(v)}$$

under the finite element discretization, where

$$\mathbf{M}^{(v)}_{v,(i,j)} = \int_{-R_v}^{R_v} v\psi_i(v)\psi_j(v)dv, \tag{4.53}$$

$$\mathbf{J}_{(i,j)}^{(x)} = \int_{-R_x}^{R_x} \int_{\varepsilon \le |y| \le R_J} \left[\psi_i(x+y) - \psi_i(x) - (e^y - 1) \frac{\partial \psi_i}{\partial x}(x) \right] k(y) dy \psi_j(x) dx. \tag{4.54}$$

Also

$$(F(\cdot,t), w)$$
$$= \int_{\mathbb{R}\times\mathbb{R}_+} v \int_{\varepsilon \le |y| \le R_j} \left[h(x+y,t) - h(x,t) - \frac{\partial h}{\partial x}(x,t)(e^y - 1) \right] k(y) dy w(x,v,t) dx dv, \tag{4.55}$$

which can be writen as

$$(F(\cdot,t), w) = H^{(x)} \otimes W_v^{(v)},$$

with

$$W_{v,i}^{(v)} = \int_{-R_v}^{R_v} v \psi_i(v) dv, \tag{4.56}$$

$$H_i^{(x)} = \int_{-R_x}^{R_x} \int_{\varepsilon \le |y| \le R_J} \left[h(x+y) - h(x) - (e^y - 1) \frac{\partial h}{\partial x}(x) \right] k(y) dy \psi_i(x) dx. \tag{4.57}$$

4.3.4 Results

The time changed Lévy process model (4.37)-(4.38) is computed with paramters $\sigma = 0.2, C = 0.05, G = M = 10, Y = 1.6,\ \kappa = 2.9, \sigma_v = 2.2, \rho = -0.4$ and $K = 10, \varepsilon = 10^{-5}, \Delta t = 0.1,\ T = 1$. The computing space domain is $[-6,6] \times [0,4]$, with 256×16 uniform grids.

As of the boundary conditions on the volatility v there is no exact rule which boundary conditions must be enforced. It is desirable to use a Neumann condition at

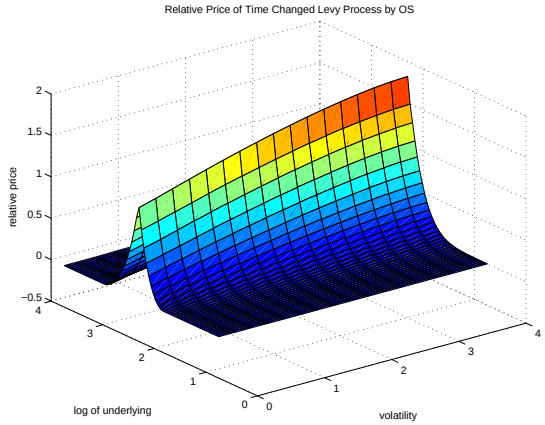

Figure 4.3: Relative European call prices of time changed Lévy process (4.37)-(4.38) by OS

$v = 0$ since if a Neumann condition is enforced at $v = 0$, it can be easily extended to the three space dimensional case. In the computation, $u_v|_{v=0} = 0.15$, and $u_v|_{v=4} = 0$ is enforced and the estimation meet the true behavior at $v = 0$ quite well. Finally the GMRES with restarts is used for the resulting linear equations.

For the time changed Lévy process model (4.37)-(4.38) the computing by operator splitting method takes 24.6 seconds on a Intel Celeron CPU 2.2GHz with 256MB of memory. Compared with the Carr-Madan FFT method, results show that the operator splitting method is numerically stable and has the monotonicity preserving property as in the case of a pure CGMY model. And the results also have fairly good accuracy in this case, where the boundary condition at $v = 0$ is estimated by a simplified Neumann condition. The relative prices and price difference by the operator splitting (OS) and FFT method are shown in Figure 4.3-4.4.

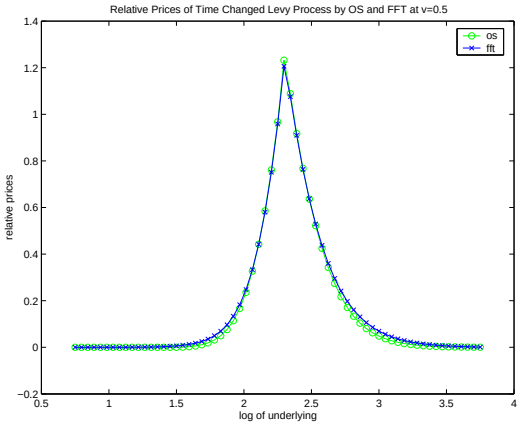

(a) Relative prices at v=0.5

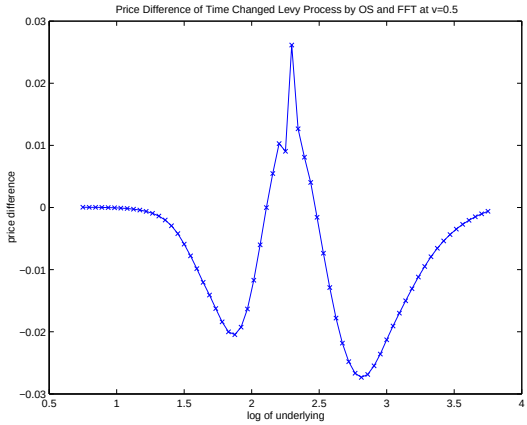

(b) Price difference at v=0.5

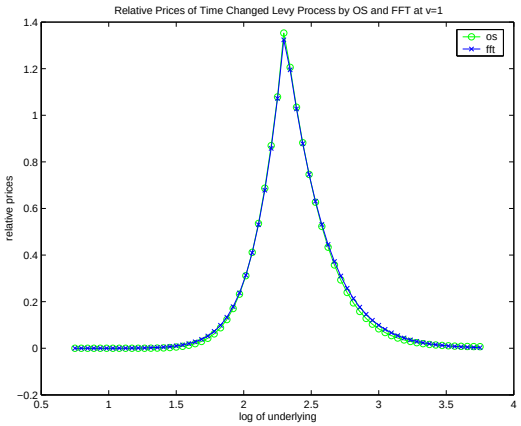

(c) Relative prices at v=1.0

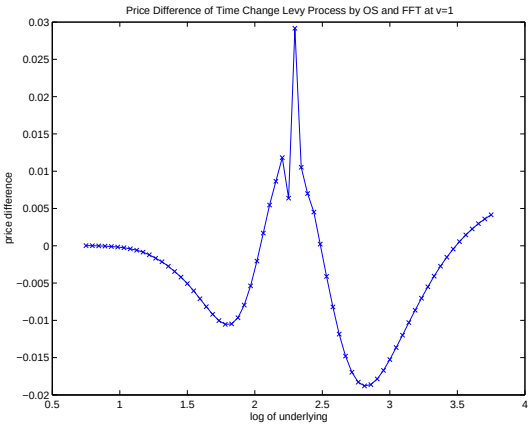

(d) Price difference at v=1.0

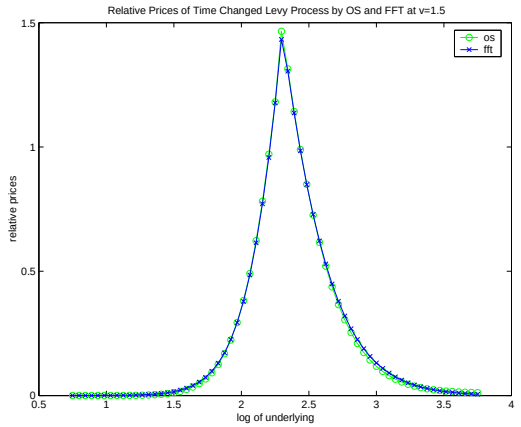

(e) Relative prices at v=1.5

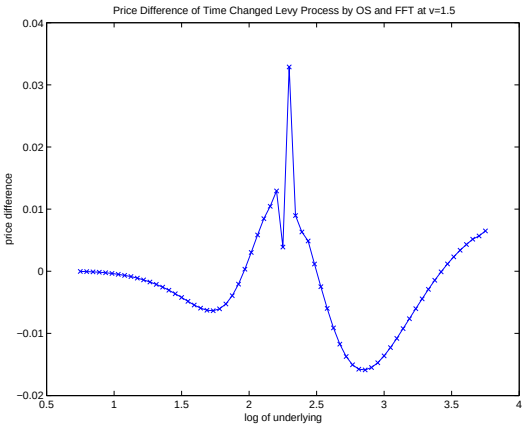

(f) Price difference at v=1.5

Figure 4.4: European call prices under time changed Lévy process (4.37)-(4.38) by OS and FFT

4.4 Operator Splitting for 3-D PIDEs

4.4.1 Stochastic Skew Model

In the stochastic skew model [CW04], the positive jumps and negative ones are further separated and treated independently:

$$X_t = rt + (L^R_{T^R_t} - \xi^R T^R_t) + (L^L_{T^L_t} - \xi^L T^L_t), \tag{4.58}$$

where $L^i_t = \sigma B^i_t + J^i_t, i = R, L$ denote Lévy processes that exhibit right (positive) and left (negative) skewness; $\xi^i, i = R, L$ denote convexity adjustments; and $v^i_t = \partial T^i_t / \partial t, i = R, L$ follow

$$dv^i_t = \kappa(1 - v^i_t)dt + \sigma_v \sqrt{v^i_t} dZ^i_t, \ i = R, L, \tag{4.59}$$

with $dB^i_t dZ^i_t = \rho^i dt, i = R, L$.

The corresponding PIDE has three variables in space dimension [Car04]:

$$\begin{aligned}
&\tfrac{\partial u}{\partial t}(x, v_R, v_L, t) + \left[r - \tfrac{\sigma^2(v_R + v_L)}{2} \right] \tfrac{\partial u}{\partial x}(x, v_R, v_L, t) \\
&+\kappa(1 - v_R)\tfrac{\partial u}{\partial v_R}(x, v_R, v_L, t) + \kappa(1 - v_L)\tfrac{\partial u}{\partial v_L}(x, v_R, v_L, t) \\
&+\tfrac{\sigma^2(v_R + v_L)}{2}\tfrac{\partial^2 u}{\partial x^2}(x, v_R, v_L, t) \\
&+\sigma\rho^R\sigma_V v_R \tfrac{\partial^2 u}{\partial x \partial v_R}(x, v_R, v_L, t) + \sigma\rho^L\sigma_V v_L \tfrac{\partial^2 u}{\partial x \partial v_L}(x, v_R, v_L, t) \\
&+\tfrac{\sigma_v^2 v_R}{2}\tfrac{\partial^2 u}{\partial v_R^2}(x, v_R, v_L, t) + \tfrac{\sigma_v^2 v_L}{2}\tfrac{\partial^2 u}{\partial v_L^2}(x, v_R, v_L, t) \\
&+v_R \textstyle\int_0^\infty \left[u(x + y, v_R, v_L, t) - u(x, v_R, v_L, t) - \tfrac{\partial u}{\partial x}(x, v_R, v_L, t)(e^y - 1) \right] k^R(y) dy \\
&+v_L \textstyle\int_{-\infty}^0 \left[u(x + y, v_R, v_L, t) - u(x, v_R, v_L, t) - \tfrac{\partial u}{\partial x}(x, v_R, v_L, t)(e^y - 1) \right] k^L(y) dy \\
&-ru(x, v_R, v_L, t) = 0.
\end{aligned} \tag{4.60}$$

Assuming $r = 0$ and after a change of variable $T - t \to t$, the 3-D PIDE becomes:

$$\begin{aligned}
&\frac{\partial u}{\partial t}(x, v_R, v_L, t) \\
&= -\frac{\sigma^2(v_R + v_L)}{2}\frac{\partial u}{\partial x}(x, v_R, v_L, t) + \kappa(1 - v_R)\frac{\partial u}{\partial v_R}(x, v_R, v_L, t) \\
&\quad +\kappa(1 - v_L)\frac{\partial u}{\partial v_L}(x, v_R, v_L, t) + \frac{\sigma^2(v_R + v_L)}{2}\frac{\partial^2 u}{\partial x^2}(x, v_R, v_L, t) \\
&\quad +\sigma\rho^R\sigma_V v_R\frac{\partial^2 u}{\partial x \partial v_R}(x, v_R, v_L, t) + \sigma\rho^L\sigma_V v_L\frac{\partial^2 u}{\partial x \partial v_L}(x, v_R, v_L, t) \\
&\quad +\frac{\sigma_v^2 v_R}{2}\frac{\partial^2 u}{\partial v_R^2}(x, v_R, v_L, t) + \frac{\sigma_v^2 v_L}{2}\frac{\partial^2 u}{\partial v_L^2}(x, v_R, v_L, t) \\
&\quad +v_R\int_0^\infty \left[u(x + y, v_R, v_L, t) - u(x, v_R, v_L, t) - \frac{\partial u}{\partial x}(x, v_R, v_L, t)(e^y - 1)\right] k^R(y)dy \\
&\quad +v_L\int_{-\infty}^0 \left[u(x + y, v_R, v_L, t) - u(x, v_R, v_L, t) - \frac{\partial u}{\partial x}(x, v_R, v_L, t)(e^y - 1)\right] k^L(y)dy,
\end{aligned} \tag{4.61}$$

with boundary conditions

$$u(x, v, 0) = (e^x - K)^+,$$

$$u(-\infty, v, t) = 0, \ \frac{\partial u}{\partial x}(x, v, t) = e^x, \text{ when } x \text{ is large,}$$

$$g_{1R}(u, u_t, u_x, u_{v_R}, u_{v_L}, \cdot)|_{v_R=0} = 0,$$

$$g_{2R}(u, u_t, u_x, u_{v_R}, u_{u_L}, \cdot)|_{v_R=\infty} = 0,$$

$$g_{1L}(u, u_t, u_x, u_{v_R}, u_{v_L}, \cdot)|_{v_L=0} = 0,$$

$$g_{2L}(u, u_t, u_x, u_{v_R}, u_{v_L}, \cdot)|_{v_L=\infty} = 0.$$

4.4.2 Operator Splitting in Diffusion Step

Let $\sigma_+^2(\varepsilon) = \int_0^\varepsilon y^2 k(y)dy$, $\sigma_-^2(\varepsilon) = \int_{-\varepsilon}^0 y^2 k(y)dy$. The diffusion step is

$$\frac{\partial u}{\partial t}(x, v_R, v_L, t) = -\frac{\sigma^2(v_R + v_L) + v_R\sigma_+^2(\varepsilon) + v_L\sigma_-^2(\varepsilon)}{2}\frac{\partial u}{\partial x}(x, v_R, v_L, t)$$

$$
\begin{aligned}
&+\kappa(1-v_R)\frac{\partial u}{\partial v_R}(x,v_R,v_L,t)+\kappa(1-v_L)\frac{\partial u}{\partial v_L}(x,v_R,v_L,t)\\
&+\frac{\sigma^2(v_R+v_L)+v_R\sigma_+^2(\varepsilon)+v_L\sigma_-^2(\varepsilon)}{2}\frac{\partial^2 u}{\partial x^2}(x,v_R,v_L,t)\\
&+\sigma\rho^R\sigma_V v_R\frac{\partial^2 u}{\partial x\partial v_R}(x,v_R,v_L,t)+\sigma\rho^L\sigma_V v_L\frac{\partial u}{\partial x\partial v_L}(x,v_R,v_L,t)\\
&+\frac{\sigma_v^2 v_R}{2}\frac{\partial^2 u}{\partial v_R^2}(x,v_R,v_L,t)+\frac{\sigma_v^2 v_L}{2}\frac{\partial^2 u}{\partial v_L^2}(x,v_R,v_L,t),
\end{aligned}
\tag{4.62}
$$

with

$$u(-\infty,v_R,v_L,t)=0,\ \frac{\partial u}{\partial x}(x,v_R,v_L,t)=e^x,\ \text{when } x \text{ is large,}$$

$$g_{1R}^D(u,u_t,u_x,u_{v_R},u_{v_L},\cdot)|_{v_R=0}=0,$$

$$g_{2R}^D(u,u_t,u_x,u_{v_R},u_{v_L},\cdot)|_{v_R=\infty}=0,$$

$$g_{1L}^D(u,u_t,u_x,u_{v_R},u_{v_L},\cdot)|_{v=0}=0,$$

$$g_{2L}^D(u,u_t,u_x,u_{v_R},u_{v_L},\cdot)|_{v=\infty}=0,$$

$$u(x,v_R,v_L,t)|_{t=t_n}=u_n,$$

$$\Longrightarrow u_n^*.$$

The g_{1i}^D, g_{2i}^D, $i=R,L$, denote the boundary conditions for the diffusion step at $v=0$ and $v=\infty$, respectively. Again note that g_{1i}^D, g_{2i}^D, $i=R,L$ are different from g_{1i}, g_{2i}, $i=R,L$.

The operator is discretized by the finite difference with a eleven-point stencil as the following. Denote $u_{i,j,k}, i=0,...,N_x, j=0,...,N_{v_R}, k=0,...,N_{v_L}$ be grid point values, let

$$\frac{\partial u}{\partial x}\approx\frac{u_{i,j,k}-u_{i-1,j,k}}{h_x},\tag{4.63}$$

$$\frac{\partial u}{\partial v_R} \approx \begin{cases} \frac{u_{i,j+1,k}-u_{i,j,k}}{h_{v_R}}, & 1-v_R \geq 0; \\ \frac{u_{i,j,k}-u_{i,j-1,k}}{h_{v_R}}, & 1-v_R < 0, \end{cases} \tag{4.64}$$

$$\frac{\partial u}{\partial v_L} \approx \begin{cases} \frac{u_{i,j,k+1}-u_{i,j,k}}{h_{v_L}}, & 1-v_L \geq 0; \\ \frac{u_{i,j,k}-u_{i,j,k-1}}{h_{v_L}}, & 1-v_L < 0, \end{cases} \tag{4.65}$$

$$\frac{\partial^2 u}{\partial x^2} \approx \frac{u_{i+1,j,k} - 2u_{i,j,k} + u_{i-1,j,k}}{h_x^2}, \tag{4.66}$$

$$\frac{\partial^2 u}{\partial v_R^2} \approx \frac{u_{i,j+1,k} - 2u_{i,j,k} + u_{i,j-1,k}}{h_{v_R}^2}, \tag{4.67}$$

$$\frac{\partial^2 u}{\partial v_L^2} \approx \frac{u_{i,j,k+1} - 2u_{i,j,k} + u_{i,j,k-1}}{h_{v_L}^2}, \tag{4.68}$$

$$\frac{\partial^2 u}{\partial x \partial v_R} \approx \frac{u_{i+1,j+1,k} - 2u_{i,j,k} + u_{i-1,j-1,k}}{2h_x h_{v_R}} - \frac{h_x}{2h_{v_R}}\frac{\partial^2 u}{\partial x^2} - \frac{h_{v_R}}{2h_x}\frac{\partial^2 u}{\partial v_R^2}, \tag{4.69}$$

$$\frac{\partial^2 u}{\partial x \partial v_L} \approx \frac{u_{i+1,j,k+1} - 2u_{i,j,k} + u_{i-1,j,k-1}}{2h_x h_{v_L}} - \frac{h_x}{2h_{v_L}}\frac{\partial^2 u}{\partial x^2} - \frac{h_{v_L}}{2h_x}\frac{\partial^2 u}{\partial v_L^2}, \tag{4.70}$$

Then

$$\begin{aligned} \mathcal{L}u \approx\ & \frac{\sigma\rho^L\sigma_v v_L}{2h_x h_{v_L}} u_{i-1,j,k-1} \\ +\ & \left[\frac{1}{h_{v_L}^2}\left(\frac{\sigma_v^2}{2}v_L - \frac{h_{v_L}}{2h_x}\sigma\rho^L\sigma_v v_L\right) - \frac{\kappa(1-v_L)1_{\{1-v_L<0\}}}{h_{v_L}}\right] u_{i,j,k-1} \\ +\ & \frac{\sigma\rho^R\sigma_v v_R}{2h_x h_{v_R}} u_{i-1,j-1,k} \\ +\ & \left[\frac{1}{h_{v_R}^2}\left(\frac{\sigma_v^2}{2}v_R - \frac{h_{v_R}}{2h_x}\sigma\rho^R\sigma_v v_R\right) - \frac{\kappa(1-v_R)1_{\{1-v_R<0\}}}{h_{v_R}}\right] u_{i,j-1,k} \end{aligned}$$

$$
\begin{aligned}
&+ \left\{ \frac{1}{h_x^2} \left[\frac{\sigma^2(v_R+v_L)}{2} - \frac{h_x}{2h_{v_R}} \sigma\rho^R \sigma_v v_R - \frac{h_x}{2h_{v_L}} \sigma\rho^L \sigma_v v_L \right] + \frac{\sigma^2(v_R+v_L)}{2h_x} \right\} u_{i-1,j,k} \\
&+ \left\{ -\frac{1}{h_x^2} \left[\sigma^2(v_R+v_L) - \frac{h_x}{h_{v_R}} \sigma\rho^R \sigma_v v_R - \frac{h_x}{h_{v_L}} \sigma\rho^L \sigma_v v_L \right] \right. \\
&\quad - \frac{1}{h_{v_R}^2} \left(\sigma_v^2 v_R - \frac{h_{v_R}}{h_x} \sigma\rho^R \sigma_v v_R \right) - \frac{1}{h_{v_L}^2} \left(\sigma_v^2 v_L - \frac{h_{v_L}}{h_x} \sigma\rho^L \sigma_v v_L \right) \\
&\quad - \frac{\sigma\rho^R \sigma_v v_R}{h_x h_{v_R}} - \frac{\sigma\rho^L \sigma_v v_L}{h_x h_{v_L}} - \frac{\sigma^2(v_R+v_L)}{2h_x} \\
&\quad \left. - \frac{\kappa(1-v_R)\mathrm{sign}(1-v_R)}{h_{v_R}} - \frac{\kappa(1-v_L)\mathrm{sign}(1-v_L)}{h_{v_L}} \right\} u_{i,j,k} \\
&+ \frac{1}{h_x^2} \left[\frac{\sigma^2(v_R+v_L)}{2} - \frac{h_x}{2h_{v_R}} \sigma\rho^R \sigma_v v_R - \frac{h_x}{2h_{v_L}} \sigma\rho^L \sigma_v v_L \right] u_{i+1,j,k} \\
&+ \left[\frac{1}{h_{v_R}^2} \left(\frac{\sigma_v^2}{2} v_R - \frac{h_{v_R}}{2h_x} \sigma\rho^R \sigma_v v_R \right) + \frac{\kappa(1-v_R)1_{\{1-v_R \geq 0\}}}{h_{v_R}} \right] u_{i,j+1,k} \\
&+ \frac{\sigma\rho^R \sigma_v v_R}{2h_x h_{v_R}} u_{i+1,j+1,k} \\
&+ \left[\frac{1}{h_{v_L}^2} \left(\frac{\sigma_v^2}{2} v_L - \frac{h_{v_L}}{2h_x} \sigma\rho^L \sigma_v v_L \right) + \frac{\kappa(1-v_L)1_{\{1-v_L \geq 0\}}}{h_{v_L}} \right] u_{i,j,k+1} \\
&+ \frac{\sigma\rho^L \sigma_v v_L}{2h_x h_{v_L}} u_{i+1,j,k+1}. \qquad (4.71)
\end{aligned}
$$

4.4.3 Operator Splitting in Jump Step

The jump step is

$$
\begin{aligned}
&\frac{\partial u}{\partial t}(x, v_R, v_L, t) \\
&= v_R \int_\varepsilon^\infty \left[u(x+y, v_R, v_L, t) - u(x, v_R, v_L, t) - \frac{\partial u}{\partial x}(x, v_R, v_L, t)(e^y - 1) \right] k^R(y) dy \\
&\quad + v_L \int_{-\infty}^{-\varepsilon} \left[u(x+y, v_R, v_L, t) - u(x, v_R, v_L, t) - \frac{\partial u}{\partial x}(x, v_R, v_L, t)(e^y - 1) \right] k^L(y) dy,
\end{aligned} \qquad (4.72)
$$

with

$$
u(x, v_R, v_L, t)|_{t=t_n} = u_n^*, \implies u_{n+1}.
$$

Let $u(x, v_R, v_L, t) - h(x,t) \to u(x, v_R, v_L, t)$, we have

$$\begin{aligned}
&\frac{\partial u}{\partial t}(x, v_R, v_L, t) + \frac{\partial h}{\partial t}(x,t) \\
&= v_R \int_\varepsilon^\infty \left[u(x+y, v_R, v_L, t) - u(x, v_R, v_L, t) - \frac{\partial u}{\partial x}(x, v_R, v_L, t)(e^y - 1) \right] k^R(y) dy \\
&\quad + v_R \int_\varepsilon^\infty \left[h(x+y, t) - h(x,t) - \frac{\partial h}{\partial x}(x,t)(e^y - 1) \right] k^R(y) dy \\
&\quad + v_L \int_{-\infty}^{-\varepsilon} \left[u(x+y, v_R, v_L, t) - u(x, v_R, v_L, t) - \frac{\partial u}{\partial x}(x, v_R, v_L, t)(e^y - 1) \right] k^L(y) dy \\
&\quad + v_L \int_{-\infty}^{-\varepsilon} \left[h(x+y, t) - h(x,t) - \frac{\partial h}{\partial x}(x,t)(e^y - 1) \right] k^L(y) dy. \qquad (4.73)
\end{aligned}$$

That is

$$\begin{aligned}
&\frac{\partial u}{\partial t}(x, v_R, v_L, t) \\
&= v_R \int_\varepsilon^\infty \left[u(x+y, v_R, v_L, t) - u(x, v_R, v_L, t) - \frac{\partial u}{\partial x}(x, v_R, v_L, t)(e^y - 1) \right] k^R(y) dy \\
&\quad + v_L \int_{-\infty}^{-\varepsilon} \left[u(x+y, v_R, v_L, t) - u(x, v_R, v_L, t) - \frac{\partial u}{\partial x}(x, v_R, v_L, t)(e^y - 1) \right] k^L(y) dy \\
&\quad + F(x, v_R, v_L, t), \qquad (4.74)
\end{aligned}$$

where

$$\begin{aligned}
F(x, v_R, v_L, t) &= -\frac{\partial h}{\partial t}(x,t) \\
&+ v_R \int_\varepsilon^\infty \left[h(x+y, t) - h(x,t) - \frac{\partial h}{\partial x}(x,t)(e^y - 1) \right] k^R(y) dy \\
&+ v_L \int_{-\infty}^{-\varepsilon} \left[h(x+y, t) - h(x,t) - \frac{\partial h}{\partial x}(x,t)(e^y - 1) \right] k^L(y) dy, \qquad (4.75)
\end{aligned}$$

with

$$u(x, v_R, v_L, t)|_{t=t_n} = u_n^* \text{ (or: } u_n^* - h(x,t) \text{) },$$

$$\Longrightarrow u^{n+1}.$$

Let $V = H^1_{-\mu}(\mathbb{R} \times \mathbb{R}^2_+)$ as defined similarly in the 1-D case. The variational formulation reads: find $u \in L^2(V;(0,T)) \cap H^1(V^*;(0,T))$, such that

$$\frac{d}{dt}(u(\cdot,t),w)_{L^2_{-\mu}(\mathbb{R}\times\mathbb{R}^2_+)} = (\mathcal{L}u(\cdot,t),w)_{V^*\times V} + (F(\cdot,t),w)_{V^*\times V},\ \forall w \in V, \tag{4.76}$$

$$u(\cdot,0) = 0.$$

where

$$\begin{aligned}
(\mathcal{L}u,w) &= \int_{\mathbb{R}\times\mathbb{R}^2_+} v_R \int_\varepsilon^\infty \Big[\, u(x+y,v_R,v_L,t) - u(x,v_R,v_L,t) \\
&\qquad -\frac{\partial u}{\partial x}(x,v_R,v_L,t)(e^y-1)\Big] k(y)dy w(x,v_R,v_L,t)dxdv_Rdv_L \\
&+ \int_{\mathbb{R}\times\mathbb{R}^2_+} v_L \int_{-\infty}^{-\varepsilon} \Big[\, u(x+y,v_R,v_L,t) - u(x,v_R,v_L,t) \\
&\qquad -\frac{\partial u}{\partial x}(x,v_R,v_L,t)(e^y-1)\Big] k(y)dy w(x,v_R,v_L,t)dxdv_Rdv_L.
\end{aligned} \tag{4.77}$$

The stiffness matrix is given by

$$\mathbf{A} = \mathbf{J}^{(\mathbf{x}+)} \otimes \mathbf{M}^{(\mathbf{v_R})}_{\mathbf{v_R}} \otimes \mathbf{M}^{(\mathbf{v_L})} + \mathbf{J}^{(\mathbf{x}-)} \otimes \mathbf{M}^{(\mathbf{v_R})} \otimes \mathbf{M}^{(\mathbf{v_L})}_{\mathbf{v_L}},$$

where

$$\mathbf{M}^{(v)}_{v,(i,j)} = \int_{-R_v}^{R_v} v\psi_i(v)\psi_j(v)dv, \tag{4.78}$$

$$\mathbf{M}^{(v)}_{(i,j)} = \int_{-R_v}^{R_v} \psi_i(v)\psi_j(v)dv, \tag{4.79}$$

$$\mathbf{J}^{(x+)}_{(i,j)} = \int_{-R_x}^{R_x}\int_\varepsilon^{R_J} \left[\psi_i(x+y) - \psi_i(x) - (e^y-1)\frac{\partial\psi_i}{\partial x}(x)\right] k(y)dy\psi_j(x)dx, \tag{4.80}$$

$$\mathbf{J}^{(x-)}_{(i,j)} = \int_{-R_x}^{R_x}\int_{-R_J}^{-\varepsilon} \left[\psi_i(x+y) - \psi_i(x) - (e^y-1)\frac{\partial\psi_i}{\partial x}(x)\right] k(y)dy\psi_j(x)dx. \tag{4.81}$$

For the right hand side,

$$
\begin{aligned}
&(F(\cdot,t),w)\\
&= \int_{\mathbb{R}\times\mathbb{R}^2_+} v_R \int_{\varepsilon}^{\infty} \left[h(x+y,t)-h(x,t)-\frac{\partial h}{\partial x}(x,t)(e^y-1)\right] k(y)dywdxdv_Rdv_L\\
&\quad + \int_{\mathbb{R}\times\mathbb{R}^2_+} v_L \int_{-\infty}^{-\varepsilon} \left[h(x+y,t)-h(x,t)-\frac{\partial h}{\partial x}(x,t)(e^y-1)\right] k(y)dywdxdv_Rdv_L.
\end{aligned}
\tag{4.82}
$$

The above equation can be writen as

$$
(F(\cdot,t),w) = H^{(x+)} \otimes W^{(v_R)}_{v_R} \otimes W^{(v_L)} + H^{(x-)} \otimes W^{(v_R)} \otimes W^{(v_L)}_{v_L},
$$

with

$$
W^{(v)}_{v,i} = \int_{-R_v}^{R_v} v\psi_i(v)dv, \tag{4.83}
$$

$$
W^{(v)}_{i} = \int_{-R_v}^{R_v} \psi_i(v)dv, \tag{4.84}
$$

$$
H^{(x+)}_i = \int_{-R_x}^{R_x}\int_{\varepsilon}^{R_J} \left[h(x+y)-h(x)-(e^y-1)\frac{\partial h}{\partial x}(x)\right] k(y)dy\psi_i(x)dx, \tag{4.85}
$$

$$
H^{(x-)}_i = \int_{-R_x}^{R_x}\int_{-R_J}^{-\varepsilon} \left[h(x+y)-h(x)-(e^y-1)\frac{\partial h}{\partial x}(x)\right] k(y)dy\psi_i(x)dx. \tag{4.86}
$$

4.4.4 Results

A stochastic skew model is computed with paramters $\sigma = 0.2$, $C = 0.05$, $G = M = 10$, $Y = 1.6$, $\kappa = 2.9$, $\sigma_v = 2.2$, $\rho^R = \rho^L = -0.4$ and $K = 10$, $\varepsilon = 10^{-5}$, $\Delta t = 0.1$, $T = 1$. The computing space domain is $[-6,6]\times[0,4]\times[0,4]$, with $256\times16\times16$ uniform grids.

Same as in the case of 2-D PIDEs, there is no exact rule that certain boundary conditions on the volatility v_R and v_L must be enforced. It is desirable to use

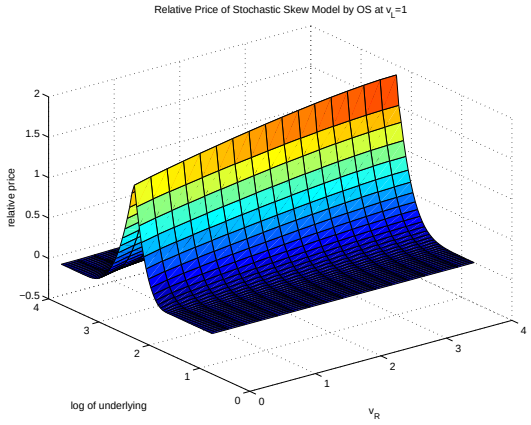

Figure 4.5: Relative European call prices of stochastic skew model by OS at v_L=1

Neumann conditions at $v_R = 0$, $v_L = 0$ since it greatly reduces the complexity on the boundary conditions. If not, every boundary condition is again a time dependent PDE problem with two space dimensions, which makes the original problem more inextricable.

In the computation, $u_{v_i}|_{v_i=0} = 0.15$, and $u_{v_i}|_{v_i=4} = 0$, $i = R, L$ are enforced and the estimation meets the true behavior at $v_i = 0, i = R, L$ quite well. Finally GMRES with restarts is used for the resulting linear equations and the results are compared with the Carr-Madan FFT method.

For the stochastic skew model, the computation by the operator splitting takes 130 minutes on a SUN SPARC Ultra-60 workstation with 512MB of memory. The results show that the operator splitting method is numerically stable and has the monotonicity preserving property as in the lower dimensional cases. And the results also have fairly good accuracy in this case, where the boundary conditions at $v_i = 0, i = R, L$ are estimated by simplified Neumann conditions. The relative prices and price difference by the OS and FFT method are shown in Figure 4.5-4.8.

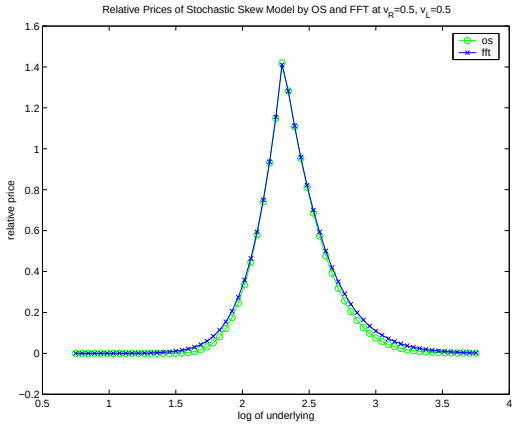

(a) Relative prices at $v_L = 0.5$

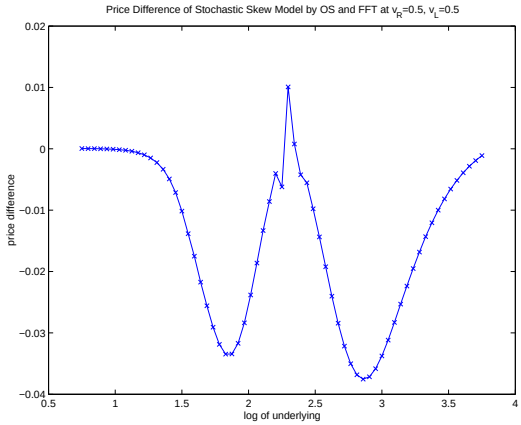

(b) Price difference at $v_L = 0.5$

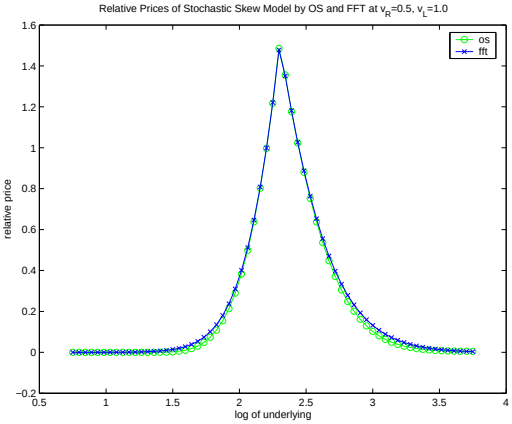

(c) Relative prices at $v_L = 1.0$

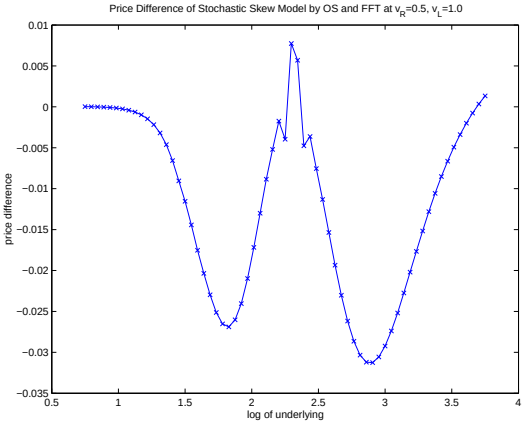

(d) Price difference at $v_L = 1.0$

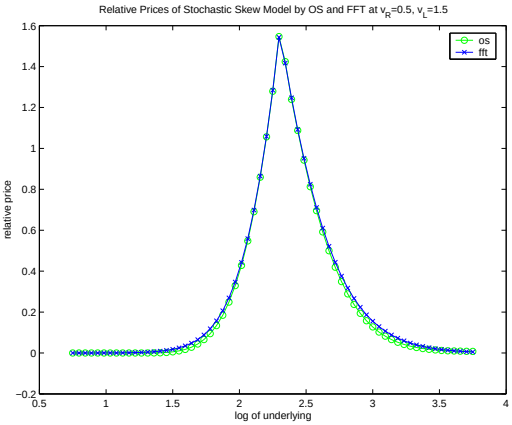

(e) Relative prices at $v_L = 1.5$

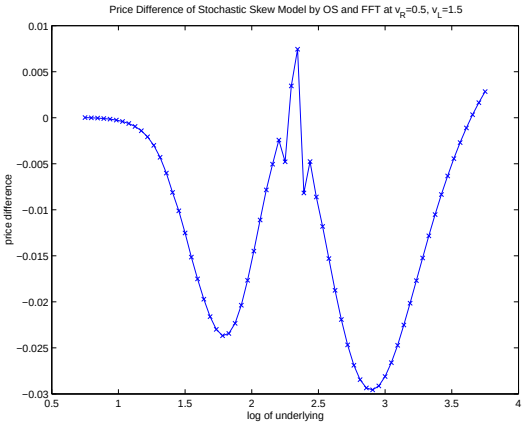

(f) Price difference at $v_L = 1.5$

Figure 4.6: European call prices under stochastic skew model by OS and FFT at $v_R = 0.5$

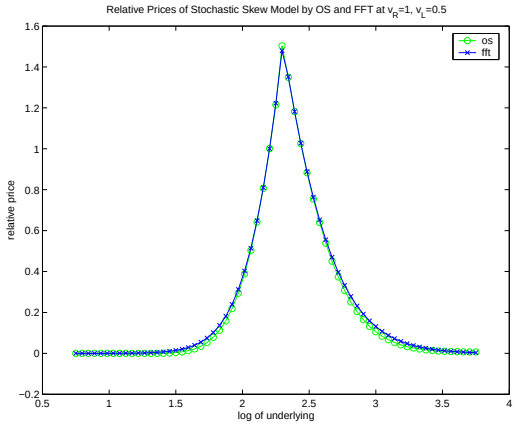

(a) Relative prices at $v_L = 0.5$

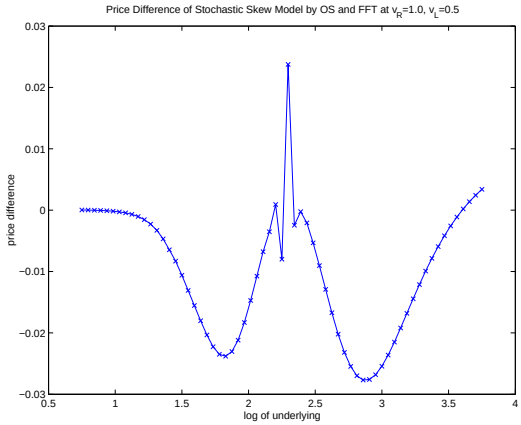

(b) Price difference at $v_L = 0.5$

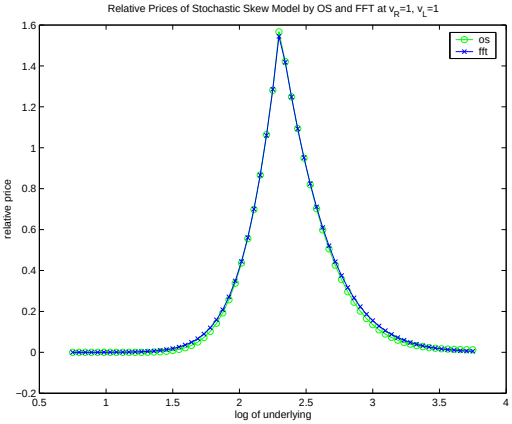

(c) Relative prices at $v_L = 1.0$

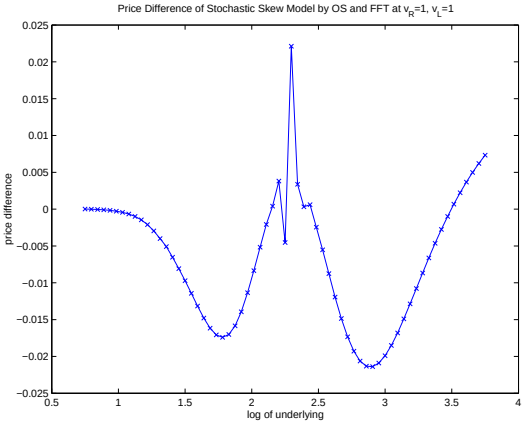

(d) Price difference at $v_L = 1.0$

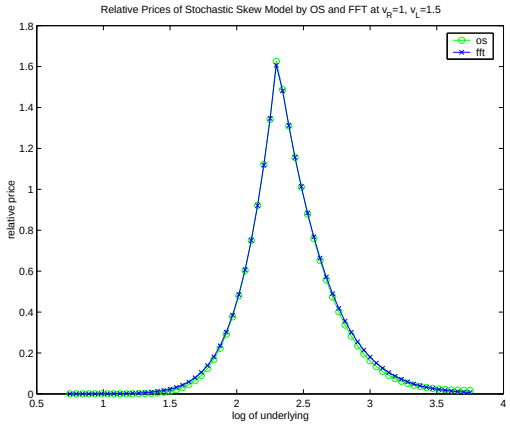

(e) Relative prices at $v_L = 1.5$

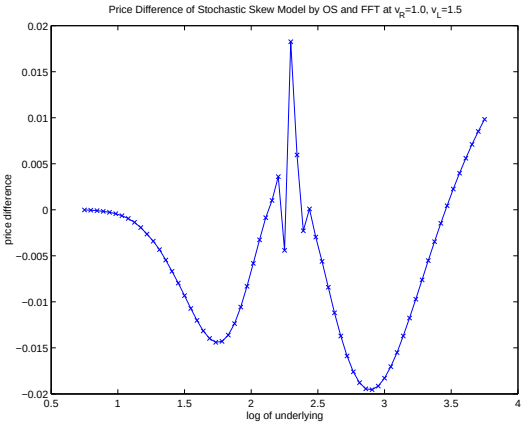

(f) Price difference at $v_L = 1.5$

Figure 4.7: European call prices under stochastic skew model by OS and FFT at $v_R = 1.0$

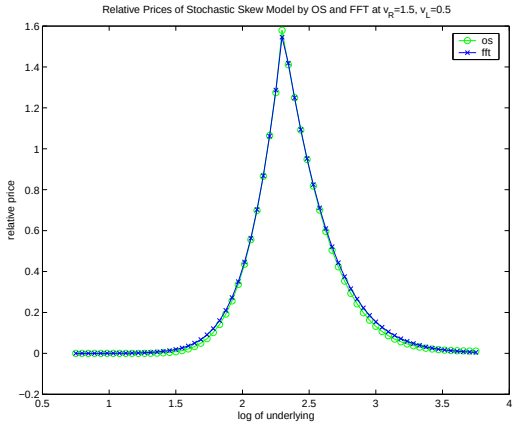

(a) Relative prices at $v_L = 0.5$

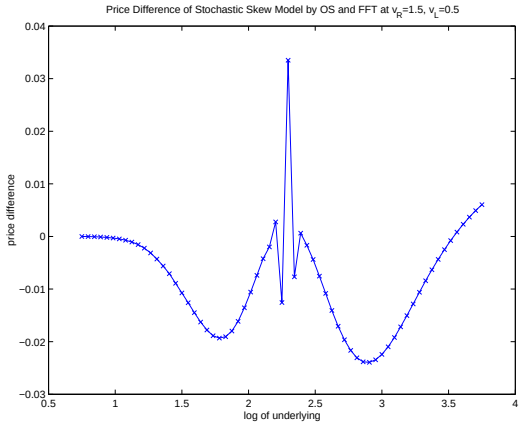

(b) Price difference at $v_L = 0.5$

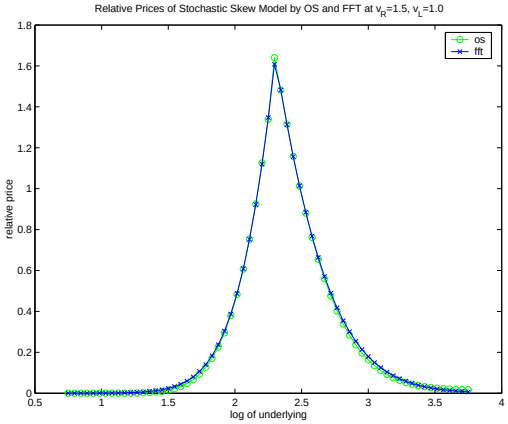

(c) Relative prices at $v_L = 1.0$

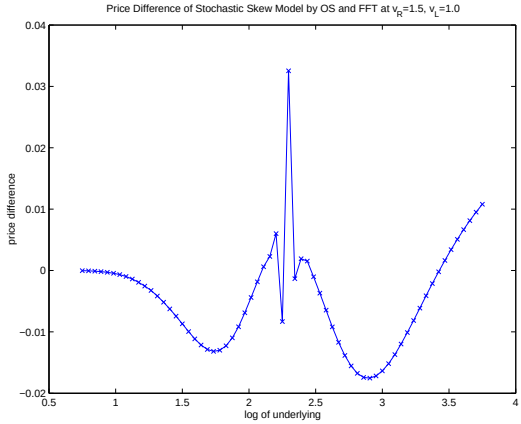

(d) Price difference at $v_L = 1.0$

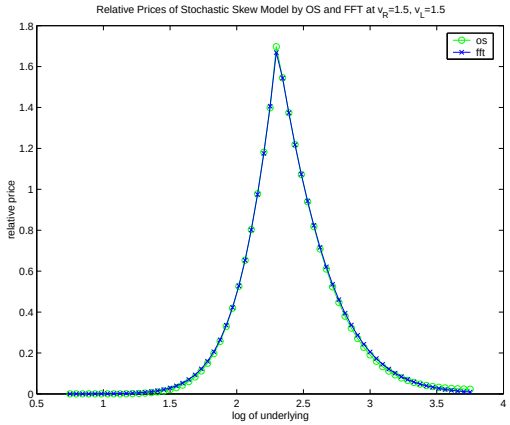

(e) Relative prices at $v_L = 1.5$

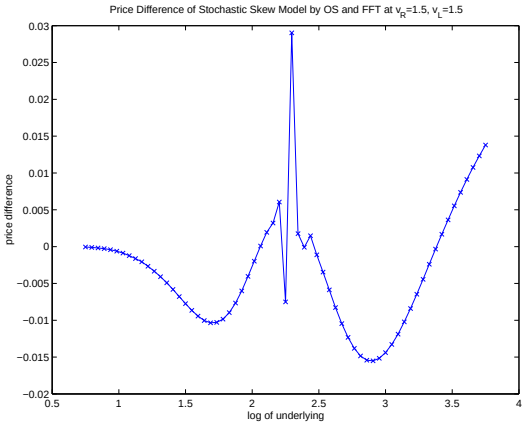

(f) Price difference at $v_L = 1.5$

Figure 4.8: European call prices under stochastic skew model by OS and FFT at $v_R = 1.5$

4.5 Concluding Remarks

In this chapter an operator splitting method is proposed to solve partial integro-differential equations in high space dimensions. It uses a finite difference scheme to solve the diffusion part. The main reason to choose the finite difference is its monotonicity preserving property and its superiority in handling convection-diffusion type evolution partial differential equations. On the other hand, the method uses a finite element scheme on the jump part since the finite element discretization of the integral operator readily results in a sparse matrix.

The computations are carried out for the partial integro-differential equations with one, two, and three space dimensions and the results show that the operator splitting method is numerically stable and has the monotonicity preserving property with fairly good accuracy, compared with the Carr-Madan FFT approach on European options.

The method has the same limitations as the other operator splitting methods when dealing with boundary conditions. Generally adjustments are needed on the boundary conditions for every substep. Based on the fact that the current literature does not have an agreement on what exact boundary conditions on volatility dimensions should be enforced on those partial differential equations, the boundary conditions are estimated by simplified Neumann conditions. Furthermore, the problem of the boundary conditions and the rigid analysis of stability of the scheme are open for further research.

Appendix A

Characteristic Functions of Log Stock Price for Stochastic Volatility Models

A.1 Heston Model

The Heston model for stock price under risk neutral measure is [Hes93]

$$dS_t = (r-q)S_t dt + \sqrt{v_t} S_t dB_t^{(1)},$$

$$dv_t = \kappa(\theta - v_t)dt + \beta\sqrt{v_t} dB_t^{(2)},$$

with $dB_t^{(1)} dB_t^{(2)} = \rho dt$, where q denotes the dividend yield, κ denotes the rate of mean reversion, θ denotes the long term mean and β denotes the volatility of the process v_t. The characteristic function of log stock price is

$$\phi_{Heston}(u; t, \kappa, \theta, \beta, \sigma_0^2, \rho, S_0) = \exp(iu(\log(S_0) + (r-q)t) - b(t)\sigma_0^2 - c(t)), \quad \text{(A.1)}$$

where

$$b(t) = \frac{2\psi(1 - \mathrm{e}^{-\eta t})}{2\eta - (\eta - \kappa^*)(1 - \mathrm{e}^{-\eta t})}, \quad \text{(A.2)}$$

$$c(t) = \frac{\kappa\theta}{\beta^2}\left[2\ln\left(1 - \frac{\eta - \kappa^*}{2\eta}(1 - \mathrm{e}^{-\eta t})\right) + (\eta - \kappa^*)t\right], \quad \text{(A.3)}$$

with $\eta = \sqrt{(\kappa^*)^2 + 2\beta^2\psi}$, $\kappa^* = \kappa - iu\beta\rho$, $\psi = (iu + u^2)/2$.

A.2 Bates Model

The Bates model for stock price under risk neutral measure is [Bat96]

$$dS_t = (r - q - \lambda\zeta)S_t dt + \sqrt{v_t} S_t dB_t^{(1)} + JS_t dq_t \ ,$$

$$dv_t = \kappa(\theta - v_t)dt + \beta\sqrt{v_t} dB_t^{(2)},$$

with $\mathrm{E}[dB_t^{(1)} dB_t^{(2)}] = \rho$, and $\zeta = \exp(\mu + \frac{1}{2}\delta^2) - 1$. q_t is a Poisson process with arrival rate λv_t, and J denotes jump size with $\log(1 + J) \sim N(\mu, \delta^2)$. The characteristic function of log stock price is

$$\begin{aligned} \phi_{Bates}(u; t, \kappa, \theta, \beta, \sigma_0^2, \rho, \lambda, \mu, \delta, S_0) &= \exp(iu(\log(S_0) + (r - q)t) - b(t)\sigma_0^2 - c(t)) \\ &\times \exp\left(-iut\lambda(\mathrm{e}^{\mu + \frac{1}{2}\delta^2} - 1) + t\lambda(\mathrm{e}^{-\frac{1}{2}\delta^2 u^2 + iu\mu} - 1)\right), \end{aligned} \tag{A.4}$$

with $b(t)$, $c(t)$ as in (A.2)-(A.3).

A.3 BNS Model with Gamma SV (BNSSG)

The BNSSG model for log stock price under risk neutral measure is [BNNS02]:

$$dx_t = (r - q - \lambda k(-\rho) - \frac{1}{2}\sigma_t^2)dt + \sigma_t dB_t + \rho dZ_t, \tag{A.5}$$

where Z_t is a background driving Lévy process independent of B_t, and σ_t^2 follows

$$d\sigma_t^2 = -\lambda\sigma_t^2 dt + dZ_t,$$

with a marginal Gamma(a, b) law. The associated cumulant function of Z_t is $k(u) = -au(b + u)^{-1}$. The characteristic function of log stock price is

$$\phi_{BNSSG}(u; t, \rho, \lambda, a, b, \sigma_0^2, S_0) = \exp(iu(\log(S_0) + (r - q - a\lambda\rho(b - \rho)^{-1})t))$$

$$\begin{aligned} &\times \quad \exp\left(-\frac{1}{2}\lambda^{-1}(u^2+iu)(1-\mathrm{e}^{-\lambda t})\sigma_0^2\right) \\ &\times \quad \exp\left(a(b-f_2)^{-1}\left(b\log\left(\frac{b-f_1}{b-iu\rho}\right)+f_2\lambda t\right)\right), \end{aligned} \tag{A.6}$$

with

$$f_1 = iu\rho - \frac{1}{2}(u^2+iu)(1-\mathrm{e}^{-\lambda t}), \tag{A.7}$$

$$f_2 = iu\rho - \frac{1}{2}(u^2+iu). \tag{A.8}$$

A.4 BNS Model with IG SV (BNSSIG)

The BNSSIG model for log stock price follows (A.5) and σ_t^2 follows [BNNS02],

$$d\sigma_t^2 = -\lambda\sigma_t^2 dt + dZ_t,$$

with a marginal inverse Gamma IG(a,b) law. The associated cumulant function of Z_t is $k(u) = -uab^{-1}(1+2ub^{-2})^{-1/2}$. The characteristic function of log stock price is

$$\begin{aligned} &\phi_{BNSSIG}(u;t,\rho,\lambda,a,b,\sigma_0^2,S_0) \\ &= \quad \exp(iu(\log(S_0)+(r-q-\rho\lambda ab^{-1}(1-2\rho b^{-2})^{-1/2})t)) \\ &\times \quad \exp\left(-\frac{1}{2}\lambda^{-1}(u^2+iu)(1-\mathrm{e}^{-\lambda t})\sigma_0^2\right) \\ &\times \quad \exp\left(a\left(\sqrt{b^2-2f_1}-\sqrt{b^2-2iu\rho}\right)\right) \\ &\times \quad \exp\left(\frac{2af_2}{\sqrt{2f_2-b^2}}\left(\arctan\left(\sqrt{\frac{b^2-2iu\rho}{2f_2-b^2}}\right)-\arctan\left(\sqrt{\frac{b^2-2f_1}{2f_2-b^2}}\right)\right)\right), \end{aligned} \tag{A.9}$$

with f_1,f_2 as in (A.7)-(A.8).

A.5 NIGSA Model

The construction of the NIGSA and models hereafter can be found in [CGMY03].

$$\begin{aligned}\phi_{NIGSA}(u;t,\sigma,\nu,\theta,\kappa,\eta,\lambda,S_0) &= \exp(iu(\log(S_0)+(r-q)t)) \\ &\times \frac{\Phi_{CIR}(-i\psi_{NIG}(u;1,\nu,\theta),t,\sigma;\kappa,\eta,\lambda)}{\Phi_{CIR}(-i\psi_{NIG}(-i;1,\nu,\theta),t,\sigma;\kappa,\eta,\lambda)^{iu}},\end{aligned} \tag{A.10}$$

where

$$\psi_{NIG}(u;\sigma,\nu,\theta)=\sigma\left(\frac{\nu}{\sigma}-\sqrt{\frac{\nu^2}{\sigma^2}-\frac{2\theta iu}{\sigma^2}+u^2}\right), \tag{A.11}$$

and

$$\Phi_{CIR}(u,t,y_0;\kappa,\eta,\lambda)=\frac{\exp(\frac{\kappa^2\eta t}{\lambda^2})}{\left(\cosh(\frac{\gamma t}{2})+\frac{\kappa}{\gamma}\sinh(\frac{\gamma t}{2})\right)^{\frac{2\kappa\eta}{\lambda^2}}}\exp\left(\frac{2iuy_0}{\kappa+\gamma\coth(\frac{\gamma t}{2})}\right), \tag{A.12}$$

with $\gamma=\sqrt{\kappa^2-2\lambda^2 iu}$.

A.6 VSGA Model

$$\begin{aligned}\phi_{VGSA}(u;t,C,G,M,\kappa,\eta,\lambda,S_0) &= \exp(iu(\log(S_0)+(r-q)t)) \\ &\times \frac{\Phi_{CIR}(-i\psi_{VG}(u;1,G,M),t,C;\kappa,\eta,\lambda)}{\Phi_{CIR}(-i\psi_{VG}(-i;1,G,M),t,C;\kappa,\eta,\lambda)^{iu}},\end{aligned} \tag{A.13}$$

where

$$\psi_{VG}(u;C,G,M)=C\log\left(\frac{GM}{GM+(M-G)iu+u^2}\right), \tag{A.14}$$

and $\Phi_{CIR}(u,t,y_0;\kappa,\eta,\lambda)$ as in (A.12).

A.7 CGMYSA Model

$$\begin{aligned}
&\phi_{CGMYSA}(u;t,C,G,M,Y_p,Y_n,\zeta,\kappa,\eta,\lambda,S_0) \\
&\quad = \exp(iu(\log(S_0)+(r-q)t)) \\
&\quad \times \frac{\Phi_{CIR}(-i\psi_{CGMY}(u;1,G,M,Y_p,Y_n,\zeta),t,C;\kappa,\eta,\lambda)}{\Phi_{CIR}(-i\psi_{CGMY}(-i;1,G,M,Y_p,Y_n,\zeta),t,C;\kappa,\eta,\lambda)^{iu}}\,, \qquad \text{(A.15)}
\end{aligned}$$

where

$$\begin{aligned}
&\psi_{CGMY}(u;C,G,M,Y_p,Y_n,\zeta) \\
&\quad = C\left[\Gamma(-Y_p)\left((M-iu)^{Y_p}-M^{Y_p}\right)+\zeta\Gamma(-Y_n)\left((G+iu)^{Y_n}-G^{Y_n}\right)\right],
\end{aligned} \qquad \text{(A.16)}$$

with $\Phi_{CIR}(u,t,y_0;\kappa,\eta,\lambda)$ as in (A.12).

A.8 NIGSAM Model

$$\begin{aligned}
&\phi_{NIGSAM}(u;t,\sigma,\nu,\theta,\kappa,\eta,\lambda,S_0) \\
&\quad = \exp(iu(\log(S_0)+(r-q)t)) \\
&\quad \times \Phi_{CIR}[-i\psi_{NIG}(u;1,\nu,\theta)-u\psi_{NIG}(-i;1,\nu,\theta),t,\sigma;\kappa,\eta,\lambda], \qquad \text{(A.17)}
\end{aligned}$$

with $\psi_{NIG}(u;\sigma,\nu,\theta)$ as in (A.11) and $\Phi_{CIR}(u,t,y_0;\kappa,\eta,\lambda)$ as in (A.12).

A.9 VGSAM Model

$$\begin{aligned}
&\phi_{VGSAM}(u;t,C,G,M,\kappa,\eta,\lambda,S_0) \\
&\quad = \exp(iu(\log(S_0)+(r-q)t)) \\
&\quad \times \Phi_{CIR}[-i\psi_{VG}(u;1,G,M)-u\psi_{VG}(-i;1,G,M),t,C;\kappa,\eta,\lambda], \qquad \text{(A.18)}
\end{aligned}$$

with $\psi_{VG}(u;C,G,M)$ as in (A.14) and $\Phi_{CIR}(u,t,y_0;\kappa,\eta,\lambda)$ as in (A.12).

A.10 CGMYSAM Model

$$\begin{aligned}
&\phi_{CGMYSAM}(u;t,C,G,M,Y_p,Y_n,\zeta,\kappa,\eta,\lambda,S_0) \\
&\quad = \exp(iu(\log(S_0)+(r-q)t)) \\
&\quad \times \Phi_{CIR}[-i\psi_{CGMY}(u;1,G,M,Y_p,Y_n,\zeta)-u\psi_{CGMY}(-i;1,G,M,Y_p,Y_n,\zeta),t,C;\kappa,\eta,\lambda], \qquad \text{(A.19)}
\end{aligned}$$

with $\psi_{CGMY}(u;C,G,M,Y_p,Y_n,\zeta)$ as in (A.16) and $\Phi_{CIR}(u,t,y_0;\kappa,\eta,\lambda)$ as in (A.12).

A.11 NIGSG Model

$$\begin{aligned}
\phi_{NIGSG}(u;t,\sigma,\nu,\theta,\kappa,\lambda,\zeta,\rho,S_0) &= \exp(iu(\log(S_0)+(r-q)t)) \\
&\quad \times \Phi_{SG}(-i\psi_{NIG}(u;\sigma,\nu,\theta),\rho u;t,\kappa,\lambda,\zeta)
\end{aligned}$$

$$\times \quad \Phi_{SG}(-i\psi_{NIG}(-i;\sigma,\nu,\theta),-i\rho;t,\kappa,\lambda,\zeta)^{-iu}, \tag{A.20}$$

where

$$\begin{aligned}\Phi_{SG}(a,b;t,\kappa,\lambda,\zeta) &= \exp\left(iay_0\frac{1-\mathrm{e}^{-\kappa t}}{\kappa}\right)\\ &\times \exp\left(\Psi_{SG}\left(b+a\frac{1-\mathrm{e}^{-\kappa t}}{\kappa},a,b;\kappa,\lambda,\zeta\right)-\Psi_{SG}(b,a,b;\kappa,\lambda,\zeta)\right),\end{aligned} \tag{A.21}$$

with

$$\Psi_{SG}(x,a,b;\kappa,\lambda,\zeta)=\log\left[\left(x+\frac{i}{\zeta}\right)^{\frac{\lambda}{\kappa-i\zeta(a+\kappa b)}}(a+\kappa b-\kappa x)^{\frac{\lambda(a+\kappa b)\zeta}{\kappa((a+\kappa b)\zeta+i\kappa)}}\right], \tag{A.22}$$

and $\psi_{NIG}(u;\sigma,\nu,\theta)$ as in (A.11).

A.12 VGSG Model

$$\begin{aligned}\phi_{VGSG}(u;t,C,G,M,\kappa,\lambda,\zeta,\rho,S_0) &= \exp(iu(\log(S_0)+(r-q)t))\\ &\times \Phi_{SG}(-i\psi_{VG}(u;C,G,M),\rho u;t,\kappa,\lambda,\zeta)\\ &\times \Phi_{SG}(-i\psi_{VG}(-i;C,G,M),-i\rho;t,\kappa,\lambda,\zeta)^{-iu},\end{aligned} \tag{A.23}$$

where

$$\begin{aligned}\Phi_{SG}(a,b;t,\kappa,\lambda,\zeta) &= \exp\left(iay_0\frac{1-\mathrm{e}^{-\kappa t}}{\kappa}\right)\\ &\times \exp\left(\Psi_{SG}\left(b+a\frac{1-\mathrm{e}^{-\kappa t}}{\kappa},a,b;\kappa,\lambda,\zeta\right)-\Psi_{SG}(b,a,b,\kappa,\lambda,\zeta)\right),\end{aligned} \tag{A.24}$$

with $\Psi_{SG}(x, a, b; \kappa, \lambda, \zeta)$ as in (A.22) and $\psi_{VG}(u; C, G, M)$ as in (A.14).

A.13 NIGIG Model

$$\begin{aligned}\phi_{NIGIG}(u; t, \sigma, \nu, \theta, \kappa, \mu, \rho, S_0) &= \exp(iu(\log(S_0) + (r-q)t)) \\ &\times \Phi_{IG}(-i\psi_{NIG}(u; \sigma, \nu, \theta), \rho u; t, \kappa, \mu) \\ &\times \Phi_{IG}(-i\psi_{NIG}(-i; \sigma, \nu, \theta), -i\rho; t, \kappa, \mu)^{-iu},\end{aligned} \tag{A.25}$$

where

$$\begin{aligned}\Phi_{IG}(a, b; t, \kappa, \mu) &= \exp\left(iay_0 \frac{1 - \mathrm{e}^{-\kappa t}}{\kappa}\right) \\ &\times \exp\left(\Psi_{IG}\left(b + a\frac{1 - \mathrm{e}^{-\kappa t}}{\kappa}, a, b; \kappa, \mu\right) - \Psi_{IG}(b, a, b; \kappa, \mu)\right),\end{aligned} \tag{A.26}$$

with

$$\begin{aligned}\Psi_{IG}(x, a, b; \kappa, \mu) &= \frac{2\sqrt{\mu^2 - 2ix}}{\kappa} - \frac{\mu \log(a + \kappa b - \kappa x)}{\kappa} \\ &+ \frac{2\sqrt{\mu^2\kappa - 2i(a + \kappa b)}}{\kappa^{3/2}} \operatorname{arctanh}\left[\frac{\sqrt{\kappa}\sqrt{\mu^2 - 2ix}}{\sqrt{\mu^2\kappa - 2i(a + \kappa b)}}\right],\end{aligned} \tag{A.27}$$

and $\psi_{NIG}(u; \sigma, \nu, \theta)$ as in (A.11).

A.14 VGIG Model

$$\begin{aligned}\phi_{VGIG}(u;t,C,G,M,\kappa,\mu,\rho,S_0) &= \exp(iu(\log(S_0)+(r-q)t)) \\ &\times \Phi_{IG}(-i\psi_{VG}(u;C,G,M),\rho u;t,\kappa,\mu) \\ &\times \Phi_{IG}(-i\psi_{VG}(-i;C,G,M),-i\rho;t,\kappa,\mu)^{-iu},\end{aligned} \tag{A.28}$$

where

$$\begin{aligned}\Phi_{IG}(a,b;t,\kappa,\mu) &= \exp\left(iay_0\frac{1-\mathrm{e}^{-\kappa t}}{\kappa}\right) \\ &\times \exp\left(\Psi_{IG}\left(b+a\frac{1-\mathrm{e}^{-\kappa t}}{\kappa},a,b;\kappa,\mu\right)-\Psi_{IG}(b,a,b;\kappa,\mu)\right),\end{aligned} \tag{A.29}$$

with $\Psi_{IG}(x,a,b;\kappa,\mu)$ as in (A.27) and $\psi_{VG}(u;C,G,M)$ as in (A.14).

A.15 NIGSIG Model

$$\begin{aligned}\phi_{NIGSIG}(u;t,\sigma,\nu,\theta,\kappa,\mu,\rho,S_0) &= \exp(iu(\log(S_0)+(r-q)t)) \\ &\times \Phi_{SIG}(-i\psi_{NIG}(u;\sigma,\nu,\theta),\rho u;t,\kappa,\mu) \\ &\times \Phi_{SIG}(-i\psi_{NIG}(-i;\sigma,\nu,\theta),-i\rho;t,\kappa,\mu)^{-iu},\end{aligned} \tag{A.30}$$

where

$$\Phi_{SIG}(a,b;t,\kappa,\mu) = \exp\left(iay_0\frac{1-\mathrm{e}^{-\kappa t}}{\kappa}\right)$$

$$\times \quad \exp\left(\Psi_{SIG}\left(b + a\frac{1-\mathrm{e}^{-\kappa t}}{\kappa}, a, b; \kappa, \mu\right) - \Psi_{SIG}(b, a, b; \kappa, \mu)\right), \tag{A.31}$$

with

$$\begin{aligned}&\Psi_{SIG}(x, a, b; \kappa, \mu)\\ &\quad = \frac{\sqrt{\mu^2 - 2ix}}{\kappa} - \frac{2i(a+\kappa b)}{\kappa^{3/2}\sqrt{\mu^2\kappa - 2i(a+\kappa b)}}\operatorname{arctanh}\left[\frac{\sqrt{\kappa}\sqrt{\mu^2 - 2ix}}{\sqrt{\mu^2\kappa - 2i(a+\kappa b)}}\right],\end{aligned} \tag{A.32}$$

and $\psi_{NIG}(u; \sigma, \nu, \theta)$ as in (A.11).

A.16 VGSIG Model

$$\begin{aligned}\phi_{VGSIG}(u; t, C, G, M, \kappa, \mu, \rho, S_0) &= \exp(iu(\log(S_0) + (r-q)t))\\ &\times \Phi_{SIG}(-i\psi_{VG}(u; C, G, M), \rho u; t, \kappa, \mu)\\ &\times \Phi_{SIG}(-i\psi_{VG}(-i; C, G, M), -i\rho; t, \kappa, \mu)^{-iu},\end{aligned} \tag{A.33}$$

where

$$\begin{aligned}\Phi_{SIG}(a, b; t, \kappa, \mu) &= \exp\left(iay_0\frac{1-\mathrm{e}^{-\kappa t}}{\kappa}\right)\\ &\times \exp\left(\Psi_{SIG}\left(b + a\frac{1-\mathrm{e}^{-\kappa t}}{\kappa}, a, b; \kappa, \mu\right) - \Psi_{SIG}(b, a, b; \kappa, \mu)\right),\end{aligned} \tag{A.34}$$

with $\Psi_{SIG}(x, a, b; \kappa, \mu)$ as in (A.32) and $\psi_{VG}(u; C, G, M)$ as in (A.14).

Appendix B

Some Treatments of Parabolic Integro-Differential Equations

B.1 Finite Difference Discretization of 2-D Diffusion Operator

Inserting the finite difference schemes (4.42)-(4.46) into equation (4.41) gives

$$\begin{aligned}\mathcal{L}u \approx & \left(\frac{1}{2}v_j - \frac{h_x}{2h_v}\rho\sigma_v v_j\right)\frac{u_{i+1,j} - 2u_{i,j} + u_{i-1,j}}{h_x^2} \\ & + \left(\frac{\sigma_v^2}{2}v_j - \frac{h_v}{2h_x}\rho\sigma_v v_j\right)\frac{u_{i,j+1} - 2u_{i,j} + u_{i,j-1}}{h_v^2} \\ & + \rho\sigma_v v_j\frac{u_{i+1,j+1} - 2u_{i,j} + u_{i-1,j-1}}{2h_x h_v} - \frac{1}{2}v_j\frac{u_{i,j} - u_{i-1,j}}{h_x} \\ & + \kappa(\theta - v_j)1_{\{v_j \geq \theta\}}\frac{u_{i,j} - u_{i,j-1}}{h_v} + \kappa(\theta - v_j)1_{\{v_j < \theta\}}\frac{u_{i,j+1} - u_{i,j}}{h_v}.\end{aligned} \tag{B.1}$$

Rearranging the terms gives equation (4.47).

B.2 Finite Difference Discretization of 3-D Diffusion Operator

Inserting the finite difference schemes (4.63)-(4.70) into equation (4.62) gives

$$\begin{aligned}\mathcal{L}u \approx & \left[\frac{\sigma^2(v_R + v_L)}{2} - \frac{h_x}{2h_{v_R}}\sigma\rho^R\sigma_v v_R - \frac{h_x}{2h_{v_L}}\sigma\rho^L\sigma_v v_L\right]\frac{u_{i+1,j,k} - 2u_{i,j,k} + u_{i-1,j,k}}{h_x^2} \\ + & \left(\frac{\sigma_v^2}{2}v_R - \frac{h_{v_R}}{2h_x}\sigma\rho^R\sigma_v v_R\right)\frac{u_{i,j+1,k} - 2u_{i,j,k} + u_{i,j-1,k}}{h_{v_R}^2} \\ + & \left(\frac{\sigma_v^2}{2}v_L - \frac{h_{v_L}}{2h_x}\sigma\rho^L\sigma_v v_L\right)\frac{u_{i,j,k+1} - 2u_{i,j,k} + u_{i,j,k-1}}{h_{v_L}^2} \\ + & \sigma\rho^R\sigma_v v_R\frac{u_{i+1,j+1,k} - 2u_{i,j,k} + u_{i-1,j-1,k}}{2h_x h_{v_R}} \\ + & \sigma\rho^L\sigma_v v_L\frac{u_{i+1,j,k+1} - 2u_{i,j,k} + u_{i-1,j,k-1}}{2h_x h_{v_L}}\end{aligned}$$

$$
\begin{aligned}
- \quad & \frac{\sigma^2(v_R+v_L)}{2}\frac{u_{i,j,k}-u_{i-1,j,k}}{h_x} \\
+ \quad & \kappa(1-v_R)1_{\{1-v_R\geq 0\}}\frac{u_{i,j+1,k}-u_{i,j,k}}{h_{v_R}} + \kappa(1-v_R)1_{\{1-v_R<0\}}\frac{u_{i,j,k}-u_{i,j-1,k}}{h_{v_R}} \\
+ \quad & \kappa(1-v_L)1_{\{1-v_L\geq 0\}}\frac{u_{i,j,k+1}-u_{i,j,k}}{h_{v_L}} + \kappa(1-v_L)1_{\{1-v_L<0\}}\frac{u_{i,j,k}-u_{i,j,k-1}}{h_{v_L}}.
\end{aligned}
\tag{B.2}
$$

Rearranging the terms gives equation (4.71).

B.3 Estimation of $Q_i^{(h)}(y)$ When y Is Small

For a better understanding of $Q_i^{(h)}(y)$ of (4.34),

$$
Q_i(y,t) = \int_{-R_x}^{R_x} h(x+y,t) - h(x,t) - (e^y-1)\frac{\partial h}{\partial x}(x,t)]\psi_i(x)dx, \tag{B.3}
$$

when $0 < y < \log K - rt + R_x$, compute

$$
\begin{aligned}
Q_i(y,t) &= \int_{\log K-rt-y}^{R_x}(e^{x+y}-Ke^{-rt})\psi_i(x)dx \\
&\quad - \int_{-R_x}^{R_x}[h(x,t)+(e^y-1)\frac{\partial h}{\partial x}(x,t)]\psi_i(x)dx \\
&= \int_{\log K-rt-y}^{\log K-rt}(e^{x+y}-Ke^{-rt})\psi_i(x)dx,
\end{aligned}
\tag{B.4}
$$

$$
\begin{aligned}
\frac{d}{dy}Q_i(y,t) &= (e^{x+y}-Ke^{-rt})\psi_i(x)|_{\log K-rt-y} \\
&\quad + \int_{\log K-rt-y}^{\log K-rt} e^{x+y}\psi_i(x)dx \\
&= e^y\int_{\log K-rt-y}^{\log K-rt} e^x\psi_i(x)dx,
\end{aligned}
\tag{B.5}
$$

$$
\begin{aligned}
\frac{d^2}{dy^2}Q_i(y,t) &= e^y e^x\psi_i(x)|_{\log K-rt-y} + e^y\int_{\log K-rt-y}^{\log K-rt} e^x\psi_i(x)dx \\
&= Ke^{-rt}\psi_i(\log K-rt-y) + e^y\int_{\log K-rt-y}^{\log K-rt} e^x\psi_i(x)dx,
\end{aligned}
\tag{B.6}
$$

and

$$\begin{aligned}\frac{d^3}{dy^3}Q_i(y,t) &= -Ke^{-rt}\frac{d}{dx}\psi_i(\log K - rt - y) \\ &+ Ke^{-rt}\psi_i(\log K - rt - y) \\ &+ e^y \int_{\log K - rt - y}^{\log K - rt} e^x \psi_i(x)dx. \end{aligned} \tag{B.7}$$

For y close to zero ($0 < y < 10^{-5}$, theoretically and empirically), $Q_i(y,t)$ can be estimated by the truncated polynomial

$$Q_i(y,t) = \frac{1}{2}y^2\frac{d^2}{dy^2}Q_i(0,t) = \frac{1}{2}y^2 Ke^{-rt}\psi_i(\log K - rt), \tag{B.8}$$

since $Q_i(0,t) = 0, \frac{d}{dy}Q_i(0,t) = 0$.

B.4 Itó's Lemma for Lévy Processes

Theorem B.4.1 *Let $\{X_t; t \geq 0\}$ be a d-dimensional Lévy process with the generating triplet (A, ν, γ). For C^2 function $f : [0,T] \times \mathbb{R}^d \to \mathbb{R}$ we have*

$$\begin{aligned} f(t, X_t) &= f(0, X_0) + \int_0^t \frac{\partial f}{\partial s}(s, X_s)ds + \int_0^t \sum_{i=1}^d \frac{\partial f}{\partial x_i}(s, X_s)dX_s^i \\ &+ \frac{1}{2}\int_0^t \sum_{i,j=1}^d A_{ij}\frac{\partial^2 f}{\partial x_i \partial x_j}(s, X_s)ds \\ &+ \int_0^t \int_{\mathbb{R}^d} \left(f(s, X_s + y) - f(s, X_s) - \sum_{i=1}^d y_i \frac{\partial f}{\partial x_i}(s, X_s) \right) \mu(dy, ds), \end{aligned} \tag{B.9}$$

where μ is the Poisson random measure associated with $\{X_t; t \geq 0\}$.

Appendix C

Parameter Estimates for Stochastic Volatility Models on S&P 500 Monthly Second Monday Data

2001	κ	θ	β	σ_0^2	ρ	ape
Jan	2.9437	0.0648	0.8456	0.0803	-0.6989	0.0089
Feb	1.9132	0.0530	0.3874	0.0373	-0.7597	0.0082
Mar	2.3453	0.0601	0.5787	0.0717	-0.7728	0.0185
Apr	6.8102	0.0582	1.4897	0.1268	-0.6561	0.0129
May	2.9171	0.0475	0.4665	0.0497	-0.7209	0.0061
Jun	4.6184	0.0492	0.7487	0.0438	-0.6825	0.0067
Jul	3.3421	0.0393	0.2297	0.0299	-0.9393	0.0139
Aug	3.0228	0.0436	0.3806	0.0339	-0.7991	0.0096
Sep	5.0427	0.0540	1.0816	0.1063	-0.6718	0.0135
Oct	6.3050	0.0546	1.2170	0.1186	-0.6941	0.0082
Nov	3.9335	0.0543	0.5832	0.0682	-0.8068	0.0081
Dec	4.4344	0.0506	0.6120	0.0499	-0.7447	0.0058
2002	κ	θ	β	σ_0^2	ρ	ape
Jan	3.9979	0.0556	0.8217	0.0555	-0.7247	0.0069
Feb	3.4298	0.0441	0.3554	0.0333	-0.9136	0.0085
Mar	2.4213	0.0359	0.1711	0.0259	-1.0000	0.0101
Apr	8.7672	0.0274	0.2987	0.0335	-1.0000	0.0109
May	7.3879	0.0332	0.3179	0.0387	-1.0000	0.0091
Jun	9.8858	0.0359	0.5579	0.0550	-0.8347	0.0108
Jul	7.7349	0.0388	0.6633	0.0794	-0.7421	0.0113
Aug	4.9613	0.0441	0.5488	0.1273	-0.6878	0.0101
Sep	3.6552	0.0530	0.5879	0.1136	-0.7523	0.0117
Oct	3.6098	0.0638	0.6128	0.1438	-0.7606	0.0105
Nov	7.4011	0.0614	1.1592	0.1252	-0.7008	0.0104
Dec	3.3994	0.0574	0.4307	0.0833	-0.7159	0.0102

Table C.1: Parameter estimates for Heston model on S&P 500 monthly second Monday data

2001	κ	θ	β	σ_0^2	ρ	λ	μ	δ	ape
Jan	5.9495	0.0170	0.1887	0.0689	-0.8712	0.3014	-0.3263	0.2433	0.0082
Feb	0.2743	0.0772	0.2239	0.0324	-0.7588	0.2493	-0.0980	0.1489	0.0060
Mar	2.0437	0.0581	0.4865	0.0679	-0.8743	0.1845	0.0644	0.0809	0.0177
Apr	8.2720	0.0167	0.7388	0.1030	-0.3918	0.4013	-0.2756	0.1769	0.0113
May	1.5488	0.0339	0.3119	0.0399	-0.6792	0.3399	-0.1219	0.1423	0.0049
Jun	0.9470	0.0262	0.2046	0.0302	-0.5883	0.2883	-0.2070	0.1704	0.0036
Jul	1.3434	0.0407	0.1617	0.0303	-0.8620	0.2161	-0.0095	0.0807	0.0123
Aug	0.3648	0.0444	0.1874	0.0263	-0.6499	0.2902	-0.1861	0.0751	0.0078
Sep	5.5538	0.0223	0.9720	0.0891	-0.4968	0.4597	-0.2163	0.1327	0.0112
Oct	6.1291	0.0229	1.0121	0.0965	-0.4901	0.3807	-0.2502	0.1339	0.0060
Nov	2.9896	0.0350	0.5032	0.0546	-0.6900	0.4419	-0.1394	0.1446	0.0065
Dec	2.3181	0.0367	0.3821	0.0395	-0.6618	0.3147	-0.1491	0.1436	0.0052
2002	κ	θ	β	σ_0^2	ρ	λ	μ	δ	ape
Jan	2.6173	0.0240	0.3489	0.0380	-0.5738	0.2922	-0.2473	0.1988	0.0043
Feb	0.6708	0.0413	0.2122	0.0261	-0.6988	0.3488	-0.1676	0.0654	0.0077
Mar	1.6234	0.0356	0.1644	0.0249	-0.8743	0.2298	-0.0350	0.0824	0.0098
Apr	7.4184	0.0208	0.2129	0.0284	-0.9611	0.3660	-0.1283	0.0389	0.0101
May	3.6495	0.0227	0.1428	0.0293	-0.9671	0.3317	-0.1732	0.0000	0.0081
Jun	7.5504	0.0212	0.3915	0.0423	-0.5950	0.4608	-0.1730	0.0412	0.0089
Jul	7.2779	0.0180	0.5785	0.0632	-0.4492	0.6991	-0.1455	0.0952	0.0084
Aug	5.1145	0.0216	0.5471	0.1109	-0.4905	0.4878	-0.2070	0.0651	0.0087
Sep	2.9389	0.0252	0.5702	0.0892	-0.5791	0.3783	-0.2567	0.0000	0.0094
Oct	3.6497	0.0280	0.6044	0.1194	-0.5771	0.5790	-0.2032	0.1414	0.0068
Nov	6.2220	0.0221	0.8802	0.0924	-0.3902	0.4712	-0.2690	0.0968	0.0077
Dec	2.4107	0.0374	0.2913	0.0665	-0.7166	0.3947	-0.2018	0.0471	0.0097

Table C.2: Parameter estimates for Bates model on S&P 500 monthly second Monday data

2001	ρ	λ	a	b	σ_0^2	*ape*
Jan	-2.6766	1.1956	0.5116	15.9751	0.0445	0.0211
Feb	-3.5438	1.8018	0.8599	45.9339	0.0258	0.0095
Mar	-3.4591	4.0229	0.2723	30.3379	0.0594	0.0240
Apr	-3.7612	6.6975	0.1911	36.1461	0.0945	0.0177
May	-3.3991	1.6906	0.6244	35.3312	0.0358	0.0087
Jun	-5.7592	1.6194	1.0091	66.0018	0.0257	0.0044
Jul	-2.6073	0.6808	2.3588	44.7918	0.0235	0.0178
Aug	-3.8397	1.0292	1.3598	47.6968	0.0223	0.0115
Sep	-3.8168	5.0090	0.2027	31.7570	0.0802	0.0271
Oct	-4.0736	4.3277	0.2389	34.0704	0.0791	0.0155
Nov	-3.6225	2.1731	0.5136	34.3880	0.0471	0.0124
Dec	-3.3491	1.2603	0.8901	33.8362	0.0322	0.0085
2002	ρ	λ	a	b	σ_0^2	*ape*
Jan	-4.3607	1.6650	0.6535	37.4382	0.0317	0.0067
Feb	-3.0424	0.6338	1.7928	33.3987	0.0220	0.0127
Mar	-2.5954	0.3723	4.4818	44.1304	0.0183	0.0129
Apr	-5.0474	0.8363	2.3609	108.9459	0.0220	0.0136
May	-5.3412	1.0008	2.0130	96.3475	0.0248	0.0116
Jun	-4.7230	1.3652	0.9664	64.4450	0.0324	0.0152
Jul	-3.1256	3.0982	0.4400	47.4841	0.0533	0.0201
Aug	-3.6161	5.1141	0.3249	51.3816	0.1112	0.0157
Sep	-4.5143	3.9027	0.3344	42.9040	0.0903	0.0174
Oct	-5.4301	4.5198	0.3331	46.5674	0.1198	0.0154
Nov	-3.5629	4.8357	0.2992	37.1958	0.0881	0.0165
Dec	-2.5854	1.7348	0.6008	26.2752	0.0623	0.0156

Table C.3: Parameter estimates for BNSSG model on S&P 500 monthly second Monday data

2001	ρ	λ	a	b	σ_0^2	*ape*
Jan	-0.2696	0.0294	7.0071	0.6073	0.0363	0.0378
Feb	-0.1933	0.0299	11.4853	0.7974	0.0256	0.0162
Mar	-0.2583	0.0294	7.9176	0.6391	0.0333	0.0534
Apr	-0.2531	0.0309	7.2014	0.6532	0.0386	0.0600
May	-0.2021	0.0301	9.4455	0.7780	0.0299	0.0190
Jun	-0.2005	0.0177	21.9718	0.8208	0.0261	0.0126
Jul	-0.1730	0.0257	14.0294	0.9899	0.0258	0.0206
Aug	-0.2023	0.0191	19.2892	0.9252	0.0237	0.0183
Sep	-0.2421	0.0328	6.1986	0.6820	0.0386	0.0792
Oct	-0.2284	0.0253	12.1782	0.7162	0.0352	0.0410
Nov	-0.2099	0.0358	8.4075	0.7603	0.0351	0.0229
Dec	-0.1865	0.0245	16.5899	0.8123	0.0297	0.0138
2002	ρ	λ	a	b	σ_0^2	*ape*
Jan	-0.2222	0.0258	11.9981	0.7313	0.0275	0.0187
Feb	-0.1940	0.0338	6.2194	0.7960	0.0287	0.0201
Mar	-0.1567	0.0240	19.7918	1.0316	0.0217	0.0126
Apr	-0.1239	0.0265	11.5132	0.9375	0.0235	0.0159
May	-0.1692	0.0134	31.0958	1.0548	0.0256	0.0161
Jun	-0.1614	0.0194	14.4179	0.8646	0.0298	0.0263
Jul	-0.1948	0.0241	6.4185	0.7941	0.0347	0.0433
Aug	-0.1884	0.0214	7.8643	0.8083	0.0491	0.0554
Sep	-0.2270	0.0269	7.9793	0.7196	0.0464	0.0483
Oct	-0.2305	0.0320	8.3072	0.7111	0.0560	0.0571
Nov	-0.2223	0.0341	8.5614	0.7311	0.0438	0.0390
Dec	-0.1948	0.0389	6.9387	0.7942	0.0479	0.0272

Table C.4: Parameter estimates for BNSSIG model on S&P 500 monthly second Monday data

2001	σ	ν	θ	κ	η	λ	*ape*
Jan	0.8952	10.3627	-4.8622	5.7315	0.3649	3.2572	0.0129
Feb	0.6246	16.7447	-7.4642	1.3633	0.3171	1.0368	0.0071
Mar	1.3018	18.1673	-6.2003	4.5960	0.5345	3.4058	0.0224
Apr	1.1544	8.6808	-5.6606	12.1128	0.2961	3.6250	0.0128
May	0.7575	16.5797	-7.7752	2.5613	0.3662	1.3042	0.0049
Jun	0.4549	11.4617	-6.8433	1.4851	0.2484	0.7412	0.0042
Jul	1.1330	36.9311	-12.3784	2.2781	0.6829	-1.2237	0.0134
Aug	0.5721	17.4502	-8.7704	2.1216	0.3603	1.0410	0.0086
Sep	1.1564	11.3689	-6.8100	8.6747	0.3286	3.1572	0.0108
Oct	1.1905	11.5016	-6.8732	8.5933	0.3332	3.2278	0.0052
Nov	1.0688	17.4907	-9.0400	5.6682	0.4551	-2.4970	0.0069
Dec	0.6253	14.0387	-7.4982	2.5016	0.3531	1.1339	0.0060
2002	σ	ν	θ	κ	η	λ	*ape*
Jan	0.5869	11.8706	-7.0370	4.0954	0.3195	1.8007	0.0047
Feb	0.5726	17.8947	-9.6225	1.9266	0.3551	-0.9213	0.0088
Mar	0.4947	18.1715	-7.7394	-0.1114	1.2360	-0.3203	0.0114
Apr	1.2430	51.1248	-36.5909	11.4415	0.5975	2.0617	0.0105
May	0.8766	26.5739	-14.2343	5.0617	0.5094	1.2500	0.0086
Jun	0.9689	20.2424	-10.7956	8.5967	0.4684	1.9259	0.0086
Jul	1.4470	20.9771	-11.6146	10.2131	0.4676	2.8057	0.0085
Aug	2.0805	17.2986	-8.2879	7.2209	0.4794	2.3573	0.0090
Sep	1.5651	15.5996	-9.1882	6.2339	0.4066	2.3363	0.0093
Oct	1.7174	13.8612	-8.6015	5.9573	0.4327	2.2192	0.0069
Nov	1.1334	11.1792	-7.5938	8.2841	0.3744	-2.3497	0.0069
Dec	1.6175	21.9432	-10.1836	4.5582	0.6396	-1.8589	0.0098

Table C.5: Parameter estimates for NIGSA model on S&P 500 monthly second Monday data

2001	C	G	M	κ	η	λ	*ape*
Jan	29.1648	21.1873	32.5609	6.4487	11.4348	21.7994	0.0115
Feb	23.0721	27.6743	45.6598	2.0557	12.1893	7.7988	0.0068
Mar	64.3897	35.6721	49.3632	5.3830	25.1429	26.8375	0.0214
Apr	23.0284	14.0610	25.4510	11.4316	6.0271	21.6204	0.0135
May	19.3889	21.6750	38.8477	3.2941	9.3838	7.8714	0.0047
Jun	8.8185	14.7512	29.9269	2.4562	5.1185	4.7847	0.0046
Jul	30.1602	33.8374	58.6961	1.9815	17.3839	5.6404	0.0136
Aug	21.2897	26.9172	50.2993	3.1207	12.5383	7.9498	0.0082
Sep	23.0709	15.3568	29.2373	8.9713	6.4283	16.6707	0.0112
Oct	19.3326	13.4795	27.1129	8.9784	5.3216	14.8469	0.0060
Nov	18.2777	17.2472	35.0390	5.4223	7.8456	10.1042	0.0070
Dec	13.9708	17.9276	34.2797	3.9589	8.0502	7.7001	0.0057
2002	C	G	M	κ	η	λ	*ape*
Jan	7.5159	11.9955	25.0096	3.7882	4.1486	6.5378	0.0054
Feb	13.9188	20.9152	42.7146	2.3733	8.5040	5.1941	0.0087
Mar	16.4363	25.2591	52.7480	0.6605	4.5611	2.3371	0.0098
Apr	6.9622	14.0755	27.2046	7.5208	4.2775	1.4112	0.0137
May	27.8004	28.3573	63.0575	5.2571	15.5387	6.9389	0.0088
Jun	29.3476	24.6784	53.3843	8.8322	13.3918	10.8006	0.0088
Jul	30.4738	20.7300	41.8759	9.9693	10.0027	13.5783	0.0086
Aug	47.4528	20.3661	39.4884	7.6182	10.5001	11.5774	0.0091
Sep	34.0014	17.8196	38.4263	6.8117	8.4366	11.8338	0.0095
Oct	25.6584	13.6364	30.0108	5.9269	6.5196	9.0478	0.0071
Nov	16.8131	12.0180	26.8970	8.6356	5.4368	10.7129	0.0077
Dec	45.5252	25.2578	51.8086	5.0865	16.7020	9.7350	0.0099

Table C.6: Parameter estimates for VGSA model on S&P 500 monthly second Monday data

2001	C	G	M	Y_p	Y_n	ζ	κ	η	λ	*ape*
Jan	4.6028	15.0957	38.7336	0.5356	0.4373	1.2461	5.1298	2.0498	8.1581	0.0105
Feb	4.3393	18.2527	39.5842	0.3913	0.4075	0.8443	1.7381	2.2591	3.0794	0.0066
Mar	4.9138	20.6220	45.2493	0.5798	0.5160	1.2071	4.4662	2.0755	6.8119	0.0214
Apr	5.8621	12.9286	38.7211	0.5483	0.4303	1.3017	10.2149	1.6946	11.4612	0.0121
May	4.4059	15.9052	43.2343	0.4328	0.3885	0.9568	2.5239	2.2701	3.3687	0.0044
Jun	5.0613	12.8411	35.0649	0.2712	0.3263	0.6291	2.6639	3.0916	3.9579	0.0044
Jul	4.9405	35.2107	47.8637	0.4662	0.5048	1.0072	2.6238	2.5955	2.5379	0.0133
Aug	5.1808	21.1424	44.7099	0.3650	0.4318	0.7306	3.3625	2.9794	4.0394	0.0081
Sep	5.9988	11.5240	39.2562	0.4836	0.4192	0.9300	7.5849	1.8823	8.3989	0.0101
Oct	5.5846	10.8303	38.4322	0.4788	0.3792	1.0641	7.7041	1.7269	7.9024	0.0053
Nov	4.8411	15.8497	38.5985	0.4671	0.4652	0.9629	6.4502	1.9735	5.8312	0.0068
Dec	4.4908	15.3799	39.9917	0.4044	0.3725	0.9397	4.0009	2.7103	4.6486	0.0054
2002	C	G	M	Y_p	Y_n	ζ	κ	η	λ	*ape*
Jan	3.7035	12.5538	41.2956	0.4260	0.2972	1.1594	3.5670	2.2750	5.1844	0.0046
Feb	4.9048	17.7422	49.2535	0.3563	0.3488	0.8406	2.4106	3.1478	3.2077	0.0084
Mar	16.1400	33.2735	84.4334	0.1883	0.1255	1.2105	0.9648	3.1245	2.2810	0.0097
Apr	4.5940	12.8203	37.5642	0.2728	0.1843	0.9268	6.5130	2.6027	1.1951	0.0129
May	4.6918	23.0910	61.0328	0.4740	0.5018	0.8998	6.7164	2.4427	3.3021	0.0087
Jun	5.2119	19.6887	51.0969	0.4534	0.4403	1.0806	9.4230	2.3165	4.6509	0.0089
Jul	5.2400	15.0594	43.8581	0.5115	0.5075	0.8862	9.6934	1.7647	5.5262	0.0085
Aug	7.0087	15.8150	26.9584	0.4164	0.4597	1.2558	9.1822	1.3422	4.4015	0.0089
Sep	6.2913	13.4684	27.9655	0.3475	0.4222	1.1324	8.2070	1.3620	4.9937	0.0094
Oct	7.5193	12.4747	28.7605	0.3846	0.3599	1.2544	6.7294	1.7718	5.1174	0.0072
Nov	6.0836	9.9763	29.8685	0.3739	0.3140	1.0321	8.1983	2.0652	6.4978	0.0074
Dec	6.1628	24.3770	37.4029	0.5036	0.5675	1.0257	7.4780	1.8934	4.2448	0.0094

Table C.7: Parameter estimates for CGMYSA model on S&P 500 monthly second Monday data

2001	σ	ν	θ	κ	η	λ	*ape*
Jan	0.6610	14.5696	-25.2693	12.5979	0.2331	-2.2479	0.0187
Feb	0.3657	15.9237	-16.8139	0.3788	0.3329	-0.0221	0.0180
Mar	0.5563	15.9586	-16.5546	0.6601	0.2169	0.2721	0.0427
Apr	1.0262	15.6257	-17.9864	8.8445	0.3493	-1.5298	0.0225
May	0.6609	16.4525	-9.9083	3.0253	0.5043	-0.6553	0.0166
Jun	0.4137	11.4520	-7.0190	1.4726	0.3714	0.3381	0.0140
Jul	0.9538	37.8140	-14.2957	3.5196	1.2432	-0.2550	0.0285
Aug	0.6160	12.8138	-9.7153	21.2394	0.3369	-2.2940	0.0203
Sep	0.9072	11.0451	-11.4558	10.0393	0.2811	-0.7664	0.0158
Oct	0.9809	11.2752	-10.4831	9.9829	0.3251	-1.4379	0.0119
Nov	0.6990	16.6685	-17.6198	6.6813	0.4131	0.5000	0.0137
Dec	0.4760	13.6221	-12.8167	4.8333	0.3536	0.2554	0.0099
2002	σ	ν	θ	κ	η	λ	*ape*
Jan	0.4439	13.3264	-15.5367	5.7872	0.2891	-0.7362	0.0096
Feb	0.5176	17.8380	-10.4100	2.0598	0.5361	-0.2484	0.0199
Mar	0.4736	18.2154	-8.7402	0.0260	1.1214	-0.0129	0.0150
Apr	1.2759	51.1241	-36.5959	11.4387	0.8964	2.0589	0.0157
May	0.8217	26.5034	-15.0540	5.8662	0.6449	-0.2467	0.0147
Jun	0.9114	20.1761	-11.8094	9.4412	0.5280	-0.3565	0.0139
Jul	1.1810	20.2983	-18.7899	12.8406	0.4326	-0.8511	0.0120
Aug	1.9971	17.2368	-9.5079	7.3605	0.5659	-1.2841	0.0195
Sep	1.2445	15.2528	-13.2969	5.6182	0.4435	-0.4240	0.0179
Oct	1.1899	13.3709	-14.3774	5.3652	0.3946	0.2758	0.0149
Nov	1.0552	11.1070	-8.7910	8.8827	0.4089	-0.4767	0.0138
Dec	1.1622	16.0869	-11.3847	7.7862	0.6139	-0.4632	0.0171

Table C.8: Parameter estimates for NIGSAM model on S&P 500 monthly second Monday data

2001	C	G	M	κ	η	λ	*ape*
Jan	17.0932	8.7045	148.2002	28.4162	4.5350	20.8213	0.0236
Feb	19.7595	22.0468	186.1343	-0.6878	17.9920	-1.3091	0.0218
Mar	6.4175	6.9951	23.8705	11.3192	2.5265	1.8406	0.0341
Apr	12.1733	7.1179	39.7601	17.8308	2.8447	11.1211	0.0184
May	7.7918	10.9778	53.9272	6.8999	5.2818	-4.8867	0.0137
Jun	5.7928	8.9577	32.7173	20.6433	3.5559	-10.1605	0.0104
Jul	27.1312	32.3204	63.6766	5.7827	30.2644	-8.2306	0.0270
Aug	9.1110	13.6918	178.4991	63.6387	7.6502	-42.4528	0.0203
Sep	7.7051	7.1766	23.0106	9.7248	2.4213	1.7742	0.0187
Oct	9.0014	7.6090	54.9828	8.6758	3.0482	5.9208	0.0113
Nov	16.6638	15.0990	63.9479	6.6098	10.7882	-2.3001	0.0171
Dec	5.5349	9.1405	28.8784	9.6435	3.7566	3.5361	0.0106
2002	C	G	M	κ	η	λ	*ape*
Jan	4.5056	6.9512	46.2553	9.4129	2.5465	6.0875	0.0096
Feb	7.2588	11.9986	90.8520	31.2113	5.9557	16.4604	0.0157
Mar	15.2845	25.2953	53.3984	-0.2025	6.0748	0.1329	0.0152
Apr	6.9622	14.0755	27.2046	7.5208	4.2775	1.4112	0.0139
May	26.7813	24.9145	102.0831	12.4062	19.2099	-3.6291	0.0134
Jun	13.7301	14.0609	46.2596	13.6642	6.6385	7.5063	0.0128
Jul	26.7617	16.8542	68.3560	12.4964	10.3127	5.6104	0.0143
Aug	45.6305	18.9154	56.0436	6.2421	13.7029	3.2923	0.0179
Sep	10.0362	8.6490	30.7660	4.5351	3.4314	-0.4377	0.0155
Oct	10.9202	7.9550	34.7739	4.4417	3.6671	0.8017	0.0148
Nov	10.1923	8.1636	43.9392	8.2335	3.9263	5.4544	0.0111
Dec	45.2174	23.1618	86.1865	3.5724	25.4882	0.9095	0.0205

Table C.9: Parameter estimates for VGSAM model on S&P 500 monthly second Monday data

2001	C	G	M	Y_p	Y_n	ζ	κ	η	λ	*ape*
Jan	5.6039	6.9524	55.1788	-10.0325	0.0049	1.4783	13.1059	1.9951	8.6769	0.0214
Feb	6.2921	13.7654	54.5975	-36.6274	-0.3287	3.4837	21.6084	5.0073	16.4761	0.0194
Mar	5.9546	2.2800	52.9908	-15.7405	1.1598	0.0455	11.5042	2.3755	1.0059	0.0329
Apr	12.2818	6.2692	38.5355	0.4737	-0.2833	1.0008	17.0961	2.8257	4.7940	0.0139
May	3.0077	5.4932	49.9979	-14.3902	0.9063	0.1484	5.3704	2.0894	1.6207	0.0127
Jun	3.6749	2.7038	54.9543	-13.6116	1.2369	0.0326	10.5238	2.7212	2.8649	0.0089
Jul	5.7389	33.1933	55.0495	-14.0262	0.4213	1.4617	3.9697	7.2783	-1.1802	0.0261
Aug	6.7589	13.0583	53.9767	-13.3937	-0.0893	1.5464	32.2642	5.5272	21.3777	0.0184
Sep	7.7173	7.0811	22.9165	-0.0366	-0.0067	0.9987	9.5380	2.4169	1.5115	0.0191
Oct	2.7933	2.1228	57.6726	-21.0203	1.1746	0.1017	8.2269	0.9226	0.9257	0.0088
Nov	1.0608	6.9306	70.7205	-9.7821	0.4749	1.7758	4.4800	0.6303	0.9114	0.0130
Dec	2.2514	6.1852	51.7171	-15.9087	0.7384	0.3457	9.5649	1.5976	3.3797	0.0105
2002	C	G	M	Y_p	Y_n	ζ	κ	η	λ	*ape*
Jan	2.0785	4.0248	47.6368	-13.7172	0.7239	0.2994	8.7462	1.2068	3.1746	0.0088
Feb	3.6044	11.9174	41.7660	0.0725	0.1563	1.1704	8.0085	3.4411	1.6348	0.0166
Mar	15.3308	25.2022	54.2330	-0.4379	0.0157	1.1373	-0.1805	6.1353	0.0659	0.0142
Apr	4.6006	13.2595	37.4289	0.3054	0.1894	0.9136	7.4917	2.7306	-1.7430	0.0126
May	26.7554	25.0710	102.2361	-0.0519	0.0265	0.9949	12.5641	19.0484	-3.7898	0.0147
Jun	13.7825	13.9253	46.2524	0.1535	-0.0500	1.0051	13.7334	6.7138	4.2051	0.0119
Jul	4.3314	10.3434	44.0949	-0.4520	0.5109	0.8902	11.2758	1.6170	3.2426	0.0131
Aug	4.3046	10.9174	99.6897	-52.5662	0.4584	1.5938	6.1853	1.2281	1.2640	0.0148
Sep	4.8104	9.3111	30.8454	0.1096	0.0638	2.2657	5.0618	1.6582	0.7038	0.0165
Oct	7.6381	8.5208	28.2125	0.0299	-0.1158	1.9611	4.4405	2.5741	0.4921	0.0149
Nov	5.2688	6.8761	29.6692	0.3183	0.1062	1.1149	8.3282	1.9791	1.6843	0.0102
Dec	5.3456	21.9821	46.5806	-36.1361	0.4033	2.4640	2.9476	3.1921	-0.5032	0.0209

Table C.10: Parameter estimates for CGMYSAM model on S&P 500 second Monday data

2001	σ	ν	θ	κ	λ	ζ	ρ	ape
Jan	1.0493	14.7746	-0.1875	7.5530	1.9712	1.1118	-0.0945	0.0110
Feb	0.8186	19.5442	-5.4641	2.4769	1.7729	0.6223	-0.0615	0.0075
Mar	0.9346	12.5440	-0.2205	8.3797	2.6709	0.9986	-0.0839	0.0225
Apr	1.7424	31.4829	2.0017	9.2339	2.2051	0.5269	-0.2087	0.0135
May	0.8474	15.6149	-4.2173	4.3498	3.2314	0.5564	-0.0593	0.0047
Jun	0.8008	24.6594	-0.8993	2.1600	2.1804	0.7109	-0.1057	0.0038
Jul	0.8932	27.4089	-5.7257	2.9207	5.3960	0.3844	-0.0427	0.0141
Aug	0.7706	21.5196	-3.8238	3.1063	3.2293	0.5315	-0.0720	0.0087
Sep	2.1066	78.4946	32.2449	7.5790	2.6646	1.2237	-0.1140	0.0096
Oct	2.2818	82.3603	32.2053	7.5720	2.5312	1.0852	-0.1252	0.0046
Nov	0.9446	15.9996	-5.5994	5.6017	3.4179	0.4380	-0.1143	0.0073
Dec	0.8897	19.5321	-3.9629	4.7820	3.6116	0.6108	-0.0699	0.0051
2002	σ	ν	θ	κ	λ	ζ	ρ	ape
Jan	0.8950	24.4948	0.2855	3.7154	2.0581	1.4128	-0.0653	0.0041
Feb	0.8042	22.7490	-5.8587	3.6711	3.7669	0.4835	-0.0639	0.0082
Mar	0.8264	28.4146	-10.7049	2.2521	4.8458	0.2406	-0.0450	0.0098
Apr	0.5995	18.4425	-0.1933	6.7533	12.8072	0.2774	-0.0928	0.0096
May	0.6919	19.3789	-0.5667	6.0390	9.7452	0.3697	-0.0805	0.0077
Jun	0.7158	16.2254	-0.3209	6.5561	8.3224	0.2498	-0.1563	0.0082
Jul	1.0301	26.3519	7.5190	7.7917	5.0759	0.5986	-0.1167	0.0091
Aug	1.4376	18.4559	-0.3976	6.7066	3.3908	0.2357	-0.3102	0.0131
Sep	2.3936	95.3391	40.3196	4.6235	3.1137	0.4416	-0.2645	0.0105
Oct	2.4564	82.6383	42.8786	4.6657	3.1327	0.5054	-0.2718	0.0095
Nov	1.0512	17.4969	-0.5172	5.6750	5.8842	0.3774	-0.1436	0.0119
Dec	2.2107	86.2696	1.9124	5.2677	6.2016	0.3630	-0.1543	0.0112

Table C.11: Parameter estimates for NIGSG model on S&P 500 second Monday data

2001	C	G	M	κ	λ	ζ	ρ	*ape*
Jan	23.4454	22.0108	33.4581	8.1445	2.5161	0.0857	-1.2251	0.0128
Feb	16.7896	23.9592	38.2546	2.8039	1.9403	0.7413	-0.0381	0.0077
Mar	32.6221	19.7244	46.4582	5.7299	1.6772	0.9093	0.0380	0.0163
Apr	26.3928	20.5225	26.5394	8.7545	2.1825	0.1973	-0.5384	0.0124
May	17.6652	21.2805	34.8133	4.3972	3.1838	0.5661	-0.0455	0.0050
Jun	11.0614	24.7926	30.3918	2.4628	2.3652	0.6008	-0.1088	0.0043
Jul	21.5785	26.9557	80.3058	5.8043	11.0923	0.4883	0.0470	0.0164
Aug	18.6656	29.8783	42.7140	3.2369	3.3024	0.5578	-0.0602	0.0088
Sep	24.0037	19.7918	30.7553	7.4413	2.2778	0.1177	-0.8511	0.0110
Oct	25.8589	19.9783	31.0665	7.5069	2.1030	0.1181	-0.8986	0.0057
Nov	16.5244	18.4092	32.5119	5.0738	3.1803	0.4228	-0.1135	0.0074
Dec	21.4294	27.2702	37.5095	5.0247	3.6376	0.6443	-0.0622	0.0052
2002	C	G	M	κ	λ	ζ	ρ	*ape*
Jan	11.5328	12.9883	31.0883	11.5552	2.6873	2.3473	0.0208	0.0086
Feb	18.2933	27.6487	44.8605	3.6349	3.7925	0.5060	-0.0544	0.0082
Mar	25.5851	30.2991	74.1905	3.0265	6.5482	0.3028	0.0409	0.0098
Apr	18.9100	24.2360	124.4305	4.7035	22.9279	0.1569	0.0823	0.0099
May	18.5927	21.7633	139.4098	6.2588	22.4456	0.2157	0.0731	0.0089
Jun	19.2555	18.9580	79.2264	7.2052	15.3867	0.2756	0.0656	0.0084
Jul	20.2769	18.1341	33.2906	8.1229	7.6105	0.2522	-0.0875	0.0089
Aug	37.8251	21.4474	36.3553	5.9191	4.4684	0.0663	-0.9045	0.0094
Sep	24.8555	18.9182	33.9410	4.5612	2.4685	0.0666	-1.4215	0.0095
Oct	26.9844	17.3734	32.2316	4.5130	2.4621	0.0566	-1.8743	0.0085
Nov	23.5324	20.2709	30.4758	6.9644	3.3044	0.0859	-1.0525	0.0085
Dec	35.8742	27.9299	42.0771	3.7973	5.0449	0.1680	-0.2885	0.0110

Table C.12: Parameter estimates for VGSG model on S&P 500 second Monday data

2001	σ	ν	θ	κ	μ	ρ	ape
Jan	1.2971	13.0552	-0.7575	0.5647	-24.8176	11.0808	0.0623
Feb	1.0890	12.9447	-0.5646	0.6155	-24.7855	10.5950	0.0491
Mar	1.3752	10.8877	-9.1187	0.2000	-28.0027	11.0853	0.0406
Apr	1.6994	12.3048	-1.4476	0.2769	-24.0311	14.8654	0.0434
May	1.3221	12.4749	-0.9102	0.3560	-23.5157	13.5696	0.0191
Jun	1.4140	12.6515	-1.0058	0.3048	-23.3725	13.0314	0.0219
Jul	1.1856	12.8057	-6.6870	0.1769	-33.6919	6.2012	0.0293
Aug	0.9553	12.5017	-6.4448	0.2864	-27.1241	7.5955	0.0271
Sep	1.1826	12.1586	-8.9216	0.3956	-21.4809	11.9758	0.0415
Oct	1.9568	12.7565	-1.8822	0.2383	-23.6282	11.7177	0.0256
Nov	1.8837	12.7862	-0.6997	0.2331	-24.2030	11.3609	0.0150
Dec	1.1628	12.8377	-0.6064	0.4841	-24.4477	10.4926	0.0252
2002	σ	ν	θ	κ	μ	ρ	ape
Jan	1.0421	12.4207	-8.6655	0.2963	-26.1075	8.9174	0.0170
Feb	1.0155	12.7274	-1.1708	0.3503	-25.2162	9.9453	0.0371
Mar	0.9706	12.7475	-0.4726	0.5344	-24.6146	10.7869	0.0311
Apr	1.1045	12.6709	-0.6039	0.2856	-25.1389	9.8589	0.0166
May	1.0150	12.7315	-0.5872	0.4908	-24.6427	10.7297	0.0250
Jun	1.1475	12.5971	-0.7189	0.3623	-24.3484	10.8122	0.0197
Jul	1.4467	14.2811	-4.4819	0.2597	-25.3007	10.9272	0.0240
Aug	1.6004	12.8513	-0.9268	0.4218	-22.5801	16.7485	0.0312
Sep	1.4179	12.8119	-7.1982	0.4429	-21.9354	14.1039	0.0247
Oct	1.3142	12.7067	-11.1140	0.5616	-23.0611	14.8602	0.0230
Nov	1.7994	13.7314	-1.6312	0.3828	-21.3275	15.9875	0.0261
Dec	1.6834	12.7621	-1.0514	0.3387	-22.1274	13.7453	0.0177

Table C.13: Parameter estimates for NIGIG model on S&P 500 second Monday data

2001	C	G	M	κ	μ	ρ	*ape*
Jan	12.6949	8.2555	38.3019	0.2060	-29.0530	11.0582	0.0317
Feb	14.2974	9.9271	69.3139	0.1955	-25.5316	11.4828	0.0222
Mar	13.5431	8.3599	69.6352	0.2079	-25.5654	10.5328	0.0401
Apr	14.1352	9.6139	69.8129	0.1945	-25.5723	11.5346	0.0931
May	13.7314	9.4800	72.5386	0.1995	-24.7185	11.3487	0.0128
Jun	13.2340	9.7023	70.5691	0.2059	-24.8592	10.9124	0.0107
Jul	14.5983	9.5625	70.4344	0.1853	-26.1847	12.1741	0.0613
Aug	13.6311	10.1725	68.1876	0.2078	-25.6600	10.5569	0.0309
Sep	11.3409	9.0241	38.1481	0.4831	-18.0595	5.9239	0.0390
Oct	11.5926	8.4834	66.7344	0.2875	-22.8262	8.0484	0.0221
Nov	13.7650	9.6405	69.4910	0.1998	-25.2527	11.1883	0.0301
Dec	13.2876	9.3282	69.2560	0.2043	-25.2475	10.6928	0.0118
2002	C	G	M	κ	μ	ρ	*ape*
Jan	14.6129	9.2822	72.2026	0.1845	-26.1082	12.1937	0.0136
Feb	13.6929	10.6599	66.8758	0.2129	-25.4342	10.5192	0.0199
Mar	14.2640	11.0528	66.5400	0.1974	-26.1361	11.6708	0.0303
Apr	14.1662	12.1102	67.4540	0.2114	-25.5182	11.1500	0.0298
May	32.0233	18.4278	114.8709	0.1064	-49.4931	21.0677	0.0131
Jun	33.1941	20.7677	32.4307	0.1964	-32.9437	14.4331	0.0161
Jul	25.6355	16.6399	24.5013	0.2367	-28.3487	14.2530	0.0245
Aug	16.0618	8.0134	76.7963	0.1785	-24.8183	13.6626	0.0379
Sep	14.2819	10.2205	50.2544	0.6060	-21.2405	6.4183	0.0242
Oct	14.7319	8.3417	85.8286	0.1835	-25.3808	12.3467	0.0918
Nov	13.3315	8.8164	69.6279	0.1954	-26.0056	10.9458	0.0636
Dec	40.1234	14.1940	32.4224	0.1506	-26.3162	25.4217	0.0167

Table C.14: Parameter estimates for VGIG model on S&P 500 second Monday data

2001	σ	ν	θ	κ	μ	ρ	ape
Jan	1.3180	6.7081	-2.1952	0.1334	-22.7445	10.0380	0.0287
Feb	0.9660	12.4988	-7.1021	0.1729	-26.0109	9.2367	0.0227
Mar	1.4709	7.9929	-1.6613	0.1247	-23.6587	10.5103	0.0384
Apr	1.1105	7.4129	-2.1345	0.2944	-18.2536	9.1380	0.0393
May	1.3864	9.8548	-2.2940	0.0982	-29.7291	11.9383	0.0123
Jun	0.8544	12.0437	-8.3694	0.1613	-26.6604	7.8935	0.0119
Jul	0.8883	12.6192	-6.9390	0.0649	-57.9300	6.9146	0.0234
Aug	0.8902	12.4385	-6.3987	0.1747	-26.8029	8.4441	0.0238
Sep	1.0195	9.3285	-4.5853	0.3863	-19.9904	8.8109	0.0409
Oct	0.7567	7.8490	-4.9864	0.5377	-21.4517	6.9909	0.0189
Nov	1.6578	9.4818	-1.5970	0.1143	-24.0323	9.0349	0.0129
Dec	1.2648	10.5781	-6.1275	0.0848	-34.1913	10.1824	0.0105
2002	σ	ν	θ	κ	μ	ρ	ape
Jan	1.3907	8.7231	-7.2636	0.0660	-38.2352	10.0112	0.0094
Feb	0.9509	12.5867	-4.6926	0.2047	-26.4617	8.8431	0.0202
Mar	0.8773	12.6093	-3.2570	0.1978	-27.0396	8.1055	0.0189
Apr	1.7191	34.1649	-8.3247	0.0779	-43.8389	18.2747	0.0127
May	1.5840	23.7915	-5.4130	0.0883	-38.4484	15.7326	0.0124
Jun	1.2939	13.6756	-0.8202	0.1549	-25.1036	10.4778	0.0146
Jul	1.3974	13.5775	-0.9759	0.1760	-23.9387	11.7007	0.0234
Aug	2.2428	47.5938	-53.0258	0.5139	-16.2329	6.9509	0.0307
Sep	1.2711	12.2279	-6.2404	0.4309	-21.7564	11.3170	0.0244
Oct	1.1838	14.2836	-13.9712	0.6084	-25.5094	11.4765	0.0226
Nov	0.9744	9.9904	-6.4785	0.4259	-22.9446	9.3458	0.0191
Dec	1.6781	13.8356	-0.4975	0.1842	-23.2837	13.3703	0.0154

Table C.15: Parameter estimates for NIGSIG model on S&P 500 second Monday data

2001	C	G	M	κ	μ	ρ	*ape*
Jan	15.4166	8.7383	7.8235	0.0793	-32.8823	19.2063	0.0308
Feb	9.4304	9.3229	29.3790	0.0442	-77.8818	-2.5362	0.0197
Mar	13.5230	8.9265	8.0210	0.0944	-28.8250	15.6088	0.0378
Apr	12.4648	10.4324	15.4208	0.2910	-17.4295	8.0477	0.0426
May	8.3552	11.0032	44.5077	0.1932	-41.2371	0.3239	0.0140
Jun	5.8308	8.5418	25.5850	0.1235	-40.9233	-0.3021	0.0106
Jul	17.8992	15.1418	47.5151	0.0463	-80.3893	-1.5083	0.0243
Aug	9.5173	9.7004	28.7863	0.0405	-82.9284	-8.1144	0.0179
Sep	11.0177	9.8086	15.1100	0.3194	-14.9451	5.6069	0.0423
Oct	6.1267	7.8898	45.8382	0.6939	-48.7116	0.5787	0.0186
Nov	12.6497	9.5832	10.2879	0.1227	-24.2495	10.8921	0.0135
Dec	7.1973	9.4724	30.4383	0.1379	-41.2980	-0.6080	0.0112

2002	C	G	M	κ	μ	ρ	*ape*
Jan	4.3531	6.8824	26.4771	0.1617	-36.7839	-0.1366	0.0108
Feb	12.0518	11.3130	43.6196	0.0491	-72.5588	2.5741	0.0163
Mar	17.1301	15.7909	49.3056	0.0483	-76.5089	-0.5029	0.0164
Apr	55.4037	31.6506	34.1489	0.0577	-54.6905	26.1434	0.0129
May	37.8174	23.5074	23.3575	0.0658	-46.2092	21.4848	0.0128
Jun	32.8065	23.3158	33.3930	0.1598	-29.3281	12.6323	0.0166
Jul	30.0731	20.1368	43.3112	0.2466	-26.0455	11.5340	0.0243
Aug	18.9363	14.0044	53.8278	0.8837	-89.8736	0.5244	0.0285
Sep	10.3171	9.8663	51.3508	0.7363	-68.0670	0.9548	0.0238
Oct	9.8050	8.4662	56.2503	0.7997	-65.3149	0.1962	0.0217
Nov	7.6310	8.6880	44.3736	0.5954	-68.4720	1.0271	0.0186
Dec	13.4366	12.4615	44.0463	0.3943	-42.7383	-0.0283	0.0168

Table C.16: Parameter estimates for VGSIG model on S&P 500 second Monday data

Appendix D

Standard Errors for Four Stochastic Volatility Models on S&P 500 Monthly Second Monday Data

2001	κ	θ	β	σ_0^2	ρ
Jan	0.16598	0.00053	0.03352	0.00112	0.01093
Feb	0.19721	0.00090	0.02519	0.00039	0.02557
Mar	0.24612	0.00108	0.04136	0.00151	0.02776
Apr	0.41079	0.00049	0.07534	0.00320	0.01329
May	0.20772	0.00035	0.02323	0.00051	0.02143
Jun	0.37515	0.00040	0.04456	0.00064	0.01573
Jul	0.72053	0.00066	0.06833	0.00085	0.22808
Aug	0.29304	0.00046	0.03031	0.00044	0.03809
Sep	0.24211	0.00047	0.04324	0.00169	0.01283
Oct	0.27327	0.00037	0.04695	0.00191	0.01402
Nov	0.29007	0.00044	0.03768	0.00109	0.03348
Dec	0.37978	0.00038	0.04163	0.00075	0.02565
2002	κ	θ	β	σ_0^2	ρ
Jan	0.33334	0.00050	0.04996	0.00102	0.01532
Feb	0.39499	0.00054	0.03761	0.00057	0.06794
Mar	0.59154	0.00095	0.05597	0.00070	0.29198
Apr	2.82551	0.00030	0.17710	0.00206	0.54555
May	1.38981	0.00028	0.10088	0.00137	0.27180
Jun	1.12955	0.00024	0.08876	0.00178	0.10686
Jul	0.49461	0.00021	0.05594	0.00190	0.04785
Aug	0.20396	0.00038	0.04257	0.00192	0.04286
Sep	0.20307	0.00057	0.03879	0.00191	0.03623
Oct	0.15338	0.00061	0.03227	0.00188	0.02838
Nov	0.51176	0.00047	0.07577	0.00331	0.02428
Dec	0.39892	0.00072	0.04985	0.00188	0.06167

Table D.1: Standard errors for Heston model on S&P 500 second Monday data with traditional method

2001	κ	θ	β	σ_0^2	ρ
Jan	0.20327	0.00054	0.04241	0.00139	0.01089
Feb	0.31435	0.00124	0.03531	0.00040	0.02407
Mar	0.26227	0.00108	0.04585	0.00166	0.02773
Apr	0.45765	0.00049	0.08866	0.00364	0.01290
May	0.27590	0.00035	0.02958	0.00057	0.02027
Jun	0.53086	0.00042	0.06533	0.00067	0.01564
Jul*	0.00000	0.00023	0.00000	0.00068	0.00000
Aug	0.34303	0.00045	0.03571	0.00045	0.03685
Sep	0.25989	0.00047	0.04753	0.00181	0.01262
Oct	0.30916	0.00038	0.05315	0.00210	0.01359
Nov	0.31383	0.00043	0.03965	0.00110	0.03257
Dec	0.44228	0.00037	0.05025	0.00078	0.02513
2002	κ	θ	β	σ_0^2	ρ
Jan	0.46351	0.00052	0.07161	0.00119	0.01493
Feb	0.48428	0.00059	0.03999	0.00057	0.06213
Mar	1.62457	0.00240	0.06500	0.00090	0.14905
Apr	3.26375	0.00028	0.10870	0.00217	0.19058
May	1.83713	0.00025	0.08279	0.00152	0.14108
Jun	1.58701	0.00026	0.11531	0.00228	0.09806
Jul	0.61171	0.00023	0.06721	0.00231	0.04829
Aug	0.20012	0.00040	0.04298	0.00190	0.04187
Sep	0.19455	0.00058	0.03858	0.00183	0.03522
Oct	0.15510	0.00062	0.03183	0.00187	0.02738
Nov	0.61900	0.00049	0.09382	0.00384	0.02386
Dec	0.41132	0.00076	0.04739	0.00180	0.04862

Table D.2: Standard errors for Heston model on S&P 500 second Monday data with proposed method

2001	ρ	λ	a	b	σ_0^2
Jan	0.48548	0.20361	0.05656	3.38795	0.00161
Feb	0.28133	0.39363	0.11770	5.19231	0.00099
Mar	0.39048	0.45635	0.02542	3.82575	0.00272
Apr	0.33470	0.44617	0.01227	3.44653	0.00311
May	0.32531	0.21708	0.04684	4.08864	0.00100
Jun	0.25570	0.12083	0.04413	3.32693	0.00043
Jul	0.88138	0.51854	0.85467	28.76354	0.00142
Aug	0.38668	0.25761	0.19031	8.05556	0.00082
Sep	0.46921	0.36666	0.01654	4.31965	0.00271
Oct	0.53313	0.34423	0.01790	4.40806	0.00292
Nov	0.46599	0.30162	0.04558	4.75363	0.00178
Dec	0.35067	0.23175	0.08907	4.67286	0.00106
2002	ρ	λ	a	b	σ_0^2
Jan	0.32598	0.17470	0.04268	2.91190	0.00088
Feb	0.44687	0.20780	0.34710	8.18444	0.00090
Mar	1.20290	0.29344	2.22406	31.02360	0.00135
Apr	2.13284	0.45138	0.84101	68.89187	0.00171
May	1.28110	0.34191	0.39848	33.21582	0.00134
Jun	0.99959	0.28346	0.14616	16.46844	0.00132
Jul	0.40543	0.33691	0.04742	7.38717	0.00180
Aug	0.48824	0.29272	0.03184	7.52769	0.00290
Sep	0.76611	0.29392	0.03020	7.35673	0.00305
Oct	0.90333	0.26043	0.02353	7.37051	0.00368
Nov	0.39581	0.44453	0.02503	4.44864	0.00342
Dec	0.47897	0.33785	0.09006	6.46493	0.00255

Table D.3: Standard errors for BNSSG model on S&P 500 second Monday data with traditional method

2001	ρ	λ	a	b	σ_0^2
Jan	0.27131	0.10846	0.06024	2.53043	0.00138
Feb	0.21623	0.23197	0.07801	3.76149	0.00072
Mar	0.26594	0.38778	0.01988	2.89642	0.00237
Apr	0.23883	0.47710	0.01050	2.51185	0.00323
May	0.20428	0.18009	0.03873	2.58507	0.00089
Jun	0.21530	0.08720	0.03200	3.04457	0.00034
Jul	0.42712	0.16511	0.41501	10.56508	0.00092
Aug	0.25484	0.32472	0.29759	5.66819	0.00116
Sep	0.33230	0.66183	0.01974	2.44517	0.00473
Oct	0.29538	0.37617	0.01652	2.39929	0.00339
Nov	0.27141	0.22355	0.03242	3.10569	0.00139
Dec	0.21539	0.25129	0.11882	2.85886	0.00135
2002	ρ	λ	a	b	σ_0^2
Jan	0.22004	0.13194	0.03130	2.30498	0.00067
Feb	0.26521	0.13581	0.30908	4.19477	0.00085
Mar	0.50507	0.07982	0.84998	11.32920	0.00093
Apr	0.97635	0.19935	0.36307	28.60550	0.00097
May	0.61312	0.19855	0.24951	14.31517	0.00093
Jun	0.56076	0.21678	0.07791	10.44191	0.00087
Jul	0.24848	0.42992	0.03724	4.53942	0.00220
Aug	0.29781	0.29088	0.01952	4.26945	0.00280
Sep	0.40472	0.27903	0.01949	3.90481	0.00269
Oct	0.48324	0.27078	0.01546	3.71070	0.00338
Nov	0.31033	0.36005	0.01623	3.93449	0.00249
Dec	0.24056	0.26295	0.05266	3.11045	0.00218

Table D.4: Standard errors for BNSSG model on S&P 500 second Monday data with proposed method

2001	σ	ν	θ	κ	η	λ
Jan	0.06846	0.80366	0.23139	0.36683	0.02615	0.30323
Feb	0.03259	0.94298	0.49540	0.14311	0.03174	0.08932
Mar	0.29384	3.94298	0.59296	0.52295	0.10976	0.66334
Apr	0.07267	0.53532	0.27990	0.64006	0.01687	0.43906
May	0.03513	0.78206	0.44177	0.20922	0.02046	0.10424
Jun	0.01102	0.28803	0.22916	0.16593	0.01473	0.05843
Jul	0.23770	7.76718	2.95342	0.48794	0.16209	0.31736
Aug	0.03861	1.23579	0.70922	0.29187	0.02800	0.13981
Sep	0.05119	0.50205	0.26145	0.26765	0.01224	0.19683
Oct	0.04354	0.38739	0.23603	0.24857	0.00967	0.17017
Nov	0.09024	1.45080	0.77690	0.47675	0.03144	0.27207
Dec	0.03499	0.79047	0.49736	0.35374	0.02475	0.14775

2002	σ	ν	θ	κ	η	λ
Jan	0.02604	0.51261	0.27637	0.25312	0.01244	0.14067
Feb	0.04614	1.61285	1.11499	0.34462	0.03460	0.15098
Mar	0.05269	2.13457	1.36931	0.36867	2.75556	0.09274
Apr	0.50180	28.64089	30.83331	6.57369	0.13635	1.32391
May	0.13916	4.43472	3.29940	1.46117	0.05983	0.40523
Jun	0.08660	1.87419	1.37731	1.04004	0.03103	0.34112
Jul	0.11588	1.75245	1.18436	0.62013	0.02714	0.28401
Aug	0.15506	1.34694	0.80508	0.32142	0.02701	0.19782
Sep	0.10498	1.15100	0.84440	0.32864	0.01999	0.18026
Oct	0.08642	0.74421	0.57774	0.22580	0.01614	0.13496
Nov	0.06383	0.57597	0.48184	0.45883	0.01544	0.25677
Dec	0.22524	3.15512	1.78814	0.64932	0.07084	0.29392

Table D.5: Standard errors for NIGSA model on S&P 500 second Monday data with traditional method

2001	σ	ν	θ	κ	η	λ
Jan	0.04763	0.54196	0.20292	0.42476	0.01823	0.24806
Feb	0.02726	0.76622	0.39811	0.15005	0.03074	0.08665
Mar	0.14615	1.88527	0.45387	0.47198	0.05590	0.39595
Apr	0.14008	1.37652	0.25667	1.33055	0.04364	0.86041
May	0.02975	0.60964	0.36500	0.23393	0.02066	0.10942
Jun	0.01029	0.26776	0.20422	0.14268	0.01272	0.05072
Jul	0.14194	4.73067	2.07307	0.39325	0.10292	0.20791
Aug	0.03145	1.00336	0.58629	0.26524	0.02357	0.11915
Sep	0.04995	0.48079	0.25198	0.29080	0.01207	0.19766
Oct	0.04065	0.34860	0.22113	0.26555	0.00908	0.16555
Nov	0.07354	1.14566	0.66887	0.46825	0.02651	0.24659
Dec	0.02992	0.59796	0.40872	0.43950	0.02645	0.16817
2002	σ	ν	θ	κ	η	λ
Jan	0.02592	0.47049	0.26332	0.31437	0.01249	0.15863
Feb	0.03672	1.18348	0.82811	0.36810	0.03365	0.15163
Mar	0.03075	1.18567	0.94305	0.05221	0.38853	0.02958
Apr*	0.14967	12.41848	16.87799	1.76271	0.06455	0.00000
May	0.08554	2.53980	2.04394	1.37860	0.04097	0.32968
Jun	0.06155	1.28134	0.98651	1.22267	0.02185	0.28723
Jul	0.09578	1.38164	1.05522	0.67440	0.02277	0.26984
Aug	0.13463	1.14399	0.68554	0.30312	0.02358	0.17901
Sep	0.11387	1.24045	0.88242	0.36943	0.02094	0.19549
Oct	0.08361	0.70375	0.53931	0.22899	0.01577	0.13328
Nov	0.05460	0.50636	0.45664	0.47744	0.01310	0.22344
Dec	0.16078	2.26450	1.36889	0.52208	0.05293	0.23112

Table D.6: Standard errors for NIGSA model on S&P 500 second Monday data with proposed method

2001	C	G	M	κ	η	λ
Jan	0.54648	0.39329	0.42079	0.30106	0.34647	0.52357
Feb	3.06391	2.15331	2.81635	0.15331	1.68455	0.79757
Mar	2.21227	0.96083	1.33449	0.39657	1.24565	1.25614
Apr	0.42939	0.30751	0.49340	0.51590	0.18324	0.61143
May	1.92661	1.19674	1.91117	0.23207	0.88632	0.70272
Jun	0.53132	0.50916	0.90102	0.19218	0.32951	0.38233
Jul	9.53958	5.88226	10.02798	0.44605	5.21370	1.49973
Aug	3.31821	2.43806	3.81807	0.30023	1.83563	1.07386
Sep	2.16565	0.83925	1.23027	0.30729	0.54340	1.18328
Oct	1.36887	0.54333	0.86572	0.27822	0.33119	0.88940
Nov	2.52496	1.32210	2.42241	0.45095	0.94924	1.25849
Dec	1.71742	1.23863	2.00860	0.43799	0.92617	1.04773

2002	C	G	M	κ	η	λ
Jan	0.58659	0.55547	0.89497	0.24804	0.30160	0.56974
Feb	2.23547	1.91071	3.95842	0.33573	1.27102	0.83128
Mar	4.02176	2.96140	9.69266	0.28629	4.19612	0.47012
Apr	1.47604	2.00825	3.36409	2.78571	0.98419	5.68999
May	8.44439	4.37059	12.14610	1.51102	3.88135	2.44994
Jun	5.29476	2.32160	6.06906	1.06656	1.98403	1.92394
Jul	4.08737	1.52529	3.00282	0.57971	1.14969	1.47670
Aug	7.03842	1.60267	3.24812	0.36410	1.31060	1.18866
Sep	4.77967	1.36968	3.13457	0.37567	0.98118	1.16254
Oct	2.36452	0.68657	1.52216	0.22219	0.50604	0.64920
Nov	1.81184	0.73080	1.35229	0.49524	0.50090	1.18029
Dec	12.27832	3.59376	8.24663	0.73595	3.77974	1.96466

Table D.7: Standard errors for VGSA model on S&P 500 second Monday data with traditional method

2001	C	G	M	κ	η	λ
Jan	0.26166	0.03127	0.03472	0.01797	0.06820	0.03302
Feb	3.47557	2.47012	3.00466	0.20111	2.05422	1.00885
Mar	1.07480	0.14836	0.18063	0.05541	0.36788	0.14452
Apr	0.22188	0.01072	0.01954	0.01239	0.03223	0.02216
May	1.92319	1.19902	1.71913	0.29436	0.95594	0.84084
Jun	0.58914	0.56448	0.97587	0.21541	0.37122	0.43329
Jul	6.01326	3.55455	6.90416	0.40707	3.21037	1.01875
Aug	3.30959	2.41677	3.88255	0.32725	1.83986	1.10311
Sep	2.11250	0.81650	1.17407	0.33916	0.53071	1.21329
Oct	1.28798	0.50875	0.80271	0.30412	0.31203	0.88895
Nov	2.03781	1.05911	2.00605	0.44317	0.77425	1.11480
Dec	1.58384	1.12943	1.71611	0.55061	0.89786	1.20248
2002	C	G	M	κ	η	λ
Jan	0.55290	0.51056	0.79696	0.31061	0.28560	0.64228
Feb	1.93660	1.70729	3.18660	0.41152	1.26455	0.94767
Mar	2.89458	2.12723	7.32317	0.35984	5.77281	0.51206
Apr	1.38502	1.57899	3.68268	1.52394	0.97556	1.30024
May	5.65008	2.95911	8.32107	1.38134	2.65533	1.95936
Jun	4.42017	1.93999	5.34149	1.21376	1.65763	1.79570
Jul	3.54423	1.31584	2.64783	0.65929	0.99429	1.41440
Aug	6.57891	1.47448	3.17162	0.35559	1.21059	1.09307
Sep	16.34503	4.49551	10.83678	1.17707	3.22267	3.67565
Oct	2.63408	0.75780	1.66310	0.24506	0.56233	0.71496
Nov	1.90003	0.75858	1.42636	0.54448	0.52353	1.24419
Dec	8.40251	2.43213	6.41815	0.57632	2.54628	1.38289

Table D.8: Standard errors for VGSA model on S&P 500 second Monday data with proposed method

BIBLIOGRAPHY

[AF03] R. A. Adams and J. J. F. Fournier. *Sobolev Spaces*. Academic Press, New York, 2003. Second edition.

[App04] D. Applebaum. *Lévy Processes and Stochastic Calculus*. Cambridge University Press, 2004.

[AR01] S. Asmussen and J. Rosiński. Approximations of small jumps of Lévy processes with a view towards simulation. *Journal of Applied Probability*, 38:482–493, 2001.

[Bat96] D. Bates. Jumps and stochastic volatility: exchange rate processes implicit in Deutsche mark options. *Review of Financial Studies*, 9:69–107, 1996.

[Bat00] D. Bates. Post-'87 crash fears in the S&P 500 futures option market. *Journal of Econometrics*, 94:181–238, 2000.

[Ber96] J. Bertoin. *Lévy Processes*. Cambridge University Press, 1996.

[BN97] O. Barndorff-Nielson. Normal inverse Gaussian distributions and the modeling of stochastic volatility models. *Scandinavian Journal of Statistics*, 24:1–13, 1997.

[BNNS02] O. Barndorff-Nielson, E. Nicolato, and N. Shephard. Some recent developments in stochastic volatility modelling. *Quantitative Finance*, 2:11–23, 2002.

[BNS02] O. Barndorff-Nielson and N. Shephard. Econometric analysis of realised volatility and its use in estimating stochastic volatility models. *Journal of the Royal Statistical Society,Series B*, 64:253–280, 2002.

[BS73] F. Black and M. Scholes. The pricing of options and corporate liabilities. *Journal of Political Economy*, 81:637–659, 1973.

[Car04] P. Carr. The PIDE for option values in the R^3 model. 2004. Bloomberg working paper.

[CGMY03] P. Carr, H. Geman, D. Madan, and M. Yor. Stochastic volatility for Lévy processes. *Mathematical Finance*, 13:345–382, 2003.

[CIR85] J. Cox, J. Ingersoll, and S. Ross. A theory of the term structure of interest rates. *Econometrica*, 53:385–408, 1985.

[CM98] P. Carr and D. Madan. Option valuation using the fast Fourier transform. *Journal of Computational Finance*, 2:61–73, 1998.

[CT03] R. Cont and P. Tankov. *Financial Modelling with Jump Processes*. Chapman & Hall/CRC, 2003.

[CV03] R. Cont and E. Voltchkova. A finite difference scheme for option pricing in jump diffusion and exponential Lévy models. 2003. Research report.

[CW02] P. Carr and L. Wu. Time-changed Lévy processes and option pricing. 2002. Working paper.

[CW04] P. Carr and L. Wu. Stochastic skew in currency options. 2004. Bloomberg working paper.

[Dup94] B. Dupire. Pricing with a smile. *Risk*, 7:18–20, 1994.

[Eng82] R. F. Engle. Autoregressive conditional heteroscedasticity with estimates of the variance United Kingdom inflation. *Econometrica*, 50(4):987–1008, 1982.

[Fel51] W. Feller. Two singular diffusion problems. *Annals of Mathematics*, 54:173–182, 1951.

[FPS00] J.-P. Fouque, G. Papanicolaou, and R. Sircar. *Derivatives in Financial Markets with Stochastic Volatility*. Cambridge University Press, 2000.

[FPSS03] J.-P. Fouque, G. Papanicolaou, R. Sircar, and K. Solna. Maturity cycles in implied volatility. 2003. Working paper.

[GMY01] H. Geman, D. Madan, and M. Yor. Time changes for Lévy processes. *Mathematical Finance*, 11:79–96, 2001.

[Hes93] S. Heston. A closed-form solution for options with stochastic volatility with applications to bond and currency options. *Review of Financial Studies*, 6:327–343, 1993.

[HM02] A. Hirsa and D. B. Madan. Pricing American options under variance gamma. 2002. Research report.

[HMS04] N. Hilber, A.-M. Matache, and C. Schwab. Sparse wavelet methods for option pricing under stochastic volatility. 2004. Research report.

[HV03] W. Hundsdorfer and J.G. Verwer. *Numerical Solution of Time-Dependent Advection-Diffusion-Reaction Equations.* Springer-Verlag, Berlin Heidelberg, 2003.

[HW87] J. Hull and A. White. The pricing of options on assets with stochastic volatilities. *Journal of Finance*, 42:281–300, 1987.

[IT04] S. Ikonen and J. Toivanen. Operator splitting methods for American options with stochastic volatility. 2004. in European Congress on Computational Methods in Applied Sciences and Engineering.

[JLL90] P. Jaillet, D. Lamberton, and B. Lapeyre. Variational inequalities and the pricing of American options. *Acta Applicandae Mathematicae*, 21:263–289, 1990.

[JS03] J. Jacod and A. N. Shiryaev. *Limit Theorems for Stochastic Processes.* Springer-Verlag, Berlin, Heidelberg, 2003. Second edition.

[Kle02] F. Klebaner. Option price when the stock is a semimartingale. *Electronic Communications in Probability*, 7:79–83, 2002.

[Kou02] S. G. Kou. A jump diffusion model for option pricing. *Management Science*, 48:1086–1101, 2002.

[KS97] I. Karatzas and S. E. Shreve. *Brownian Motion and Stochastic Calculus.* Springer-Verlag, New York, 1997. Second edition.

[MCC98] D. Madan, P. Carr, and E. Chang. The variance gamma process and option pricing. *European Finance Review*, 2:79–105, 1998.

[Mer73] R. Merton. Theory of rational option pricing. *Bell Journal of Economics*, 4:141–183, 1973.

[Mer76] R. Merton. Option pricing when the underlying stock returns are discontinuous. *Journal of Financial Economics*, 4:125–144, 1976.

[MNS03] A.-M. Matache, P.-A. Nitsche, and C. Schwab. Wavelet Galerkin pricing of American options on Lévy driven assets. 2003. Technical report.

[MvPS03] A.-M. Matache, T. von Petersdorff, and C. Schwab. Fast deterministic pricing of options on Lévy driven assets. 2003. Technical report.

[MW03] D. Madan and X. Wu. Standard errors for financial market data analysis. 2003. Working paper.

[RY99] D. Revus and M. Yor. *Continuous Martingales and Brownian Motion.* Springer-Verlag, 1999. Third edition.

[Sat99] K.-I. Sato. *Lévy Processes and Infinitely Divisible Distributions.* Cambridge University Press, 1999.

[Sch03] W. Schoutens. *Lévy Processes in Finance.* Wiley, New York, 2003.

[Smo03] A. Smolianski. Finite-element/level-set/operator-splitting (FELSOS) approach for computing two-fluid unsteady flows with free moving interfaces. 2003. Working paper.

[vPS03] T. von Petersdorff and C. Schwab. Wavelet discretizations of parabolic integrodifferential equations. *SIAM Journal on Numerical Analysis*, 41(1):159–180, 2003.

[Yan71] N. N. Yanenko. *The Method of Fractional Steps*. Springer-Verlag, Berlin Heidelberg, 1971.